

ISSN : 0003-2778

Scopus®

Indexed



JOURNAL OF THE ANATOMICAL SOCIETY OF INDIA



An Official Publication of Anatomical Society of India

Full text online at www.jasi.org.in
Submit articles online at <https://review.jow.medknow.com/jasi>

Editor-in-Chief
Dr. Vishram Singh

JOURNAL OF THE ANATOMICAL SOCIETY OF INDIA

Print ISSN: 0003-2778

GENERAL INFORMATION

About the Journal

Journal of the Anatomical Society of India (ISSN: Print 0003-2778) is peer-reviewed journal. The journal is owned and run by Anatomical Society of India. The journal publishes research articles related to all aspects of Anatomy and allied medical/surgical sciences. Pre-Publication Peer Review and Post-Publication Peer Review Online Manuscript Submission System Selection of articles on the basis of MRS system Eminent academicians across the globe as the Editorial board members Electronic Table of Contents alerts Available in both online and print form. The journal is published quarterly in the months of January, April, July and October.

Scope of the Journal

The aim of the *Journal of the Anatomical Society of India* is to enhance and upgrade the research work in the field of anatomy and allied clinical subjects. It provides an integrative forum for anatomists across the globe to exchange their knowledge and views. It also helps to promote communication among fellow academicians and researchers worldwide. The Journal is devoted to publish recent original research work and recent advances in the field of Anatomical Sciences and allied clinical subjects. It provides an opportunity to academicians to disseminate their knowledge that is directly relevant to all domains of health sciences.

The Editorial Board comprises of academicians across the globe.

JASI is indexed in Scopus, available in Science Direct.

Abstracting and Indexing Information

The journal is registered with the following abstracting partners:

Baidu Scholar, CNKI (China National Knowledge Infrastructure), EBSCO Publishing's Electronic Databases, Ex Libris – Primo Central, Google Scholar, Hinari, Infotrieve, Netherlands ISSN center, ProQuest, TdNet, Wanfang Data

The journal is indexed with, or included in, the following:

SCOPUS, Science Citation Index Expanded, IndMed, MedInd, Scimago Journal Ranking, Emerging Sources Citation Index.

Impact Factor* as reported in the 2020 Journal Citation Reports* (Clarivate Analytics, 2021): 0.15

Information for Authors

Article processing and publication charges will be communicated by the editorial office. All manuscripts must be submitted online at <https://review.jow.medknow.com/jasi>.

Subscription Information

A subscription to JASI comprises 4 issues. Prices include postage. Annual Subscription Rate for non-members-		
Rates of Membership (with effect from 1.1.2019)		
	India	International
Ordinary membership	INR 1500	US \$ 100
Couple membership	INR 2250	
Life membership	INR 8000	US \$ 900
Subscription Rates (till 31st August)		
Individual	INR 6000	US \$ 650
Library/Institutional	INR 12000	US \$ 1000
Trade discount of 10% for agencies only		
Subscription Rates (after 31st August)		
Individual	INR 6500	US \$ 700
Library/Institutional	INR 12500	US \$ 1050
<i>The Journal of Anatomical Society of India</i> (ISSN: 0003-2778) is published quarterly. Subscriptions are accepted on a prepaid basis only and are entered on a calendar year basis. Issues are sent by standard mail Priority rates are available upon request.		

Information to Members/Subscribers

All members and existing subscribers of the Anatomical Society of India are requested to send their membership/existing subscription fee for the current year to the Treasurer of the Society on the following address: Prof (Dr.) Punit Manik, Treasurer, ASI, Department of Anatomy, KGMU, Lucknow - 226003. Email: punitamanik@yahoo.co.in. All payments should be made through an account payee bank draft drawn in favor of the **Treasurer, Anatomical Society of India**, payable at **Lucknow** only, preferably for **Allahabad Bank, Medical College Branch, Lucknow**. Outstation cheques/drafts must include INR 70 extra as bank collection charges.

All complaints regarding non-receipt of journal issues should be addressed to the Editor-in-Chief, JASI at editorjasi@gmail.com. The new subscribers may, please contact wkhlpmedknow_subscriptions@wolterskluwer.com.

Requests of any general information like travel concession forms, venue of next annual conference, etc. should be addressed to the General Secretary of the Anatomical Society of India.

For mode of payment and other details, please visit www.medknow.com/subscribe.asp

Claims for missing issues will be serviced at no charge if received within 60 days of the cover date for domestic subscribers, and 3 months for subscribers outside India. Duplicate copies cannot be sent to replace issues not delivered because of failure to notify publisher of change of address. The journal is published and distributed by Wolters Kluwer India Pvt. Ltd. Copies are sent to subscribers directly from the publisher's address. It is illegal to acquire copies from any other source. If a copy is received for personal use as a member of the association/society, one cannot resale or give-away the copy for commercial or library use.

The copies of the journal to the subscribers are sent by ordinary post. The editorial board, association or publisher will not be responsible for non receipt of copies. If any subscriber wishes to receive the copies by registered post or courier, kindly contact the publisher's office. If a copy returns due to incomplete, incorrect or changed address of a subscriber on two consecutive occasions, the names of such subscribers will be deleted from the mailing list of the journal. Providing complete, correct and up-to-date address is the responsibility of the subscriber.

Nonmembers: Please send change of address information to subscriptions@medknow.com.

Advertising Policies

The journal accepts display and classified advertising. Frequency discounts and special positions are available. Inquiries about advertising should be sent to Wolters Kluwer India Pvt. Ltd, advertise@medknow.com.

The journal reserves the right to reject any advertisement considered unsuitable according to the set policies of the journal.

The appearance of advertising or product information in the various sections in the journal does not constitute an endorsement or approval by the journal and/or its publisher of the quality or value of the said product or of claims made for it by its manufacturer.

Copyright

The entire contents of the JASI are protected under Indian and international copyrights. The Journal, however, grants to all users a free, irrevocable, worldwide, perpetual right of access to, and a license to copy, use, distribute, perform and display the work publicly and to make and distribute derivative works in any digital medium for any reasonable non-commercial purpose, subject to proper attribution of authorship and ownership of the rights. The journal also grants the right to make small numbers of printed copies for their personal non-commercial use.

Permissions

For information on how to request permissions to reproduce articles/information from this journal, please visit www.jasi.org.in.

Disclaimer

The information and opinions presented in the Journal reflect the views of the authors and not of the Journal or its Editorial Board or the Publisher. Publication does not constitute endorsement by the journal. Neither the JASI nor its publishers nor anyone else involved in creating, producing or delivering the JASI or the materials contained therein, assumes any liability or responsibility for the accuracy, completeness, or usefulness of any information provided in the JASI, nor shall they be liable for any direct, indirect, incidental, special, consequential or punitive damages arising out of the use of the JASI. The JASI, nor its publishers, nor any other party involved in the preparation of material contained in the JASI represents or warrants that the information contained herein is in every respect accurate or complete, and they are not responsible for any errors or omissions or for the results obtained from the use of such material. Readers are encouraged to confirm the information contained herein with other sources.

Addresses

Editorial Office

Dr. Vishram Singh, Editor-in-Chief, JASI
OC-5/103, 1st floor, Orange County Society,
Ahinsa Khand-I, Indrapuram, Ghaziabad,
Delhi, NCR- 201014.
Email: editorjasi@gmail.com

Published by

Wolters Kluwer India Pvt. Ltd
A-202, 2nd Floor, The Qube,
C.T.S. No.1498A/2 Village Marol, Andheri (East),
Mumbai - 400 059, India.
Phone: 91-22-66491818
Website: www.medknow.com

Printed at

Nikedra Art Printers Pvt. Ltd Bhandup (W) , Mumbai - 400078, India.

JOURNAL OF THE ANATOMICAL SOCIETY OF INDIA

Print ISSN: 0003-2778

EDITORIAL BOARD

Editor-in-Chief

Dr. Vishram Singh, MBBS, MS, PhD (hc), FASI, FIMSA
Adjunct Professor, Department of Anatomy, KMC, Mangalore, Manipal Academy of Higher Education, Manipal, Karnataka

Joint-Editor

Dr. Murlimanju B.V.
Associate Professor, Department of Anatomy, KMC, Mangalore, Manipal Academy of Higher Education, Manipal, Karnataka

Managing Editor

Dr. C. S. Ramesh Babu
Associate Professor, Department of Anatomy, Muzaffarnagar Medical College, Muzaffarnagar, Uttar Pradesh

Associate Editor

Dr. D. Krishna Chaitanya Reddy
Assistant Professor, Department of Anatomy, Kamini Academy of Medical Sciences and Research Center, Hyderabad

Section Editors

Clinical Anatomy

Dr. Vishy Mahadevan, PhD, FRCS(Ed), FRCS
Prof of Surgical Anatomy, The Royal College of Surgeons of England, London, UK

Histology

Dr. G.P. Pal, MS, DSc, Prof & Head, Department of Anatomy, MDC & RC, Indore, India

Gross and Imaging Anatomy

Dr. Srijit Das, Department of Human and Clinical Anatomy, College of Medicine and Health Sciences, Sultan Qaboos University, Muscat, Oman

Medical Education

Dr. Deepa Singh
Professor, Department of Anatomy, HIMS, Swami Rama Himalayan University, Jolly Grant, Dehradun, Uttarakhand

Neuroanatomy

Dr. T.S. Roy, MD, PhD
Prof & Head, Department of Anatomy, AIIMS, New Delhi

Embryology

Dr. Gayatri Rath, MS, FAMS
Professor and Head, Department of Anatomy, NDMC Medical College, New Delhi

Genetics

Dr. Rima Dada, MD, PhD
Prof, Department of Anatomy, AIIMS, New Delhi, India

Dental Sciences

Dr. Praveen B Kudva
Professor and Head, Department of Periodontology, Jaipur Dental College, Jaipur, Rajasthan

National Editorial Board

Dr. S.D. Joshi, Indore
Dr. G.S. Longia, Jaipur
Dr. A.K. Srivastava, Lucknow
Dr. Daksha Dixit, Belgaum
Dr. S.K. Jain, Moradabad
Dr. P.K. Sharma, Lucknow
Dr. S. Senthil Kumar, Chennai
Dr. Daisy Sahani, Chandigarh
Dr. N. Damayanti Devi, Imphal

Dr. Renu Chauhan, Delhi
Dr. Ashok Sahai, Agra
Dr. Ramesh Babu, Muzaffarnagar
Dr. T.C. Singel, Ahmedabad
Dr. P.K. Verma, Hyderabad
Dr. S.L. Jethani, Dehradun
Dr. Surajit Ghatak, Jodhpur
Dr. Brijendra Singh, Rishikesh
Dr. P. Vatsala Swamy, Pune

International Editorial Board

Dr. Yun-Qing Li, China
Dr. In-Sun Park, Korea
Dr. K.B. Swamy, Malaysia
Dr. Syed Javed Haider, Saudi Arabia
Dr. Pasuk Mahaknkrauh, Thailand
Dr. Tom Thomas R. Gest, USA

Dr. Chris Briggs, Australia
Dr. Petru Matusz, Romania
Dr. Min Suk Chung, South Korea
Dr. Veronica Macchi, Italy
Dr. Gopalakrishnakone, Singapore
Dr. Sunil Upadhyay, UK

JOURNAL OF THE ANATOMICAL SOCIETY OF INDIA

Print ISSN: 0003-2778

EXECUTIVE COMMITTEE

Office Bearers

President

Dr. Brijendra Singh (Rishikesh)

Vice President

Dr. G. P. Pal (Indore)

Gen. Secretary

Dr. S.L. Jethani (Dehradun)

Joint. Secretary

Dr. Jitendra Patel (Ahmedabad)

Treasurer

Dr. Punita Manik (Lucknow)

Joint-Treasurer

Dr. R K Verma (Lucknow)

Editor-in-Chief

Dr. Vishram Singh (Mangalore)

Joint-Editor

Dr. Murlimanju B.V (Mangalore)

Members

Dr. Avinash Abhaya (Chandigarh)
Dr. Sumit T. Patil (Portblair)
Dr. Mirnmoy Pal (Agartala)
Dr. Manish R. Gaikwad (Bhubaneswar)
Dr. Sudhir Eknath Pawar (Ahmednagar)
Dr. Rekha Lalwani (Bhopal)
Dr. Anshu Sharma (Chandigarh)
Dr. Rakesh K Diwan (Lucknow)
Dr. A. Amar Jayanthi (Trichur)
Dr. Ranjan Kumar Das (Baripada)

Dr. Rajani Singh (Rishikesh)
Dr. Anu Sharma (Ludhiana)
Dr. Pradeep Bokariya (Sevagram)
Dr. B. Prakash Babu (Manipal)
Dr. Ruchira Sethi (Varanasi)
Dr. Ashok Nirvan (Ahmedabad)
Dr. S K Deshpande (Dharwad)
Dr. Sunita Athavale (Bhopal)
Dr. Sharmistha Biswas (Kolkatta)

JOURNAL OF THE ANATOMICAL SOCIETY OF INDIA

Volume 71 | Issue 2 | April-June 2022

CONTENTS

EDITORIAL

Immunity toward COVID-19 (Novel Coronavirus Disease) in Children, an Anatomical Perspective

Vishram Singh, B. V. Murlimanju, Latha V. Prabhu.....87

ORIGINAL ARTICLES

Morphological and Anthropometrical Features of Human Ear Ossicles: A 1-Year Cadaveric Observational Study

R. S. Mudhol, Sindhu Narahari, Rajesh Radhakrishna Havaladar.....88

Intrauterine Alcohol Exposure Delays Growth and Disturbs Trabecular Morphology in 3-Week-Old *Sprague – Dawley* Rat Femur

Diana S. Pillay, Robert Ndou.....93

Participation of 1st-Year Medical Undergraduate Students in an Anatomy Exhibition as “Near-Peer” Teachers – An Innovative Method to Implement Components of the Competency-based Curriculum in India

Priyanka Daniel, John Bino Stephen, Priyanka Clementina Stephen, Suganthy Rabi.....102

The Persistent Median Artery: A New Challenger in Carpal Tunnel Imaging?

Okan Gürkan, Ferhat Çengel, Umut Erdem, Ayhan Yılmaz, Abdulkadir Polat, Elif Evrim Ekin.....109

Analysis of Workstation Posture in Diversified Professionals as a Tool to Enhance Better Understanding of Health Outcomes to Avoid Occupational Health Hazards

W M S Johnson, Jinu Merlin Koshy, Archana Rajasundram114

Morphometric Evaluation of Sacrum Volume in Healthy Women

Emrah Özcan, Ömür Karaca, Mine İslimye Taşkın, Ramazan Çetin, Aycan Büyükmert, Alper Vatansever, İlter Kuş.....119

Demonstration of the Epigastric Vessels Surface Anatomy with Equation Model: An Anatomical Feasibility Study

Suna Yıldırım Karaca, Onur İnce, Mehmet Adıyeko, Alper İleri, Tayfun Vural, Emrah Töz, Ahmet Demir, İbrahim Karaca, Alparslan Pulur, İbrahim Egemen Ertaş123

Analysis of Anatomical Variations of the Main Arteries Branching from the Abdominal Aorta by Multidetector Computed Tomography: A Prospective Study of 500 Patients in a Tertiary Center

Navneet Dabria, Anisha Galhotra, Ritu Dhawan Galhotra, Arnav Galhotra, Isha Sharma, Chandan Kakkar, Kamini Gupta, Kavita Sagar.....128

Sternalis Muscle in Living Individuals Identified with Computed Tomography

Rüstü Türkay, Sevim Özdemir, Nurdan Göçgün, Tuba S. Can, Behice K. Yılmaz, Türkan İkizceli, Ilke Ali Gürses135

Sub-Acromion Impingement Syndrome: Scapular Morphometric Analysis: A Study On Dry Bones among Eastern Indian Population

Madhumita Dutta, Ratnadeep Poddar.....140

CASE REPORTS

Coexisting Multiple and Complex Peritoneal Variations and Agenesis of Vermiform Appendix

Mehtap Tiryakioglu, Sevda Lafci Fahrioglu, Selda Onderoglu, Sezgin Ilgi146

Unilateral Absence of Round Ligament of Femur - Cadaveric Case Report

Divya Umamaheswaran, Nagajyothi Chigurupati, Prince Solomon, Rema Devi.....151

continued...

LETTERS TO EDITOR

An Optimal Palpation Method to Locate the Pubic Tubercle

Dağhan Dağdelen, Erol Benlier154

Basic Rules for Naming Sutures

Erdogan Unur, Ilyas Ucar, Selman Cikmaz, Salih Murat Akkin156

Why Should Anatomists Underline the Geometry of Some Special Structures?

Aysegul Firat, Hatice Yasemin Balaban.....158

Immunity toward COVID-19 (Novel Coronavirus Disease) in Children, an Anatomical Perspective

COVID-19 has been killing elderly individuals, and it is mysterious to see that the kids are spared. This novel coronavirus is not like the other viruses, which are dangerous for children as the morbidity is high for this age group. It is interesting to see that the initial patients in the People's Republic of China had no children. This suggests that the disease is not symptomatic in children.^[1] Children were observed to have mild clinical manifestations and may act as asymptomatic carriers.^[2] It was reported that children's mortality is less than 1%.^[3] The reason for this immune status in children is not known. However, children might have received prophylactic vaccines for the other viruses, and these vaccines might have protected the children from COVID-19 to some extent. It is also possible that the children are not exposed to the external environment and might have maintained good pulmonary health.

However, we hypothesized that the children have the primary lymphoid organ, thymus, which might have provided immunity to COVID-19. The thymus is a temporary organ, attaining its largest size at puberty and involutes after that. People are more susceptible to viral infections with the thymus regressing due to the aging process. It is a primary lymphoid organ in which maturation of "T" lymphocytes takes place. These "T" lymphocytes are essential to invade against foreign pathogens. It was reported that thymectomy during early childhood was leading to decline in the immunologic function following the cytomegalovirus infection.^[4] The age groups between 17 and 29 years were the most common people infected with COVID-19 because, by this age, the thymus gland involutes, and these people are susceptible to the antigen load.

Grafting of thymus tissue into the neonatally thymectomized mice has prevented immunological deficiency.^[5] From this perspective, we opine that the transplantation of thymic tissue in COVID-19 patients may be beneficial. Thymic tissue may create an adaptive immune response when the coronavirus attacks the body. Even transfusion of serum taken from children may help these patients. The serum of children can be tested for severe acute respiratory syndrome coronavirus 2 antibodies. It is believed that the thoughts penned herewith may stimulate the researchers in considering new therapeutic strategies and discussing the investigations, which deals with the biomarkers and virulence of COVID-19.

**Vishram Singh, B. V. Murlimanju,
Latha V. Prabhu**

*Department of Anatomy, Kasturba Medical College, Mangalore, Manipal
Academy of Higher Education, Manipal, Karnataka, India*

*Address for correspondence: Dr. B. V. Murlimanju,
Department of Anatomy, Kasturba Medical College,
Mangalore - 575 004, Karnataka, India.
E-mail: flutemist@gmail.com*

References

1. Li Q, Guan X, Wu P, Wang X, Zhou L, Tong Y, *et al.* Early transmission dynamics in Wuhan, China, of Novel coronavirus-infected pneumonia. *N Engl J Med* 2020;382:1199-207.
2. Shen K, Yang Y, Wang T, Zhao D, Jiang Y, Jin R, *et al.* Diagnosis, treatment, and prevention of 2019 novel coronavirus infection in children: Experts' consensus statement. *World J Pediatr* 2020;16:223-31.
3. Qiu H, Wu J, Hong L, Luo Y, Song Q, Chen D. Clinical and epidemiological features of 36 children with coronavirus disease 2019 (COVID-19) in Zhejiang, China: An observational cohort study. *Lancet Infect Dis* 2020;20:689-96.
4. Sauce D, Larsen M, Fastenackels S, Duperrier A, Keller M, Grubeck-Loebenstien B, *et al.* Evidence of premature immune aging in patients thymectomized during early childhood. *J Clin Invest* 2009;119:3070-8.
5. Miller JF. Revisiting thymus function. *Front Immunol* 2014;5:411.

This is an open access journal, and articles are distributed under the terms of the Creative Commons Attribution-NonCommercial-ShareAlike 4.0 License, which allows others to remix, tweak, and build upon the work non-commercially, as long as appropriate credit is given and the new creations are licensed under the identical terms.

Article Info

Received: 06 June 2022
Accepted: 06 June 2022
Available online: 30 June 2022

Access this article online	
Quick Response Code: 	Website: www.jasi.org.in
	DOI: 10.4103/jasi.jasi_86_22

How to cite this article: Singh V, Murlimanju BV, Prabhu LV. Immunity toward COVID-19 (novel coronavirus disease) in children, an anatomical perspective. *J Anat Soc India* 2022;71:87.

Morphological and Anthropometrical Features of Human Ear Ossicles: A 1-Year Cadaveric Observational Study

Abstract

Introduction: The ossicular chain formed by malleus, incus, and stapes, is considered an essential content of the middle ear and is responsible for the transmission of sound vibrations from the tympanic membrane to the oval window. This study aims to evaluate the morphology and anthropometry of ossicles from human cadavers. **Material and Methods:** This is a cross-sectional study conducted in the Department of Otorhinolaryngology and Head-and-Neck Surgery of KAHER's JN Medical College, Belagavi, for 1 year. Twenty fresh cadavers (40 sets of ossicles) were dissected using zero-degree endoscope. With gentle manipulation, ossicles were removed to study anthropometry and morphology of each middle ear bone using osseous sizer. **Results:** Among the three bones, based on mean measurements, the heaviest bone was incus (19.08 mg), followed by malleus (16.65 mg) and the lightest bone was stapes (2.28 mg). The longest bone among the three bones was malleus (7.18 mm), followed by incus (5.71 mm) and stapes (2.70 mm). Malleus showed variations in the distal ends, incus showed variation in the lenticular process and the obturator foramen of stapes had different shapes. **Discussion and Conclusion:** With a rapid rise in the demand for ossiculoplasty in India, knowledge of morphology and possible anthropometric variation existing in Indian subjects is needed to add up to a better understanding of middle ear dynamics.

Keywords: *Incus, malleus, morphology, ossicles, ossiculoplasty, stapes*

Introduction

The special function of hearing is carried out by a small organ like ear and it only makes it more interesting that inside this miniature ear structure, there are three minor bones- malleus(hammer), incus(anvil) and stapes(stirrup) tactically positioned to form a semi rigid structure acting like a bony cable for transmitting sound in the middle ear.^[1] The malleus is the first bone and is attached to the eardrum and the stirrup or the stapes is attached to the oval window. The incus is bridged between them, and articulates with both the bones on its either side. This arrangement, along with the ventilation, is the driving force of middle ear mechanics. Discontinuity or fixity of the ossicular chain leads to conductive hearing loss. An eroded incudo-stapedial joint, an absent incus or an absent incus and stapes superstructure together leads to ossicular discontinuity in increasing order of frequency of hearing loss.^[2] To restore appropriate sound transmission, ossicular

chain reconstruction has to be performed. Several factors have to be considered when selecting a material to use for ossicular reconstruction. This includes ease of availability, stiffness, stability, biocompatibility, and cost-effectiveness. According to Mudhol *et al.*, autografts were preferred for ossicular reconstruction because they had a very low extrusion rate. However, with the development of newer bioactive synthetic prosthesis and moldable materials, the extrusion rate has become low. Hence, we can expect biosynthetic materials to be more popular.^[3] To study the morphology and anthropometry of middle ear ossicles during surgery is difficult. Studying them on cadavers gives a better understanding about its variations and dimensions. The knowledge of these ossicle dimensions, their variations, and their morphometric data will help the otologists during reconstructive surgery and also aid in designing better prosthesis.

Objective

This study aims to evaluate the morphology and anthropometry of ossicles from human cadavers.

How to cite this article: Mudhol RS, Narahari S, Havaldar RR. Morphological and anthropometrical features of human ear ossicles: A 1-year cadaveric observational study. *J Anat Soc India* 2022;71:88-92.

**R. S. Mudhol,
Sindhu Narahari,
Rajesh Radhakrishna
Havaldar**

Department of ENT and Head and Neck Surgery, J.N. Medical College, KLE Academy of Higher Education and Research, Belagavi, Karnataka, India

Article Info

Received: 05 April 2021

Revised: 08 February 2022

Accepted: 25 March 2022

Available online: 30 June 2022

Address for correspondence:

*Dr. Sindhu Narahari,
Department of ENT and Head and Neck Surgery, J.N. Medical College, KLE Academy of Higher Education and Research, Belagavi, Karnataka, India.
E-mail: sindhunarahari.13@gmail.com*

Access this article online

Website: www.jasi.org.in

DOI:
10.4103/jasi.jasi_67_21

Quick Response Code:



This is an open access journal, and articles are distributed under the terms of the Creative Commons Attribution-NonCommercial-ShareAlike 4.0 License, which allows others to remix, tweak, and build upon the work non-commercially, as long as appropriate credit is given and the new creations are licensed under the identical terms.

For reprints contact: WKHLRPMedknow_reprints@wolterskluwer.com

Material and Methods

This is a cross-sectional study carried out over a period of 1 year (January 2019 to December 2019) from available cadavers for dissection during the study period in J. N. Medical College, Belagavi. All cadavers subjected to dissection were included except temporal bones with any evidence of previous surgeries and those bones with history or evidence of trauma. Each cadaver was numbered categorically and postauricular (Wilde's) incision was taken. Using the instruments shown in Figure 1, dissection was carried out. Skin and subcutaneous tissue till the periosteal layer was dissected and the external auditory canal was entered. The tympanic membrane was meticulously dissected from the malleus. All three ossicles were visualized using a zero-degree endoscope and their muscle attachments were separated. With gentle

manipulation, ossicles were removed. All three ossicles were washed with the hydrogen peroxide solution and each set of ossicles was stored in a clean box after labeling it. Each ossicle was weighed using an Mettler Toledo™ digital analytical balance with 0.1 mg readability electronic weighing machine and its measurements were taken using an osseous sizer. Photographs were taken from a fixed distance using the NIKON™ D3500 DSLR camera. This study was approved by the Institutional Ethics Committee on human subjects research of Jawaharlal Nehru Medical College, Belagavi (MDC/DOME/51) on 24/11/18.

All measurements were noted and their mean, median, and standard deviation were calculated. Statistical analysis was done by Chi-square test, Paired *t*-test, Independent *t*-test and Karl Pearson's correlation coefficient method using Statistical Package for Social Sciences version 24 (SPSS™ 24). Developed on 2016 March, IBM Developer by Norman H Nie, Dale H Bent, C. Hadlai Hull Chicago.

Results

A total of 20 cadavers (40 sets of ossicles) were evaluated, as shown in Figure 2. About 70% were male and 30% were female cadavers.

Malleus

The weight ranged from 12 mg to 21 mg with an average of 16.65 mg. The total length of the malleus ranged from 6 mm to 9 mm with an average of 7.19 mm. The length of the manubrium ranged from 2.5 mm to 5 mm with an



Figure 1: Instruments used for dissection and measurements



Figure 2: Set of 40 ossicles obtained from 20 cadavers

average of 4.21 mm. The maximum width of the head ranged from 1.5 mm to 4.5 mm and an average of 2.44 mm. There is no statistical difference between the right and left sides. Out of 40 sets of ossicles, morphologically malleus showed very less variations except that the distal end of 13 bones was straight (30%) and 27 bones were curved (70%) as shown in Figure 3. There was no statistical difference noted between the right and left sides [Table 1].

Incus

The weight of the incus ranged from 12 mg to 28 mg with an average of 19.8 mg. The total length of the incus ranged from 4.40 mm to 7 mm with an average of 6.74 mm. The total width of the body ranged from 3 mm to 5.50 mm with an average of 3.80 mm. The length of the long process ranged from 2.50 mm to 4.50 mm with an average of 3.80 mm. Out of 40 sets of ossicles, the morphology of the incus showed variation which could be developmental or maybe necrosis of the lenticular process. In 28 (70%) bones, a fully developed lenticular process was seen and in 12 (30%) bones an underdeveloped or necrosis lenticular process was observed [Figure 3]. There was no statistical difference noted between the right and left sides [Table 2].

Stapes

The weight ranged from 1.50 mg to 3 mg with an average of 2.29 mg [Table 3]. The total height of the stapes ranged from 2 mm to 3.5 mm with an average of 2.7 mm. The

length of the footplate ranged from 2 mm to 3 mm with an average of 2.42 mm. The width of the footplate ranged from 1 mm to 2 mm with an average of 1.26 mm. The length of the anterior crus ranged from 1 mm to 2.5 mm with an average of 1.66 mm. The length of the posterior crus ranged from 1.5 mm to 2.5 mm with an average of 2.08 mm. The width of the head ranged from 0.5 mm to 1.5 mm and an average of 1 mm. Out of 40 sets of ossicles, we found 18 (45%) bones having a triangular shaped and around 22 (55%) bones having an oval-shaped obturator foramen, as shown in Figure 3.

Among all three bones, the heaviest bone was incus (19.08 mg), followed by malleus (16.65 mg) and the lightest bone was stapes (2.28 mg). The longest bone among the three was malleus (7.18 mm), followed by incus (5.71 mm) and last being stapes (2.70 mm).

Discussion

The human auditory system is a remarkable engineering design that is made up of complex geometries. Although the knowledge of the ossicular chain has been there for around 500 years, there are only a small number of morphometrical studies done on ear ossicles.^[4] Quam and Rak provided

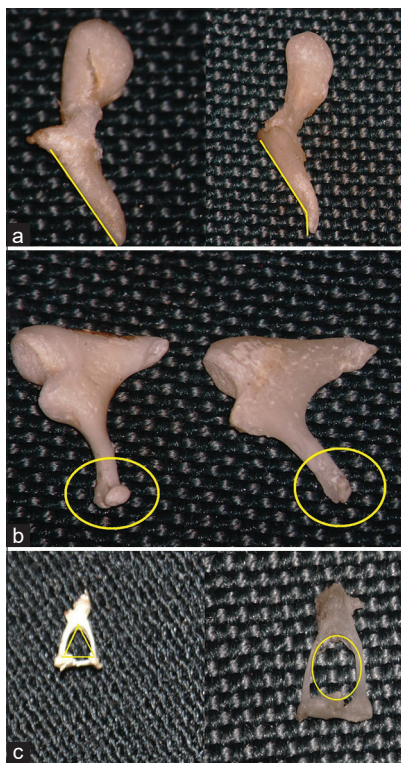


Figure 3: (a) Straight and curved distal end of manubrium. (b) Fully developed lenticular process and underdeveloped/necrosed lenticular process. (c) Triangular shaped and oval shaped obturator foramen

Table 1: Characteristics of malleus

Parameters	Sides	n	Minimum	Maximum	Range	Mean
Weight	Right	20	12.00	21.00	9.00	16.60
	Left	20	13.00	20.00	7.00	16.70
	Overall	20	12.50	20.50	8.00	16.65
Length	Right	20	6.00	8.50	2.50	7.08
	Left	20	6.00	9.00	3.00	7.28
	Overall	20	6.00	8.80	2.80	7.19
Length of manubrium	Right	20	2.50	5.00	2.50	4.15
	Left	20	2.50	5.00	2.50	4.25
	Overall	20	2.50	5.00	2.50	4.21
Maximum width	Right	20	1.50	4.50	3.00	2.43
	Left	20	1.50	4.50	3.00	2.43
	Overall	20	1.50	4.50	3.00	2.44

Table 2: Characteristics of incus

	Sides	n	Minimum	Maximum	Range	Mean±SD
Weight	Right	20	13.00	26.00	13.00	19.65±3.75
	Left	20	12.00	28.00	16.00	18.50±4.48
	Overall	20	12.50	27.00	14.50	19.08±4.04
Length	Right	20	4.50	7.00	2.50	5.68±0.86
	Left	20	4.40	7.00	2.60	5.74±0.93
	Overall	20	4.50	7.00	2.50	5.74±0.87
Length of long process	Right	20	2.50	4.50	2.00	3.50±0.51
	Left	20	2.50	4.50	2.00	3.38±0.56
	Overall	20	2.50	4.50	2.00	3.45±0.50
Width of body	Right	20	3.00	5.50	2.50	3.80±0.85
	Left	20	3.00	5.00	2.00	3.78±0.68
	Overall	20	3.00	5.30	2.30	3.80±0.77

SD: Standard deviation

the foremost set of well-defined measurements by determining the X- and Y-axis of the bone following which all the distances and angles were calculated.^[5] However, Hallgrímsson *et al.* gave one of the most efficient and accurate methods by using computed tomography which provided the measurements of ossicles.^[6]

A comparison of morphometry of malleus in our study with other studies is shown in Table 4. The weight in our study ranged from 12 to 21 mg with an average of 16.65 mg which was slightly low compared to other studies. The length of malleus in our study ranged from 6 to 9 mm with an average of 7.19 mm which is almost similar to other studies. A comparison of morphometry of incus with other studies is shown in Table 5. The length of incus in the present study is almost similar to other studies. The width of the incus is lesser compared to other studies. The mean weight of incus in our study was found to be 19.8 mg which was lesser than that reported by Jyoti and Shama. in India (23.8 mg).^[13] This suggests that considerable variations in anthropometry and morphology exist in the same country and hence, designing appropriate prosthesis is a challenge as there are no generalized fixed measurements. A comparison of morphometry of stapes is shown in Table 6. According to David Victor *et al.*,^[10] the mean total height of stapes is 3.44 mm. The height of the stapes in our study is lesser compared to other studies; the length and width of the footplate are similar in measurements as compared to other studies. In the present study, out of the 40 stapes specimens, the length of the anterior and posterior crus was equal in five specimens and in all other specimens, the posterior crus was longer than the anterior crus. Differences in the shape of foramen obturatum ranging from circular, oval, triangular to even tunnel shaped are mentioned in different studies.^[9,16] Sarrat *et al.*, distinguished numerous shapes of obturator foramen of stapes as round, oval, or angled.^[17] In our study, we observed triangular-shaped foramen in 45% of the bones and oval shaped in 55%. Ossiculoplasty is performed by a large number of surgeons using a wide variety of prosthesis materials. According to a study done by Mudhol *et al.*, there was significant betterment in hearing in people with ossiculoplasty done using autologous incus as compared to titanium prosthesis.^[18] Surgeons operating in the middle ear should be aware of the dimensions and the possible variations that can be present in the region to perform the needed and anticipated corrections without causing any instability to the structural integrity in middle ear dynamics. Reckoning this, ossicles are of significant importance in reconstructive efforts and a careful assessment of this region should be carried out during ossiculoplasty.

Since it is not practical to assess all the finer details of these structures in live patients, it becomes essential to assess, interpret and analyze with an alternative, the only feasible possibility being cadaveric studies. Till date, very

Table 3: Characteristics of stapes

Parameters	Sides	n	Minimum	Maximum	Range	Mean±SD
Weight	Right	20	1.80	3.00	1.20	2.39±0.47
	Left	20	1.50	3.00	1.50	2.17±0.46
	Overall	20	1.70	3.00	1.30	2.29±0.43
Length	Right	20	2.00	3.50	1.50	2.70±0.38
	Left	20	2.00	3.50	1.50	2.70±0.38
	Overall	20	2.00	3.50	1.50	2.70±0.38
Length of foot plate	Right	20	2.00	3.00	1.00	2.43±0.37
	Left	20	2.00	3.00	1.00	2.40±0.38
	Overall	20	2.00	3.00	1.00	2.42±0.37
Width of foot plate	Right	20	1.00	2.00	1.00	1.28±0.38
	Left	20	1.00	2.00	1.00	1.23±0.38
	Overall	20	1.00	2.00	1.00	1.26±0.37
Length of anterior crus	Right	20	1.00	2.50	1.50	1.63±0.46
	Left	20	1.00	2.50	1.50	1.68±0.41
	Overall	20	1.00	2.50	1.50	1.66±0.42
Length of posterior crus	Right	20	1.50	2.50	1.00	2.05±0.36
	Left	20	1.50	2.50	1.00	2.10±0.31
	Overall	20	1.50	2.50	1.00	2.08±0.32
Width of head	Right	20	0.50	1.50	1.00	1.00±0.28
	Left	20	0.50	1.50	1.00	1.00±0.28
	Overall	20	0.50	1.50	1.00	1.00±0.28

SD: Standard deviation

Table 4: A comparison of morphometry of malleus with other studies

Author	Length of malleus (mm)	Length of manubrium (mm)
Present study	7.19	4.21
Radha ^[7]	7.4	4.2
Unur <i>et al.</i> ^[8]	7.7	4.7
Harneja ^[9]	7.15	4.22
Kumar ^[10]	8	4.17
Singh <i>et al.</i> ^[11]	7.9	4.76

Table 5: Comparison of morphometry of incus with other studies

Author	Length of incus (mm)	Width (mm)
Present study	6.47	3.80
Arensburg <i>et al.</i> ^[12]	6.4	5.1
Jyoti ^[13]	6.3	4.4
Kumar ^[10]	7.04	5.31

Table 6: Comparison of morphometry of stapes with other studies

Author	Height of stapes	Length of foot plate	Width of foot plate
Present study (mm)	2.7	2.42	1.26
Unur <i>et al.</i> , 2002 ^[8]	3.22±0.31	2.57±0.33	1.29±0.22
Harneja ^[9]	3.12±0.21	2.68±0.27	1.26±0.08
Wadhwa <i>et al.</i> , 2005 ^[14]	3.41±0.20	2.97±0.31	0.39±0.10
Rathava <i>et al.</i> , 2014 ^[15]	3.33±0.25	2.78±0.15	1.34±0.13

few Indian studies have been done on ossicles. Most of them were done using various digital software, graph sheets, or Vernier calipers for measuring ossicles. These measurements may be associated with errors. In this study, an attempt has been made for the first time to use an osseous sizer, a more accurate tool for the assessment of ossicular morphometry.

Conclusion

With a rapid rise in demand for ossiculoplasty in our country, this study assesses the possible morphology and anthropometric variation that can exist in Indian cadavers with an intention to add up to the present understanding of middle ear dynamics. With considerable inter- and intra-regional variations in the morphology and anthropometry, we also expect that the effort of this study will motivate several others to carry out temporal bone dissections with an intention to supplement the present understanding with additional information on ossicles and also be conserved in ossicular banks by practicing appropriate safeguarding and sterilization approaches for forthcoming use as homograft in ossiculoplasty. These collected ossicles may be used to substitute eroded middle ear ossicles as an alternative to the commercially available prosthesis.

Ethics approval

Approval was obtained from the Ethics Committee of KLE Academy of Higher Education and Research. The procedures used in this study adhere to the tenets of the Declaration of Helsinki.

Financial support and sponsorship

Nil.

Conflicts of interest

There are no conflicts of interest.

References

- Saha R, Srimani P, Mazumdar A, Mazumdar S. Morphological variations of middle ear ossicles and its clinical implications. *J Clin Diagn Res* 2017;11:C01-4.
- Mills GC, Alperin JB, Trimmer KB. Studies on variant glucose-6-phosphate dehydrogenases: G6PD Fort Worth. *Biochem Med* 1975;13:264-75.
- Mudhol RS, Naragund AI, Shruthi VS. Ossiculoplasty: Revisited. *Indian J Otolaryngol Head Neck Surg* 2013;65:451-4.
- Noussios G, Chouridis P, Kostretzis L, Natsis K. Morphological and morphometrical study of the human ossicular Chain: A review of the literature and a meta-analysis of experience over 50 years. *J Clin Med Res* 2016;8:76-83.
- Quam R, Rak Y. Auditory ossicles from southwest Asian Mousterian sites. *J Hum Evol* 2008;54:414-33.
- Hallgrímsson B, Zelditch ML, Parsons TE, Kristensen E, Young NM, Boyd SK. Morphometrics and biological anthropology in the postgenomic age. In: *Biological Anthropology of the Human Skeleton*. 2nd ed. 2007; p. 207-235.
- Radha K. Morphological and morphometric study of malleus in South Indian population. *Int J Anat Res* 2016;4:2342-4.
- Unur E, Ulger H, Ekinci N. Morphometrical and morphological variations of middle ear ossicles in the newborn. *Erciyes Tip Derg* 2002;24:57-63.
- Harneja NK, Chaturvedi RP. A study of the human ear ossicles. *Indian J Otolaryngol* 1973;25:154-60.
- Kumar DV, Chaitanya K, Singh V, Reddy DS. A morphometric study of human middle ear ossicles in cadaveric temporal bones of Indian population and a comparative analysis. *J Anat Soc India* 2018;67:12-7.
- Singh K, Chhabra S, Sirohiwal B, Yadav S. Morphometry of malleus a possible tool in sex determination. *J Forensic Res* 2012;3:152. doi:10.4172/2157-7145.1000152.
- Arensburg B, Harell M, Nathan H. The human middle ear ossicles, Morphometry and taxonomic implications. *J Hum Evol* 1981;10:199-205.
- Jyoti KC, Shama SN. A study of morphological and morphometrical analysis of human incus. *Int J Curr Res* 2015;7:16102-4.
- Wadhwa S, Kaul JM, Agarwal AK. Morphometric study of stapes and its clinical implications. *J Anat Soc India* 2005;54:1-9.
- Rathava JK, Dilip VG, Vidya KS, Urvik CK, Pratik NT, Mital MP, *et al.* Osteometric dimension of stapes. *J Res Med Dent Sci* 2014;2:30-3.
- Dass R, Grewal BS, Thapar SP. Human stapes and its variations. I. General features. *J Laryngol Otol* 1966;80:11-25.
- Sarrat R, García Guzmán A, Torres A. Morphological variations of human ossicula tympani. *Acta Anat (Basel)* 1988;131:146-9.
- Naragund AI, Mudhol RS, Harugop AS, PH Patil. Ossiculoplasty with autologous incus versus titanium prosthesis: A comparison of anatomical and functional results. *Indian J Otol* 2011;17:75-9.

Intrauterine Alcohol Exposure Delays Growth and Disturbs Trabecular Morphology in 3-Week-Old *Sprague – Dawley* Rat Femur

Abstract

Introduction: The consequence of gestational alcohol exposure ranges from stillbirth to miscarriage and fetal alcohol syndrome (FAS). FAS is one of the deleterious causes of congenital disabilities, mental and growth retardation. Several studies suggest that low birth weight and impaired bone growth, as well as a decrease in mineralization in utero, may reduce peak bone mass and increase the risk of fractures and osteoporosis later in life. Therefore, the aim of this study was to determine the effects of intrauterine alcohol exposure on the internal architecture of the femur.

Material and Methods: Time-mated ($n = 13$) pregnant *Sprague – Dawley* dams were assigned to either the ethanol ($n = 5$), saline control ($n = 5$) or untreated control ($n = 3$) group. The former two groups were treated with 0.015 ml/g of 25.2% ethanol and 0.9% saline for the first 19 days of gestation, respectively. The untreated group received no treatment. Once born, the pups were weaned at 21 days. These rats were then terminated. From each dam, two pups were collected resulting in ethanol ($n = 10$), saline controls ($n = 10$), and untreated controls ($n = 6$). The femora of the pups were dissected and scanned using a 3D- μ CT scanner (Nikon XTH 225 L) at 15 μ m resolution. Trabecular and cortical parameters were analyzed using Volume Graphics Studio[®] software following reconstruction. **Results:** We found altered trabecular parameters in the alcohol exposed group. The diaphyseal cortical and medullary cavity proportions were also affected, particularly in the midshaft.

Discussion and Conclusion: These results indicate that gestational alcohol exposure may lower bone structural quality by disturbing the internal morphology of the osseous tissue.

Keywords: Cortical thickness, femur, gestational alcohol, internal morphology, trabeculae

**Diana S. Pillay,
Robert Ndou**

*Department of Anatomy
and Histology, School of
Medicine, Sefako Makgatho
Health Sciences University,
Ga-Rankuwa, Pretoria,
South Africa*

Introduction

The consumption of alcohol during pregnancy has well-known teratogenic consequences on fetal development.^[1] These may include spontaneous abortion, fetal growth inhibition, premature delivery, abruption placentae, and breech presentations.^[2] An offspring exposed to alcohol *in utero* can suffer an assortment of disorders and disabilities^[3] collectively described as fetal alcohol spectrum disorder. This is a nondiagnostic, umbrella term used to describe a range of effects on an offspring that result from gestational alcohol exposure.^[3] These include alcohol-related birth defects, alcohol-related neurodevelopmental disorder, partial fetal alcohol syndrome, and fetal alcohol syndrome (FAS).^[3,4]

There is limited information on changes in the internal architecture of bone following gestational alcohol exposure. However,

research shows a postnatal reduction in cortical and trabecular thickness as well as reduced bone formation rate following intrauterine alcohol exposure.^[5-7] A decrease in the bone formation rate may occur due to the disturbance in proliferation and the activity of osteoblasts,^[6,8] which may alter the internal integrity of the bone. Although studies have shown the adverse impact of alcohol consumption on cortical and trabecular parameters, no research has established the effects of gestational alcohol exposure on the internal architecture of postnatal bone development. Knowledge in this area will be useful and will help us understand weaker bones in FAS children.

Studies investigating the effects of gestational alcohol exposure on bone focus on rat fetuses,^[1,9] therefore, such research is limited among adolescents^[10] Understanding how gestational alcohol exposure affects bone postnatal development is crucial as peak bone growth occurs during adolescence.^[3] Intrauterine alcohol exposure causes shorter bones^[1,9] and delayed fetal

Article Info

Received: 09 November 2021

Accepted: 17 March 2022

Available online: 30 June 2022

Address for correspondence:

*Dr. Diana S. Pillay,
Department of Anatomy
and Histology, School of
Medicine, Sefako Makgatho
Health Sciences University,
Ga-Rankuwa, Pretoria, 0204,
South Africa.*

E-mail: diana.pillay125@gmail.com

Access this article online

Website: www.jasi.org.in

DOI:
10.4103/jasi.jasi_183_21

Quick Response Code:



How to cite this article: Pillay DS, Ndou R. Intrauterine alcohol exposure delays growth and disturbs trabecular morphology in 3-week-old *Sprague – Dawley* rat femur. *J Anat Soc India* 2022;71:93-101.

This is an open access journal, and articles are distributed under the terms of the Creative Commons Attribution-NonCommercial-ShareAlike 4.0 License, which allows others to remix, tweak, and build upon the work non-commercially, as long as appropriate credit is given and the new creations are licensed under the identical terms.

For reprints contact: WKHLRPMedknow_reprints@wolterskluwer.com

skeletal ossification,^[9] with osteoporosis and high fracture risk in postnatal life,^[9] suggesting inadequate postnatal development.

The rate of alcohol consumption during gestation is among the highest in South Africa at 13%,^[11] compared to 9.8% on average in the rest of the world.^[11] However, some conservative areas around the world^[12] and in South Africa stigmatize alcohol consumption by woman. Therefore, some women tend to drink in secret to evade the detection by their spouses and to avoid the perceived societal stigma associated with women alcohol drinkers.^[12] This behavior of secluded alcohol consumption results in binge drinking, defined as consuming four to five glasses of alcohol per occasion.^[13] This pattern of drinking poses a high risk for FAS,^[14] particularly as women may not know that they are pregnant in the initial 2 months of gestation. Considering this, we employed a model that sought to mimic binge drinking. Binge drinking causes more severe brain damage and behavioral changes than heavy chronic drinking in rats.^[15] This is thought to be due to the high peak blood alcohol concentration produced by consuming large alcohol volumes over a short duration as in binge drinking.^[12] The effects of alcohol consumption cause negative consequences to the skeleton of adults; however, it remains uncertain if this deleterious effects on the osseous tissue will continue into adolescence and adult life in cases of gestational alcohol exposure. We wondered whether prenatal alcohol exposure would affect trabecular morphological parameters in postnatal life in weight-bearing bone such as the femur. As such, we investigated this question using the femur in 3-week-old rats that were subjected to alcohol during gestation.

Material and Methods

Breeding and animal husbandry

The study received ethics approval from the Animal Ethics Screening Committee (AESC 2015/27/15C). A total of 13 female virgin *Sprague – Dawley* rats weighing between 260 and 350 g were used. All study animals were bred and kept at the Central Animal Services, University of Witwatersrand. These animals were maintained under pathogen-free conditions, temperature-controlled environment ($23^{\circ}\text{C} \pm 2^{\circ}\text{C}$) and a 12-h light/dark cycle. Pregnant dams were individually housed in plastic cages (L 430 mm \times W 220 mm \times H 200 mm), with free movement within the enclosures. The animals had unrestricted access to tap water and standard rodent diet.

Treatment with ethanol or saline

The dams ($n = 13$) were divided into either the ethanol ($n = 5$), saline control ($n = 5$) and untreated control groups ($n = 3$). Fewer animals were used in this group ($n = 3$) to reduce the number of animals required for the study and to lower the study cost. The untreated control group received neither ethanol nor saline. The experimental and saline groups were treated with 0.015 ml/g body mass of either 25.2%

ethanol or 0.9% saline control, respectively. The ethanol administered was to mimic a chronic binge drinking model as a relatively large dose was given once a day. The treatment was administered by oral gavage for 19 days from the 1st day of gestation as determined by the presence of a vaginal plug.

Determination of maternal blood alcohol levels

To determine blood alcohol levels in the dams, whole blood was collected from the tail vein into heparinized microcapillary tubes, one hour after alcohol administration. Microcapillary tubes were spun in a microhaematocrit centrifuge (Haematokrit 210, Hetich, Germany) at 3000 rpm for 10 min. Plasma alcohol determination was carried out using the BioVision Ethanol Colorimetric Assay Kit (BioVision incorporation, Milpitas, USA) according to the manufacturer's instructions. All reactions and readings were done in an alcohol-free environment using an iMark Bio-rad Microplate Absorbance Reader (Bio-rad Laboratories Inc, USA). All blood samples were centrifuged, and serum stored at -80°C until analyzed for Blood Alcohol Concentration [BioVision Ethanol Colorimetric/Fluorometric Assay Kit (catalog #K620-100)] (BAC).

Allocation of pups

The dams were allowed to litter naturally, and the pups remained with their dams until termination at 21 days of age where they were terminated by a lethal pentobarbital intraperitoneal injection. From each dam, two pups were collected resulting in: ethanol ($n = 10$), saline controls ($n = 10$), and untreated controls ($n = 6$).

Skeletal harvesting

Upon termination, the skeletal samples were then individually immersed and stored in 10% buffered formalin to continue fixation until further processing.

Micro-focus X-ray computed tomography

Bilateral femora were scanned with a Nikon XTH 225/320 LC X-ray microtomograph. To keep the samples steady during scanning, the bones were placed in plastic tubes and mounted in low density Styrofoam, while allowing the X-rays to get to the sample with negligible absorption. The plastic container with the sample inside was then positioned on a rotating manipulator in the scanning chamber for the scanning. The scanning parameters used in this study were as follows: the scanning voltage was 70kv; the X-ray current was 400 μA , with a frame averaging of 4 and a resolution of 15 μm . Following reconstruction, VG studio Max[®]3.2 was used for the data analysis as previously described.^[16]

Parts of the femora and trabecular morphometry parameters studied

The VG studio software built in caliper was used to determine the femoral osteometric parameters. The full bone length and

bicondylar length and bicondylar breadth were measured from the femur [Table 1]. The trabecular morphometric parameters (trabecular number [TbN], thickness, spaces, and volume) were studied in the proximal and distal epiphysis of the bone [Figure 1].

A cross-sectional slice from each percentile mark was then saved for further analysis on Fiji image J. From these slices, the cross-sectional area, cortical area, and medullary canal area of the shaft were measured at 3 positions: 25th (proximal), 50th (midshaft), and 75th (distal) percentile marks [Figure 1].

Statistical analysis

The data were managed in Microsoft Excel 2016 (Microsoft Corporation) and analyzed using SPSS® version 27 (IBM®, SPSS Statistics for Windows, Armonk, NY, USA.). Analysis of variance with least significant difference *post hoc* was used for the multiple group comparisons of means. Binary logistic regression was used to predict group membership into either the ethanol or saline control group. Significance level was set at $P < 0.05$.

Results

Blood alcohol concentration

In this assay, serum for the saline control group had BAC values that were negative (or undetectable) and 81.53 mg/dl for ethanol.

Size estimation

Femoral length

All three groups in the study exhibited mean differences in femoral bone length. The ethanol group had the shortest

femora (mean = 15.65 mm ± 0.84) compared to the saline (mean = 16.01 mm ± 0.74) and untreated controls (mean = 17.16 ± 0.85) [Figure 2a]. However, femora belonging to the ethanol group were only significantly shorter when compared to the untreated controls but not the saline group (P 0.001 and P 0.140, respectively). The saline controls were also significantly shorter than the untreated group (P 0.001).

Femoral shaft volume

The phenomenon of lowest values in the ethanol group was also observed regarding shaft volume as it was lowest in the ethanol group (mean = 36.62 mm ± 6.30). It was significantly lower than the saline (mean = 44.29 mm ± 6.90 control) and untreated controls (mean = 46.90 ± 6.28) (P 0.001 for ethanol compared to both controls). No significant differences were detected between the control groups (P 0.286) [Figure 2b].

Femoral bicondylar breadth

The mediolateral (ML) dimension varied between the groups investigated with the ethanol group (mean = 3.88 mm ± 0.68) showing a significantly lower bicondylar breadth in comparison to both the controls (saline; mean = 4.34 mm ± 0.41 and untreated mean = 4.45 ± 0.42) (P 0.006 for both comparisons). No significant differences were detected between the control groups (P 0.59) [Figure 2c].

Femoral proximal and distal epiphysis volume

The size of the epiphysis showed regional similarities in the proximal and distal epiphysis among the study groupings. The proximal epiphysis had a marginally larger volume in the untreated controls (mean = 20.75 mm³ ± 1.24) compared to the saline (mean = 18.73 mm³ ± 3.39) and in the ethanol group (mean = 18.66 mm³ ± 2.86). However, no significance was observed among the three groups (P 0.113). In the distal epiphysis, a greater volume in the untreated controls (mean = 23.75 mm³ ± 3.06) compared to the saline (mean = 20.57 mm³ ± 3.91) and ethanol group (mean = 19.83 mm³ ± 2.90) was found (P 0.013 and P 0.002, respectively) [Figure 2d].

Table 1: Osteometric parameter descriptions

Parameter	Description
Full femur length	The maximum length measured between the top of the greater trochanter and the bottom of the farthest condyle
Bicondylar breadth	The distance between the medial most and lateral most points on the epicondyles
Proximal epiphysis	The part of the bone above the proximal epiphyseal growth plate
Distal epiphysis	The part of the bone below the distal epiphyseal growth plate
Cross-sectional area	The area of a slice taken from the outer margins encompassing the shaft at the 25 th , 50 th , and 75 th percentile marks
Medullary cavity area	The area of a slice taken from the outer margins encompassing the medullary canal at the 25 th , 50 th , and 75 th percentile marks
Cortical thickness	The difference between the cross-sectional area and the medullary cavity area at the shaft 25 th , 50 th and 75 th percentile marks

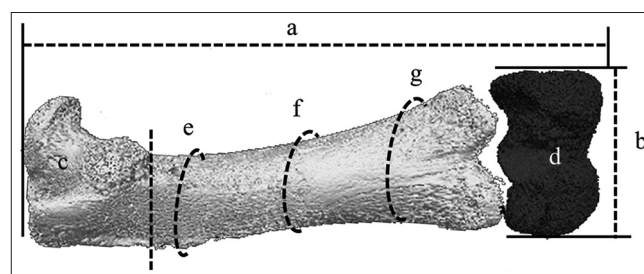


Figure 1: Three-dimensional reconstruction of a 12-week-old femur showing parts investigated. (a), Full length; (b), bicondylar breadth; (c and d), proximal and distal epiphysis. (e-g), 25th (proximal); 50th (midshaft) and 75th (distal) percentile marks, respectively

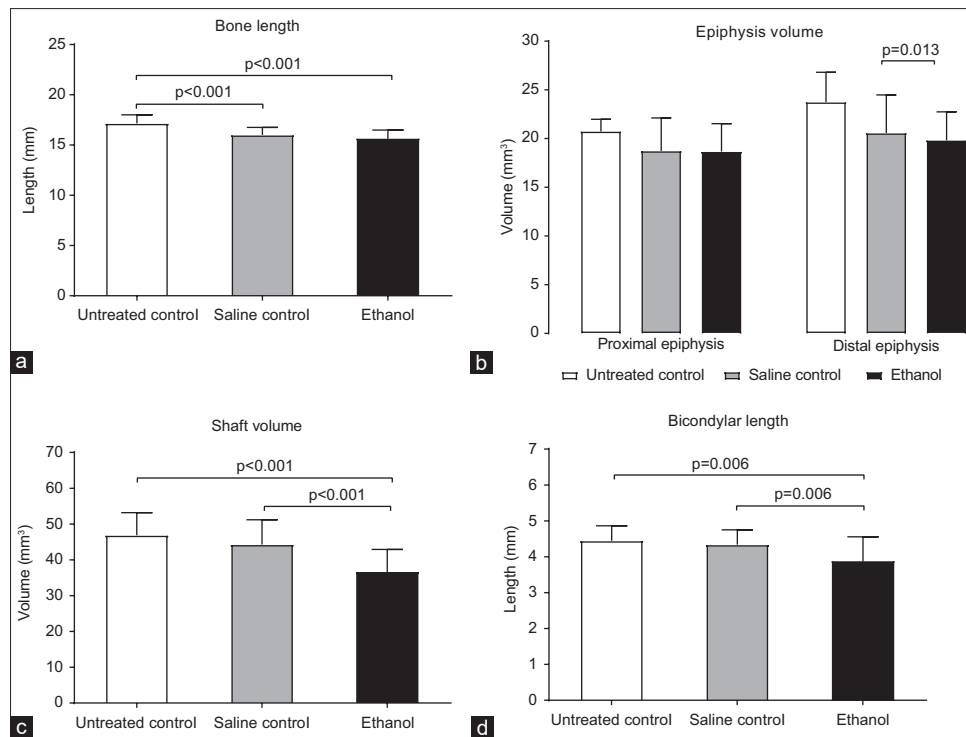


Figure 2: Size estimation; (a), bone length; (b), shaft volume; (c), bicondylar length; (d), epiphyseal volume. Represented as means for the untreated control, saline control, and ethanol group. Error bars indicate standard deviation

Trabeculae morphometry

Femoral bone to total volume ratio (bone volume/total volume)

Regarding the proximal region, bone volume total volume (BV/TV) was the highest in the untreated controls (mean = 69.75% ± 4.91) compared to the saline controls (mean = 67.18% ± 11.33) and the ethanol group (mean = 62.02% ± 10.65) [Figure 3a]. This difference was significant for the ethanol and untreated controls (P 0.041), with controls showing no significant differences (P 0.195). In distal region, the saline (mean = 69.78% ± 11.95) and untreated controls (mean = 57.43% ± 3.27) had more BV/TV than the ethanol group (mean = 52.53% ± 12.30) (P 0.004 and P < 0.001, respectively) [Figure 3a].

Femoral trabecular thickness

Regional differences were observed in the trabecular thickness among the three groups. In the proximal region, all three groups had similarities in trabecular thickness (ethanol group; mean = 0.11 mm ± 0.05, saline controls; mean = 0.13 mm ± 0.07 and untreated controls; mean = 0.11 mm ± 0.03) (P 0.313) [Figure 3b]. Conversely, the distal region revealed that the ethanol group (mean = 0.08 mm ± 0.04) had thinner trabeculae than the saline controls (mean = 0.15 mm ± 0.07) although similar to the untreated controls (mean = 0.08 mm ± 0.02) (P < 0.001 for ethanol and saline controls) [Figure 3b].

Femoral trabecular number

Trabecular distribution by the study group showed a varied pattern when stratified by epiphyseal region. The number of TbN in the proximal region was the greatest in untreated controls (mean = 6.26 mm⁻¹ ± 1.00) followed by the saline (mean = 5.76 mm⁻¹ ± 1.24) and the ethanol group (mean = 5.10 mm⁻¹ ± 1.22) [Figure 3c]. However, these differences were only significant between the ethanol and untreated controls (P < 0.009).

In the distal region, the untreated controls (mean = 7.41 mm⁻¹ ± 1.17) had more trabeculae than the saline (mean = 5.50 mm⁻¹ ± 1.21) and ethanol groups (mean = 6.38 mm⁻¹ ± 1.68) (P 0.001 and P 0.05, respectively) [Figure 3c].

Femoral trabecular spacing

Unlike the other trabecular morphometric parameters, trabeculae spacing (TbSp) showed similarities among the groups in both the proximal and distal epiphyseal regions. In the proximal region, the saline and untreated groups had a mean of 0.056 mm (±0.01), whereas the ethanol group (mean = 0.06 mm ± 0.012) had marginally wider TbSp (P 0.160 among the three groups) [Figures 3d and 4a-c]. In the distal region, all three groups had identical mean TbSp (untreated and saline control mean = 0.06 mm ± 0.007), although the ethanol group had a different standard deviation despite equal means (ethanol; mean = 0.06 ± 0.009) (P 0.97 among the three groups) [Figures 3d and 4d-f].

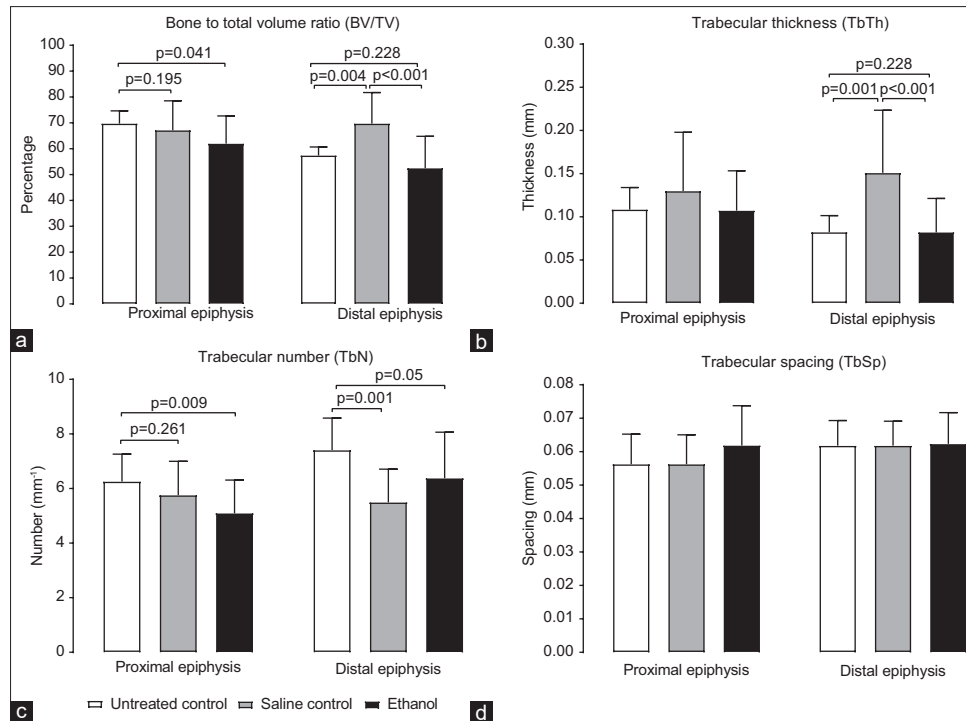


Figure 3: Trabeculae morphology. Represented as means for the animal groups (a), bone to total volume; (b), trabeculae thickness; (c), trabeculae number and (d), trabeculae spacing represented at the proximal and distal extremities. Error bars represent standard deviation

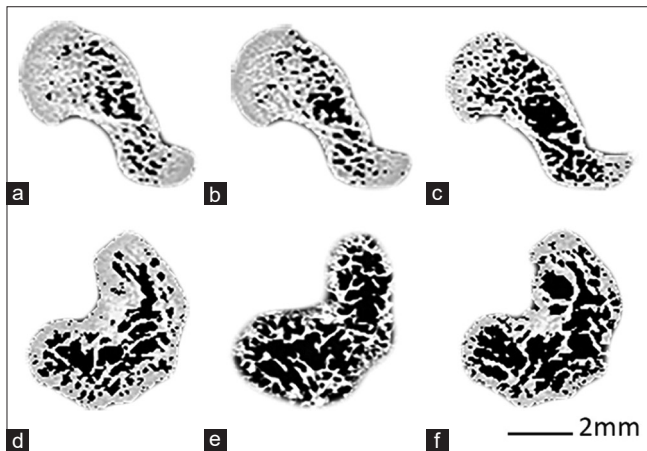


Figure 4: Trabecular morphology. Representative slices of (a), proximal end in an untreated control; (b), proximal end in a saline control; (c), proximal end of the ethanol group; (d), distal end of an untreated control; (e), distal end of saline control; (f), distal end of the ethanol group

Femoral cross-sectional area, cortical area (thickness), and medullary canal area

Proximal (25th percentile mark)

The proximal cross-sectional areas were similar in all three groups (ethanol group; mean = 4.52 mm² ± 0.89, saline controls; mean = 4.68 mm² ± 0.89 and untreated controls; mean = 4.62 mm² ± 0.72) (*P* 0.822) [Figure 5a]. Furthermore, the medullary canal area was similar in all three groups as the ethanol group had a mean of 2.21 mm² (±0.52) and the saline controls had a mean of 2.21 mm² (±0.40) and untreated controls had a

mean of 2.14 mm² (±0.68) (*P* 0.913) [Figure 5a]. With respect to cortical area (thickness) in this region, the ethanol group (mean = 2.31 mm² ± 1.07) exhibited a marginally lower value compared to the saline (mean = 2.47 mm² ± 0.96) and the untreated controls (mean = 2.48 mm² ± 0.54). No significance was detected among the three groups (*P* 0.812) [Figure 5a].

Midshaft (50th percentile mark)

The midshaft cross-sectional area was similar in all three groups studied with the untreated groups having a mean of 4.69 mm² (±0.82), saline mean = 4.66 mm² (±0.92) and the ethanol with 4.58 mm² (±0.68) (*P* 0.923) [Figure 5b]. The medullary canal area was the same in the controls (untreated and saline; mean of 2.34 mm² ± 0.42 and 2.34 mm² ± 0.43, respectively). The ethanol group (mean = 2.81 ± 0.74) had the largest medullary canal area with significant differences detected when compared to the untreated and saline controls (*P* 0.031 and *P* 0.008, respectively) [Figure 5b]. Regarding cortical area (thickness) in this region, the untreated (mean = 2.35 mm² ± 1.00) and saline controls (mean = 2.32 mm² ± 1.03) had similar values. The ethanol group (mean = 1.78 mm² ± 0.69) exhibited lower values compared to untreated and saline controls. However, significance was only detected between the ethanol and saline controls (*P* 0.044) [Figure 5b].

Distal (75th percentile mark)

The distal cross-sectional area was marginally smaller in the ethanol group (mean = 5.52 mm² ± 0.97) compared to

the saline and untreated controls (mean = 5.90 mm² ± 0.97 and 5.96 mm² ± 0.62, respectively). However, no significant differences were observed among the three groups (*P* 0.26) [Figure 5c]. The medullary canal area was marginally smaller in the ethanol group (mean = 3.89 mm² ± 0.71) compared to the saline and untreated controls (mean = 3.93 mm² ± 0.62 and 3.98 mm² ± 0.93, respectively). No significant differences were observed among the three groups (*P* 0.95) [Figure 5c]. With respect to cortical area (thickness) in this region, the ethanol group (mean = 1.62 mm² ± 0.45) exhibited a marginally lower value compared to the saline controls (mean = 1.96 mm² ± 0.90) and the untreated controls (mean = 1.98 mm² ± 0.60), although no significant differences were detected among the three groups (*P* 0.19) [Figure 5c].

Femur (3 weeks) trabecular morphometric parameters most affected by gestational ethanol

Proximal femur

The effect of gestational ethanol on length, shaft volume, proximal BV/TV, proximal trabecular thickness (TbTh), proximal TbN, proximal trabecular spacing (TbSp), proximal volume, proximal cortical thickness, midshaft cortical thickness were assessed using binary logistic regression in the ethanol and saline control groups [Table 2]. The parameters used could reliably distinguish between the two groups. A test of the full model against a constant only model was statistically significant, indicating that the predictors as a set, reliably distinguished between ethanol or saline control group membership (Chi-square = 24.443, *P* 0.004 with *df* = 9). Nagelkerke's *R*² of 0.550 indicated a moderately strong relationship between prediction and grouping. The Wald criterion demonstrated that no specific variable predicted membership [Table 3]. Prediction success overall was 78.3% (75.0% for the ethanol group and 81.8% saline controls).

Distal femur

The effect of gestational ethanol on length, shaft volume, midshaft cortical thickness, distal BV/TV, distal trabecular thickness (TbTh), distal TbN, distal TbSp, distal volume, distal ML, and distal cortical thickness was assessed using binary logistic regression in the ethanol and saline control groups [Table 4]. The parameters used could reliably distinguish between the two groups. A test of the full model against a constant only model was statistically significant, indicating that the predictors as a set, reliably distinguished between ethanol or saline control group membership (Chi-square = 36.004, *P* < 0.001 with *df* = 10). Nagelkerke's *R*² of 0.724 indicated a very strong relationship between prediction and grouping. The Wald criterion demonstrated that no specific variable predicted membership [Table 5]. Prediction success overall was 91.3% (95.8% for the ethanol group and 86.4% saline controls).

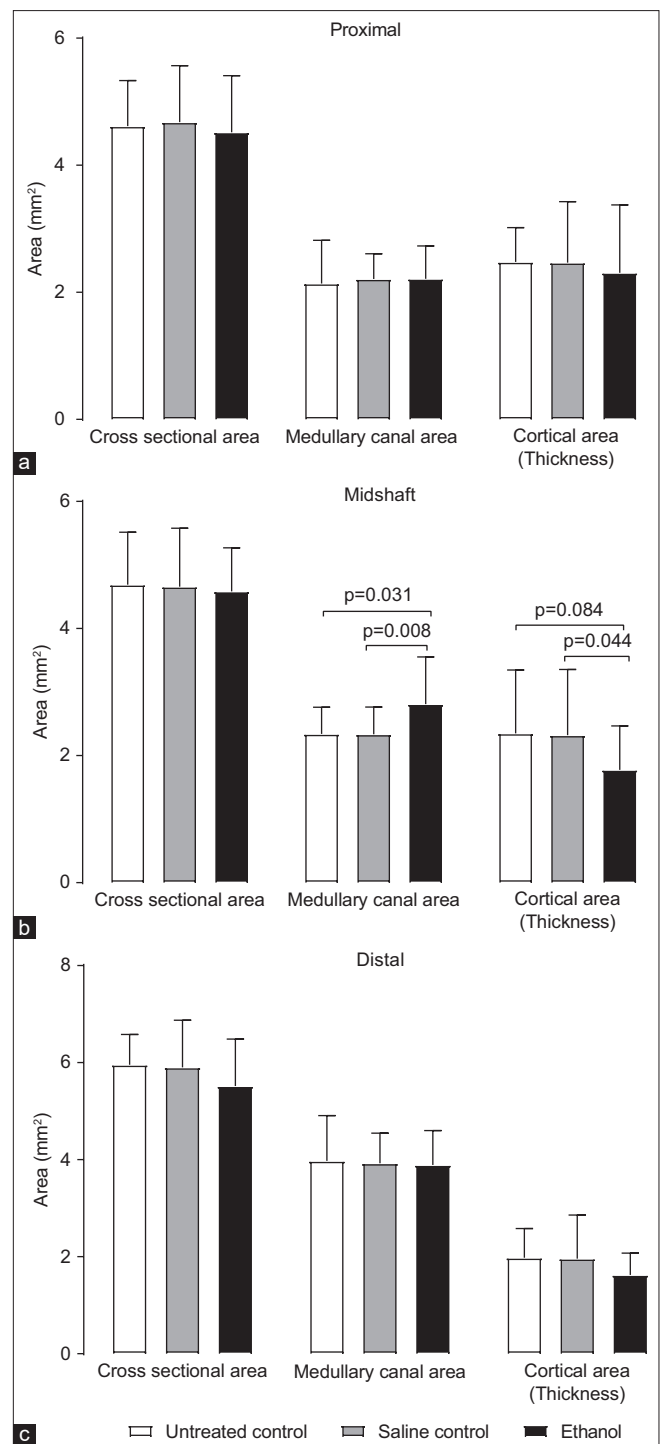


Figure 5: Cross-sectional area, medullary canal areas, and cortical thickness. Represented as means for the untreated controls, saline controls, and ethanol group; (a), at the 25th percentile mark; (b), 50th percentile mark; (c), 75th percentile mark. Error bars represent standard deviation

Discussion

The main aim was to test the hypothesis that prenatal ethanol interrupts trabecular parameters. The internal architecture was assessed from the data obtained using micro focus X-ray computed tomography (CT). Altered trabecular parameters in the alcohol exposed group were

Table 2: Femur osteometric and proximal epiphysis trabecular and cortical morphometric parameters in the equation

	Variables in the equation					
	<i>B</i>	SE	Wald	df	Significant	Exp (B)
Osteometric parameters						
Length	0.463	0.671	0.477	1	0.490	1.589
Shaft volume	-0.206	0.077	7.069	1	0.008	0.814
Epiphyseal volume	0.053	0.190	0.077	1	0.782	1.054
Proximal epiphysis trabecular and cortical morphometric parameters						
BV/TV	-0.084	0.069	1.492	1	0.222	0.919
TbTh	-4.486	14.408	0.097	1	0.756	0.011
TbN	-0.555	0.427	1.690	1	0.194	0.574
TbSp	-64.12	41.116	2.432	1	0.119	0.000
Proximal cortical thickness	0.270	0.685	0.156	1	0.693	1.311
Midschaft cortical thickness	-0.533	0.638	0.698	1	0.404	00.587
Constant	13.704	11.928	1.320	1	0.251	894,545.791

SE: Standard error, BV/TV: Bone volume to total volume, TbTh: Trabecular thickness, TbN: Trabecular number, TbSp: Trabecular spacing

Table 3: Group membership classification from osteometric and proximal epiphysis trabecular morphometric parameters of the femur

Observed Group	Classification table		
	Predicted		Percentage correct
	Ethanol	Saline control	
Ethanol	18	4	81.8
Saline control	6	18	75.0
Overall percentage			78.3

found. The diaphyseal cortical and medullary cavity proportions were also affected, particularly in the midshaft.

A concern of consuming alcohol during gestation is children considered small for age.^[3,12] Bone growth and development impact bone size and ultimately lead to stunted growth as observed in offspring of mothers who admit to drinking alcohol during gestation.^[17] Therefore, understanding bone size in research related to the effects of alcohol intake during pregnancy is crucial. In the present study, we used micro-CT data to determine the shaft volume, epiphyseal volume, length, and bicondylar length. We could not find comparable studies with respect to the shaft and epiphyseal plate volume as well as bicondylar breadth. However, numerous studies report on full bone length.^[1,9] We were concerned that length alone as a single linear measurement would not be adequate to use as a proxy for bone size. Having used micro-CT data, we were able to quantify the bone size in the form of volume in a manner that best or reliably estimates the true bone sizes.

Limb bone elongation takes place through endochondral ossification, which is entirely dependent on the existence and viability of the epiphyseal growth plate.^[18] It has been proposed that alcohol exposure during intrauterine life could result in shorter bone due to disturbances in chondrocyte number and differentiation rate as well as the size of the epiphyseal growth plate.^[2,9] Researchers^[19] have

used length (height) measurements of the growth plate and its various zones for use as a proxy of epiphyseal growth plate size. Since this measurement would be in the vertical direction, size information with respect to the horizontal aspects of the growth plate would not be captured. Furthermore, the vertical measurements of the growth plate and its various zones differ in each part of the growth plate when assessed from the ML aspect. This means that the height depends on where the researcher measures and is prone to difficulties in reproducibility. To overcome this problem, we used the measurements of surface area to gain a better estimate of the sizes of the growth plate and its zones.

We found a lower bone to tissue volume ratio in the ethanol group together with fewer and thinner trabeculae. We could not find applicable literature on gestational alcohol trabecular morphology in the femur of animals exposed to alcohol during intrauterine life. However, numerous studies elucidate the effects of alcohol use on bone strength and trabecular architecture.^[5,20,21] These studies report altered bone to volume ratio, trabecular thinning as well as fewer trabeculae with larger spaces.^[22,23] Mean TbSp appeared to be unaffected in our study as there were no group differences.

Employing a binary logistic regression showed that shaft volume, length and proximal cortical thickness were the main parameters that determined group membership into either ethanol or saline control. This means that these three parameters are affected the most in gestational alcohol exposure. When using the proximal trabeculae morphometric parameters more saline control were misclassified as belonging to the ethanol group. This suggests that there was less group variation in these parameters. This, in turn, suggests that that intrauterine ethanol effects in the femur may be minimal for the proximal aspect of the bone.

Table 4: Femur osteometric and distal epiphysis trabecular and cortical morphometric parameters in the equation

	Variables in the equation					
	<i>B</i>	SE	Wald	df	Significant	Exp (B)
Osteometric parameters						
Length	3.226	1.679	3.690	1	0.050	25.178
Bicondylar length	0.248	1.547	0.026	1	0.873	1.281
Shaft volume	-0.291	0.148	3.861	1	0.049	0.748
Epiphyseal volume	-0.176	0.277	0.403	1	0.525	0.839
Distal epiphysis trabecular and cortical morphometric parameters						
BV/TV	-0.350	0.234	2.246	1	0.134	0.704
TbTh	-13.144	42.873	0.094	1	0.759	0.000
TbN	-1.492	0.984	2.302	1	0.129	0.225
TbSp	-188.693	137.911	1.872	1	0.171	0.000
Distal cortical thickness	-2.746	1.325	4.291	1	0.038	0.064
Midschaft cortical thickness	-1.228	0.903	1.847	1	0.174	0.293
Constant	12.851	16.041	0.642	1	0.423	381,250.305

SE: Standard error, BV/TV: Bone volume to total volume, TbTh: Trabecular thickness, TbN: Trabecular number, TbSp: Trabecular spacing

Table 5: Group membership classification from osteometric and distal epiphysis trabecular morphometric parameters of the femur

Observed Group	Classification table		
	Predicted		Percentage correct
	Ethanol	Saline control	
Ethanol	19	3	86.4
Saline control	1	23	95.8
Overall percentage			91.3

Conclusion

Gestational alcohol exposure had an adverse impact on bone size at 3 weeks in postnatal life. The smaller femora observed following intrauterine alcohol exposure could be due to the altered trabecular parameters and cortical as well as medullary cavity proportions in the femoral midshaft.

Financial support and sponsorship

The study received funding from the National Research Foundation of South Africa; Grant number: TTK160826186551.

Conflicts of interest

There are no conflicts of interest.

References

1. Simpson ME, Duggal S, Keiver K. Prenatal ethanol exposure has differential effects on fetal growth and skeletal ossification. *Bone* 2005;36:521-32.
2. Miralles-Flores C, Delgado-Baeza E. Histomorphometric analysis of the epiphyseal growth plate in rats after prenatal alcohol exposure. *J Orthop Res* 1992;10:325-36.
3. O'Leary CM. Fetal alcohol syndrome: Diagnosis, epidemiology, and developmental outcomes. *J Paediatr Child Health* 2004;40:2-7.
4. May PA, Blankenship J, Marais AS, Gossage JP, Kalberg WO, Barnard R, *et al.* Approaching the prevalence of the full spectrum of fetal alcohol spectrum disorders in a South African population-based study. *Alcohol Clin Exp Res* 2013;37:818-30.
5. Diamond T, Stiel D, Lunzer M, Wilkinson M, Posen S. Ethanol reduces bone formation and may cause osteoporosis. *Am J Med* 1989;86:282-8.
6. Hogan HA, Sampson HW, Cashier E, Ledoux N. Alcohol consumption by young actively growing rats: A study of cortical bone histomorphometry and mechanical properties. *Alcohol Clin Exp Res* 1997;21:809-16.
7. Maurel DB, Jaffre C, Rochefort GY, Aveline PC, Boisseau N, Uzbekov R, *et al.* Low bone accrual is associated with osteocyte apoptosis in alcohol-induced osteopenia. *Bone* 2011;49:543-52.
8. Sampson HW, Perks N, Champney TH, DeFee B 2nd. Alcohol consumption inhibits bone growth and development in young actively growing rats. *Alcohol Clin Exp Res* 1996;20:1375-84.
9. Snow ME, Keiver K. Prenatal ethanol exposure disrupts the histological stages of fetal bone development. *Bone* 2007;41:181-7.
10. Farr JN, Khosla S. Skeletal changes through the lifespan – From growth to senescence. *Nat Rev Endocrinol* 2015;11:513-21.
11. Peltzer K, Pengpid S. Maternal alcohol use during pregnancy in a general national population in South Africa. *S Afr J Psychiatr* 2019;25:1236.
12. Olivier L, Curfs LM, Viljoen DL. Fetal alcohol spectrum disorders: Prevalence rates in South Africa. *S Afr Med J* 2016;106:S103-6.
13. Katwan E, Adnams C, London L. Childhood behavioural and developmental disorders: Association with maternal alcohol consumption in Cape Town, South Africa. *S Afr Med J* 2011;101:724, 726-7.
14. Jacobson JL, Jacobson SW, Sokol RJ, Ager JW Jr. Relation of maternal age and pattern of pregnancy drinking to functionally significant cognitive deficit in infancy. *Alcohol Clin Exp Res* 1998;22:345-51.
15. Thomas SE, Kelly SJ, Mattson SN, Riley EP. Comparison of social abilities of children with fetal alcohol syndrome to those of children with similar IQ scores and normal controls. *Alcohol Clin Exp Res* 1998;22:528-33.
16. Bouxsein ML, Boyd SK, Christiansen BA, Guldberg RE, Jepsen KJ, Müller R. Guidelines for assessment of bone microstructure in rodents using micro-computed tomography.

- J Bone Miner Res 2010;25:1468-86.
17. Lemoine P, Harousseau H, Borteyru JP, Menuet JC. Children of alcoholic parents – Observed anomalies: Discussion of 127 cases. *Ther Drug Monit* 2003;25:132-6.
 18. Lui JC, Nilsson O, Baron J. Growth plate senescence and catch-up growth. *Endocr Dev* 2011;21:23-9.
 19. Pan Z, Zhang X, Shangguan Y, Hu H, Chen L, Wang H. Suppressed osteoclast differentiation at the chondro-osseous junction mediates endochondral ossification retardation in long bones of Wistar fetal rats with prenatal ethanol exposure. *Toxicol Appl Pharmacol* 2016;305:234-41.
 20. Diez A, Serrano S, Cucurull J, Mariñoso L, Bosch J, Puig J, *et al.* Acute effects of ethanol on mineral metabolism and trabecular bone in Sprague-Dawley rats. *Calcif Tissue Int* 1997;61:168-71.
 21. Maddalozzo GF, Turner RT, Edwards CH, Howe KS, Widrick JJ, Rosen CJ, *et al.* Alcohol alters whole body composition, inhibits bone formation, and increases bone marrow adiposity in rats. *Osteoporos Int* 2009;20:1529-38.
 22. Turner RT. Skeletal response to alcohol. *Alcohol Clin Exp Res* 2000;24:1693-701.
 23. Mikosch P. Alcohol and bone. *Wien Med Wochenschr* 2014;164:15-24.

Participation of 1st-Year Medical Undergraduate Students in an Anatomy Exhibition as “Near-Peer” Teachers – An Innovative Method to Implement Components of the Competency-based Curriculum in India

Abstract

Introduction: To develop a medical professional multidimensionally, experiences must be built in the medical undergraduate curriculum using existing programs and resources. Utilizing the involvement of 1st-year medical students in an anatomy exhibition as “near-peer” teachers, we aimed to develop an interest in teaching among them and to sensitize them to the surrounding community and the need for the development of communication skills. **Material and Methods:** One hundred 1st-year medical students were involved in teaching anatomy to school students from the community during an anatomy exhibition. The students were divided into 10 groups and they demonstrated the displayed specimens for 4 days on a rotation basis. Feedback was collected to evaluate students’ responses to the program. **Results:** The feedback from the students ($n = 88$) revealed that students enjoyed the experience (97.7%) and found the experience useful for their appreciation of anatomy (87.4%). About 53.4% of students were able to communicate effectively, although 61.4% had language difficulties. Students appreciated the opportunity to interact with school students (90.9%), the need for educational outreach (94.3%) and also recommended their future involvement in teaching programs (94.3%). In making the learning experience enjoyable to the students, the factors that played a key role were their ability to communicate easily ($P = 0.019$) and their ability to appreciate the need for community outreach ($P = 0.005$). **Discussion and Conclusion:** Developing the interest of 1st-year medical students in teaching and sensitizing them to the need for improved communication skills and societal consciousness can be achieved by enabling them to act as “near-peer” teachers in school teaching programs.

Keywords: *Communication skills, competency-based curriculum, medical education, near-peer teaching, social consciousness*

Priyanka Daniel,
John Bino Stephen¹,
Priyanka
Clementina
Stephen²,
Suganthy Rabi¹

*Department of Anatomy,
Brighton and Sussex Medical
School, University of Sussex,
Brighton, UK, ¹Department of
Anatomy, Christian Medical
College, Vellore, Tamil Nadu,
²Department of Anatomy,
Jawaharlal Institute of
Postgraduate Medical Education
and Research, Puducherry, India*

Introduction

The medical curriculum globally has been gradually and steadily shifting toward competency-based medical education. Medical students are no longer required to become a competent clinician only, but they are required to embrace and exercise softer skills such as communication, professionalism, lifelong learning, and leadership as well.^[1] To train an individual in these various attributes, multiple experiences must be built in the medical undergraduate curriculum, enabling the students to acquire the requisite skills. These experiences can be designed in the form of curricular and extracurricular activities to broaden the scope of learning in a limited period. With the advent of competency-based education, there is a

greater need for identifying avenues to enrich our medical training.^[2]

One such activity planned for 1st-year medical undergraduate students at our institution was their involvement in a walk-through anatomy exhibition, conducted in the department of anatomy for higher secondary biology school students. This exhibition, which is approved by the institution, is periodically held to help the school students of the surrounding region, to understand three-dimensional human anatomy, and to create an interest in the subject. The main mode of teaching is through soft-tissue dissections, plastinates, models, charts, figures, and other audio-visual aids.^[3] [Figure 1] In this first-of-a-kind effort, the 1st-year medical undergraduate students were involved in a 4-day anatomy exhibition to describe simple

This is an open access journal, and articles are distributed under the terms of the Creative Commons Attribution-NonCommercial-ShareAlike 4.0 License, which allows others to remix, tweak, and build upon the work non-commercially, as long as appropriate credit is given and the new creations are licensed under the identical terms.

For reprints contact: WKHLRPMedknow_reprints@wolterskluwer.com

How to cite this article: Daniel P, Stephen JB, Stephen PC, Rabi S. Participation of 1st-year medical undergraduate students in an anatomy exhibition as “near-peer” teachers – An innovative method to implement components of the competency-based curriculum in India. *J Anat Soc India* 2022;71:102-8.

Article Info

Received: 27 April 2021
Accepted: 03 May 2022
Available online: 30 June 2022

Address for correspondence:

Dr. Suganthy Rabi,
Department of Anatomy,
Christian Medical College,
Vellore - 632 002,
Tamil Nadu, India.
E-mail: suganthyraabi@
cmcvellore.ac.in

Access this article online

Website: www.jasi.org.in

DOI:
10.4103/jasi.jasi_81_21

Quick Response Code:



anatomical specimens to school students. This was done to provide them a “near-peer” teaching experience to develop an interest in teaching among them, to create awareness of the surrounding community, and also to sensitize them for the need to develop communication skills in medicine.

Material and Methods

After obtaining permission from the Institutional Review Board (IRB Min. No. 12490, dated December 18, 2019) and informed consent, 100 1st-year medical students were involved in teaching anatomy to school students during “CORPORA 2018,” an anatomy exhibition, conducted by the department of anatomy over 4 days which was attended by over 5000 school students. One day before starting the study, the knowledge of basic human anatomy was tested by a multiple-choice quiz (MCQ) test to make sure that the students were aware of simple school-level anatomy. On the days of the exhibition, the MBBS students were randomly divided into 10 groups and assigned various regions of the human anatomy been displayed for the exhibition. They were required to demonstrate the displayed specimens to the visiting school students. The activity was conducted during their regular anatomy class timings of two and a half hours daily, for 4 days on a rotation basis [Figure 2]. Students were provided faculty facilitators to help them if they had any doubts or queries. After the exhibition, an anonymous feedback designed on a 5-point Likert scale as well as having descriptive feedback questions was collected to evaluate students’ responses to the program [Figure 3]. Data were summarized using frequency along with percentage, and the association between the variables was measured by constructing crosstabs and Kendall’s Tau-b correlation coefficient. The $P = 0.05$ was set as the level of significance, and IBM SPSS Statistics for Windows, version 21.0 (IBM Corp., Armonk, NY., USA).

Results

Feedback was obtained from a total of 88 (n) students. Out of a feedback from 88 (n) students, a total of 76 students

indicated their age on the feedback, which was a mean age of 18.34 years (± 0.946), and 77 students indicated their sex on the feedback, where the male students were 31 in comparison to 46 female students. The 1st-year medical students ($n = 86$) scored an overall mean of 82.71% (± 13.23) in the basic anatomy MCQ test before the start of the study, indicating their ability to be able to demonstrate specimens to school students.

The feedback collected from the students ($n = 88$) revealed that 97.7% of the students enjoyed the experience of teaching school students and 87.4% felt that this experience was useful for their appreciation of anatomy. About 53.4% of the students were able to effectively communicate with the visitors, although 61.4% had language difficulties and felt that they needed to work toward developing language and communication skills. Being involved in teaching was a new experience for many students (77.3%) and 70.1% of the students expressed that they would love to be involved in future teaching programs as well. Most of the students appreciated the opportunity to interact with school students and teachers from the community (90.9%) and felt that there was a need for outreach in education (94.3%). The majority of the students (94.3%) recommended the future involvement of medical students for anatomy exhibitions [Figure 4].

On Likert scale, scores were given for various responses as follows: strongly agree – 1, agree – 2, disagree – 3, and strongly disagree – 4 (neutral was given a value of 0). The score of the student responses to all questions was between 1 and 2, indicating the agreeability of the students with the questions posed, such as enjoyability of the experience, communication abilities, usefulness of the session for their own learning, and opportunity for community interaction. Question number 6 explored the usefulness of the time spent on the exercise and students gave a mean score of 2.39 ± 1.573 , indicating that there was a greater proportion of students disagreeing with the concept of wastage of time due to the exercise. Surprisingly, question number 9 asked the students about the fact that if



Figure 1: “CORPORA-2018, a walk-through anatomy exhibition, conducted by the Department of Anatomy for higher secondary” biology school students



Figure 2: 1st-year medical students demonstrating anatomy specimens to high-school students during the anatomy exhibition

FEEDBACK QUESTIONNAIRE FOR MBBS STUDENTS (2018 BATCH) INVOLVED IN 'CORPORA' PROGRAM						
Sex: Male/ Female			Age:			
Kindly tick only one relevant response						
Q. No.	QUESTION	Strongly agree	Agree	Neutral	Disagree	Strongly disagree
1	I enjoyed teaching school students at the CORPORA 2018 exhibition					
2	I was able to communicate easily with the visitors					
3	The specimens and models were easy to handle and explain					
4	Being involved in teaching was a new experience for me					
5	I had the opportunity to meet students and teachers from the different schools					
6	I felt being involved in CORPORA was time- consuming					
7	I felt being involved in CORPORA was useful for my appreciation of anatomy					
8	I was able to appreciate the need for outreach in education					
9	I had difficulty in explaining due to language					
10	I would love to be involved in teaching programs in the future					
11	I would recommend medical students' involvement in CORPORA in future					
	Any comments and suggestions regarding CORPORA exhibition:					

Figure 3: Feedback questionnaire used for obtaining student responses

they faced difficulty due to language issues and response score of 1.78 ± 1.208 indicated that a large proportion of the 1st-year medical students have language issues which should be taken care of early in the medical training to improve their learning during clinical years [Table 1].

Cross tabulation and statistical analysis done using Kendall's Tau-b correlation coefficient between various responses on the feedback questions revealed some important aspects [Table 2]. In making the learning experience enjoyable to the students, the factors that played a key role were their ability to communicate easily ($P = 0.019$) and their ability to appreciate the need for community outreach ($P = 0.005$). The factor that made the students communicate effectively was their appreciation for the need for outreach in education ($P = 0.016$), although communication for some was greatly hampered

by language barriers ($P = 0.051$). There was a positive correlation found between the students who understood the usefulness of the session for the appreciation of human anatomy also their willingness to be a part of such endeavors in future ($P = 0.027$).

Comments from the students were varied where many appreciated the experience, whereas some had concerns regarding not knowing the local language and the magnitude of the anatomical work at display for school students [Table 3].

Discussion

Doctors today are custodians of health, wellness, and well-being of society and are required to embrace a multidimensional approach to their practice of medicine.

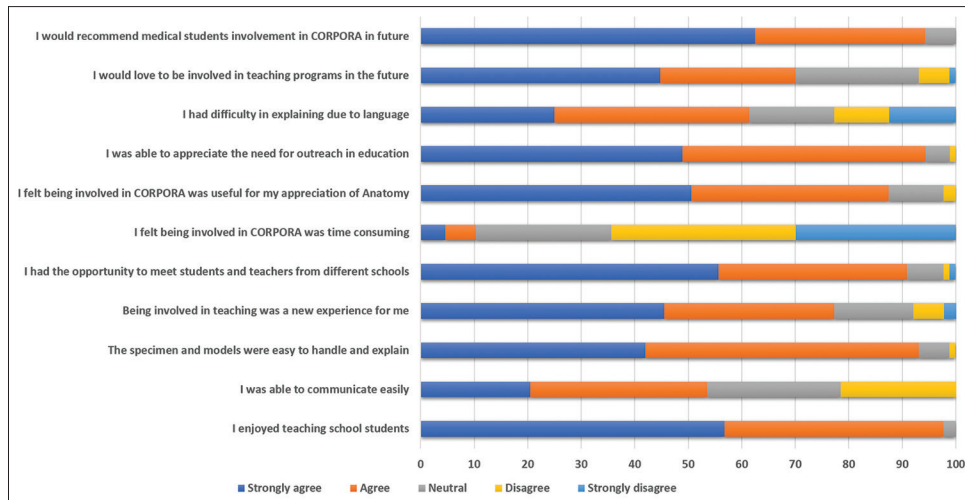


Figure 4: Graph representing student feedback obtained on a 5-point Likert scale

The medical profession requires a doctor to not only be responsible toward the treatment of his patients but also Excel in other essential roles to serve as the physicians of first contact for the community while being globally relevant.^[4] The essential roles of an Indian Medical Graduate (IMG), listed by the National Medical Commission of India, are clinician, professional, leader, communicator, and lifelong learner. Each role has required competencies laid down under it, which the graduate needs to achieve to become a competent IMG.^[5]

Teaching skills

Teaching “how to teach” has hardly ever been taught to medical undergraduate students. Medical students form future residents and faculty members of medical institutions with responsibilities including teaching and training of juniors. Teaching is also an essential aspect of physician–patient interaction and medical students tend to develop as effective communicators if exposed to training in teaching skills. In addition to these factors, it is also believed that medical students with a better understanding of teaching and learning principles become better learners.^[6]

A study done at the University of Vermont College of Medicine on the perceptions of undergraduate medical students ($n = 83$) on themselves and residents as teachers showed that medical students are interested both in learning teaching skills and teaching during medical school and during residency. Sixty-seven percent of students felt that residents played a significant role as teachers. Students appreciated the need for teaching training and many students wanted to teach during medical school (80%) and residency (93%).^[7] In our study, most of our students were exposed to a teaching opportunity for the first time in their life (77.3%) but did appreciate the usefulness of teaching and expressed their interest in being involved in teaching programs in future (70.1%).

There have been studies suggesting that when students teach, they develop a deeper and more persistent understanding of the material.^[8] Furthermore, there is enough evidence to say that when teaching is used as a mode of learning, the retention of content is better. A study done by Peets *et al.* concluded that the involvement of medical students in teaching small group sessions improves their knowledge acquisition and retention.^[9] In our study too, most of the students (87.4%) felt that there was an improvement in their understanding of the subject as a result of the teaching experience.

In a survey done by Andrew Jay *et al.* evaluating the effects of student-as-teachers (SAT) program at Mayo Medical School using a web-based survey sent to all teaching assistants in the anatomy-based SAT program over 5 years (2007–2011), indicated that participants in the anatomy-based SAT program achieved core competencies of a medical educator and felt prepared for the teaching demands of residency.^[10] In a study done by Haber *et al.*, 4th-year students were trained in the form of a 4 h session called “teaching to teach” in preparation for teaching during their internship. The course evaluations indicated that students highly supported the program (overall ratings 2000–2005: mean = 4.4 [scale 1–5], $n = 224$).^[11] Zijdenbos *et al.* in 2011 did a 1-week basic teacher training program as a part of a course called block supervised training in attitude research and teaching for the final year of internship, which was scored on a 5-point Likert scale and the mean score was found to be more than 3.0 which lead to the conclusion that the training provided raised interest among teachers and students.^[12] On comparing this to our study, the major difference is that we have initiated a near-peer teaching approach for our students at a much earlier stage in their medical career, in preparation for future teaching experiences. Although, we recognize that this program was of a short duration, this would establish

Table 1: Feedback response mean scores indicating the mean agreeability of the students for the questions given

Feedback questions	Q1	Q2	Q3	Q4	Q5	Q6	Q7	Q8	Q9	Q10	Q11
Valid responses (<i>n</i>)	88	88	88	88	88	87	87	88	88	87	88
Mean±SD	1.39±0.535	1.51±1.093	1.48±0.625	1.35±0.885	1.34±0.676	2.39±1.573	1.31±0.687	1.43±0.603	1.78±1.208	1.17±0.892	1.26±0.557

SD: Standard deviation

a foundation for all future endeavors to enable more teaching opportunities for our students.

Community sensitization

Community outreach has been an important aspect of medical education and needs to be initiated as early as possible. The importance of providing anatomical teaching to high school students has been reported in the literature.^[2] This exhibition which is conducted once in every alternate year caters to the needs of the biology students in our area which benefits not only our students but it also helps in kindling the interest of biology students toward human anatomy by live demonstration of both wet specimens and plastinates. Keeping the exhibition locally relevant, we have been able to maintain a great relationship with the surrounding community and have an immense community support in maintaining our department resources. The idea of medical students being involved in teaching was to expose them to the surrounding community in a nonthreatening way, where they can communicate and interact freely. There is much emphasis on the need for social consciousness among medical students and to develop into better doctors for the future, they need to be aware of their surrounding community and their culture. There have been no such similar reports in the literature as this was a unique initiative by our department. In our study, the students appreciated the fact that they got an opportunity to interact with students and teachers from the local community (90.9%) and also realized a need for outreach in the field of education as well. There was a statistically significant positive correlation ($P = 0.005$) between students who enjoyed the experience and those who were able to appreciate the need for community outreach. We also hope that through this experience, we can cultivate an idea of sharing of knowledge among our students.

Communication skills

Over the past decade, communication skills have been extensively incorporated in the medical curriculum globally and now form an important component of medical education. However, sensitization to the need for developing communication skills is not addressed in the medical curriculum and we need to realize that it may not occur automatically to students that there is a need for growth in this area unless challenged with targeted experiences and environments. For a 1st-year medical student, it is important to be aware of this need to work on developing this skill in his future years. In a study done by Moral *et al.* using 120 1st-year and 110 final-year students using a Communication Skill Attitude Scale, it was shown the 4th-year students were less enthusiastic about communication skills training than 1st year, indicating the importance of inculcating communication skills training at an earlier stage like in 1st year.^[13] In a study done by Joekes *et al.* to investigate whether the introduction of professional

Table 2: Correlation and statistical significance between the individual feedback questions

Questions	Correlation coefficient	P
Q1 and Q2	0.241	0.019*
Q3	0.233	0.023*
Q4	0.034	0.752
Q5	0.274	0.005*
Q6	-0.073	0.467
Q7	0.086	0.461
Q8	0.286	0.005*
Q9	-0.197	0.026*
Q10	0.063	0.559
Q11	0.148	0.177
Q2 and Q3	0.131	0.196
Q4	0.168	0.081
Q5	0.143	0.160
Q6	0.015	0.866
Q7	0.114	0.239
Q8	0.231	0.016*
Q9	-0.140	0.051*
Q10	-0.033	0.685
Q11	0.058	0.526
Q3 and Q4	0.129	0.202
Q5	0.293	0.002*
Q6	-0.152	0.114
Q7	0.103	0.288
Q8	0.166	0.099
Q9	-0.074	0.378
Q10	-0.026	0.801
Q11	0.016	0.873
Q4 and Q5	0.147	0.205
Q6	0.008	0.924
Q7	-0.008	0.939
Q8	0.087	0.422
Q9	-0.020	0.817
Q10	0.044	0.640
Q11	-0.024	0.807
Q5 and Q6	-0.020	0.831
Q7	0.062	0.585
Q8	0.277	0.009*
Q9	-0.048	0.597
Q10	0.067	0.529
Q11	0.227	0.046*
Q6 and Q7	-0.073	0.409
Q8	-0.181	0.030*
Q9	0.050	0.560
Q10	-0.085	0.373
Q11	-0.038	0.686
Q7 and Q8	0.023	0.842
Q9	-0.071	0.448
Q10	0.231	0.027*
Q11	0.219	0.062
Q8 and Q9	-0.034	0.725
Q10	0.107	0.296
Q11	0.134	0.232

Contd...

Table 2: Contd...

Questions	Correlation coefficient	P
Q9 and Q10	0.020	0.823
Q11	-0.012	0.897
Q10 and Q11	0.263	0.026*

*Significant

Table 3: Some examples of students' comments

Positive	Negative
“It was a good experience. It should be held more often” (S7)	“Some contents were given in so much depth that was a lot for 11 th graders” (S31)
“A nice, new experience” (S57)	“We were not able to communicate well due to language barrier” (S18)

development teaching in the first 2 years of a medical course improved students' observed communication skills with simulated patients ($n = 82$). Thirty-five students were given traditional preclinical curriculum and 47 students were given training in a curriculum with communication skills integrated into a “professional development” vertical module. Videod consultations were rated using the Evans interview rating scale by communication skills tutor. Results showed that students who received training scored higher ratings when compared to students who received traditional curriculum.^[14] In a study done by Taveira-Gomes *et al.*, 255 undergraduate medical students, at the Faculty of Medicine, University of Porto, completed a 1.5 h per week course over 4 months on basic communication skills. The students' final evaluation consisted of an interview with a simulated patient assessed by a teacher using a standardized framework. After 3 years, while attending internship, 68 students from the same group completed a reevaluation interview following the same procedure, which showed that medical students maintained a communication skill mean level similar to that of the original posttraining evaluation, but significant differences in specific communication abilities were detected in this group of students.^[15]

In the studies cited above, it showed that inculcating communication skills in the early years of MBBS significantly improved the communication skills of MBBS students and helped them in becoming better communicators and also helped in their attitude toward patients. In our study, students realized the need for good communication skills as a large proportion of our 1st-year medical students (61.4%) had language issues and had difficulty in communication, language barriers significantly hampering their communication abilities ($P = 0.051$). This language issue, which has been listed as some of the negative comments in the data, is since most of our students are from different parts of the country and have different mother tongues. The local language is not known to many, who are required to learn the language in the

coming years to be able to talk to the local patients in their clinical years. Highlighting that almost two-thirds of our students face this issue, there is a need for organized language teaching to help these students, which has now been included in their foundation course as a mandatory session. There was a significant positive correlation ($P = 0.019$) between the students who enjoyed the experience of teaching the school students and their ability to communicate easily with them, indicating that good communication skills help the students benefit from such experiences. We believe that it is important to create a sensitization toward the need for honing of communication skills among the students early in their training, to maximize on the communication training opportunities that they might receive in their future years, and to improve their learning during clinical years.

Conclusion

Training a medical professional is challenging and requires multiple avenues for developing these traits. A review analysis of 10 interventional studies showed that medical students had positive responses and attitudes toward new teaching methods and that new teaching strategies in medical education could positively impact learning.^[16]

Developing the interest of 1st-year medical students in teaching, sensitizing them to the need for improved communication skills, and improving social consciousness among them can be achieved by enabling them to act as “near-peer” teachers in high-school teaching programs.

In training future doctors, the added demands of the profession have to be kept in mind and avenues for growth must be provided as early as the 1st year of medical training. There is also an urgent need for innovations in medical education and the development of multiple learning opportunities in light of the new competency-based curriculum rollout in India. We believe that educational innovations can be contextual, and there should be emphasis on using the already established structure of our systems and available resources in designing such innovations rather than mimicking the ideas of a different setup elsewhere in the world.

Acknowledgments

The authors would like to thank the MBBS batch of 2018 students for their active participation in the study, the teaching and nonteaching faculty of the department of anatomy for their help in conducting the exhibition and the study, Mrs. Mahasampath Gowri for help in statistical analysis and the Institutional Review Board, Christian Medical College, Vellore, India, for ethical clearance.

Financial support and sponsorship

Nil.

Conflicts of interest

There are no conflicts of interest.

References

1. Supe A. Graduate Medical Education Regulations 2019: Competency-driven contextual curriculum. *Natl Med J India* 2019;32:257-61.
2. Shah N, Desai C, Jorwekar G, Badyal D, Singh T. Competency-based medical education: An overview and application in pharmacology. *Indian J Pharmacol* 2016;48:S5-9.
3. Koshi R, Indirani K. Clinical anatomy for high school students. *Clin Anat* 2006;19:82-3.
4. Raina SK, Kumar R, Kumar D, Chauhan R, Raina S, Chander V, *et al.* Game change in Indian Health Care System through reforms in medical education curriculum focusing on primary care – Recommendations of a joint working group. *J Family Med Prim Care* 2018;7:489-94.
5. Attitudes, Ethics and Communication Competencies for Indian Medical Graduate; 2020. Available from: https://www.nmc.org.in/wp-content/uploads/2020/01/AETCOM_book.pdf. [Last accessed on 2021 Mar 27].
6. Dandavino M, Snell L, Wiseman J. Why medical students should learn how to teach. *Med Teach* 2007;29:558-65.
7. Bing-You RG, Sproul MS. Medical students’ perceptions of themselves and residents as teachers. *Med Teach* 1992;14:133-8.
8. Fiorella L, Mayer RE. The relative benefits of learning by teaching and teaching expectancy. *Contemp Educ Psychol* 2013;38:281-8.
9. Peets AD, Coderre S, Wright B, Jenkins D, Burak K, Leskosky S, *et al.* Involvement in teaching improves learning in medical students: A randomized cross-over study. *BMC Med Educ* 2009;9:55.
10. Andrew Jay E, Starkman SJ, Pawlina W, Lachman N. Developing medical students as teachers: An anatomy-based student-as-teacher program with emphasis on core teaching competencies. *Anat Sci Educ* 2013;6:385-92.
11. Haber RJ, Bardach NS, Vedanthan R, Gillum LA, Haber LA, Dhaliwal GS. Preparing fourth-year medical students to teach during internship. *J Gen Intern Med* 2006;21:518-20.
12. Zijdenbos I, Fick T, ten Cate O. How we offer all medical students training in basic teaching skills. *Med Teach* 2011;33:24-6.
13. Moral RR, García de Leonardo C, Caballero Martínez F, Monge Martín D. Medical students’ attitudes toward communication skills learning: Comparison between two groups with and without training. *Adv Med Educ Pract* 2019;10:55-61.
14. Joekes K, Noble LM, Kubacki AM, Potts HW, Lloyd M. Does the inclusion of ‘professional development’ teaching improve medical students’ communication skills? *BMC Med Educ* 2011;11:41.
15. Taveira-Gomes I, Mota-Cardoso R, Figueiredo-Braga M. Communication skills in medical students – An exploratory study before and after clerkships. *Porto Biomed J* 2016;1:173-80.
16. Ahmady S, Khajeali N, Sharifi F, Mirmoghtadaei Z. Educational intervention to improve preclinical academic performance: A systematic review. *J Educ Health Promot* 2019;8:83.

The Persistent Median Artery: A New Challenger in Carpal Tunnel Imaging?

Abstract

Introduction: The aim of the study was to determine the incidence of the persistent median artery (PMA) at the wrist level, its correlation to age, gender, and contralateral wrist, and its position to the median nerve and its variations. **Material and Methods:** A total of 1504 wrists were evaluated using the magnetic resonance imaging examination. The proton density and T2-weighted axial images were investigated. The patients were divided into three groups according to age. The incidence of PMA, gender, and relationship with the contralateral wrist, distribution according to the age groups, and position to the median nerve were recorded. The images were first evaluated on the consensus of two radiologists and then all data were inspected by another radiologist with at least 10 years of experience in musculoskeletal radiology. **Results:** Palmar-type PMA was observed in 379 of 1504 included wrists (25.1%). The evaluation according to the age groups showed that the incidence of PMA decreased with increasing age. The median nerve variations concomitant to PMA (bifid-trifid) was found to be seen in 94 patients. In 61 of these 94 patients (64.8%), PMA was passing through the branches of the median nerve. It was observed that in 62.5% of the cases, PMA occupied an anteromedial position to the median nerve. **Discussion and Conclusion:** PMA accompanied by median nerve variations is frequently seen. The incidence of PMA decreases with increasing age. The presence of PMA and its position should be cautiously evaluated using imagery, particularly in young patients before wrist surgery.

Keywords: Anatomy, carpal tunnel, magnetic resonance imaging, median artery, median nerve

Introduction

During prenatal development, the median artery provides blood supply to the hand and forearm. Following the development of the radial and ulnar arteries, it usually regresses and disappears after birth.^[1] However, the median artery may persist during adulthood in some people, which is called the persistent median artery (PMA) and continues to supply the hand after birth.^[2] It has two subtypes: palmar, in which the PMA extends to the palm, and antebrachial, in which the PMA is shorter and ends in the forearm.^[3]

The carpal tunnel, which has a fibro-osseous structure, is formed by the flexor retinaculum (transverse carpal ligament) at the anterior side and by the carpal bones at the posterior side. Within the tunnel, nine flexor tendons and in anterior location, median nerve adjacent to flexor retinaculum is observed. Typically, no vascular

structures are located within the tunnel in the wrist in adults. However, the PMA may extend through the flexor retinaculum and the carpal tunnel adjacent to the median nerve. It may extend to the palm and form the superficial palmar arch together with the ulnar artery. The incidence of palmar PMA was between 0.6%^[4] and 26%^[5] in previous studies.

Aneurysms or thrombosis of the PMA may compress the median nerve and cause carpal tunnel syndrome. During surgical interventions, in this region or median nerve blockage, the superficially located PMA may be injured and ischemia may emerge in the perfused area.^[6] Therefore, the presence of PMA and its position to the median nerve is critical.

In this study with a large sample size, the objective was primarily to determine the incidence of PMA at the wrist level, its correlation to age, gender, contralateral wrist, and secondarily its position to the median nerve, and its variations.

This is an open access journal, and articles are distributed under the terms of the Creative Commons Attribution-NonCommercial-ShareAlike 4.0 License, which allows others to remix, tweak, and build upon the work non-commercially, as long as appropriate credit is given and the new creations are licensed under the identical terms.

For reprints contact: WKHLRPMedknow_reprints@wolterskluwer.com

How to cite this article: Gürkan O, Çengel F, Erdem U, Yılmaz A, Polat A, Ekin EE. The persistent median artery: A new challenger in carpal tunnel imaging? J Anat Soc India 2022;71:109-13.

Okan Gürkan,
Ferhat Çengel,
Umut Erdem,
Ayhan Yılmaz,
Abdulkadir Polat¹,
Elif Evrim Ekin

Departments of Radiology,
¹Orthopedics and Traumatology,
Gaziosmanpaşa Training and
Research Hospital, Istanbul,
Turkey

Article Info

Received: 28 June 2021
Revised: 01 February 2022
Accepted: 25 March 2022
Available online: 30 June 2022

Address for correspondence:

Dr. Okan Gürkan,
Gaziosmanpaşa Training and
Research Hospital, Karayolları
Mahallesi, Osmanbey Cd. 621
Sokak, 34255 Gaziosmanpaşa,
Istanbul, Turkey.
E-mail: drokan@gmail.com

Access this article online

Website: www.jasi.org.in

DOI:
10.4103/jasi.jasi_114_21

Quick Response Code:



Material and Methods

In this retrospective study following the approval of the ethics committee, magnetic resonance images (MRI) of 1578 wrists, which had been obtained for various reasons between 2015 and 2020, were evaluated. Patient age and gender, the evaluated wrist, the presence/absence of a PMA at the wrist level, the PMA's position to the median nerve, the type of median nerve, and its variations, if present, were recorded.

Among 1578 wrists, 74 patients were excluded from the study. Cases were excluded based on several criteria: (1) Poorly defined or low-quality images (without proton density [PD] and T2-weighted images); (b) insufficient clinical information (the reason of magnetic resonance [MR] examination was not recorded, the absence of information about age, gender, and other information); and (c) history of wrist surgery. The study was conducted with 1504 sequential patients.

All images were obtained using a 1.5 Tesla MR device (Signa HDxt; GE, USA). All patients were placed in the prone and arm-overhead position. The wrist was positioned in a dedicated wrist coil, so it was located at the isocenter of the magnet. The PMA was assessed on the T2 and PD axial images obtained at the level of the carpal tunnel. Slice thickness was 3 mm.

The diagnostic criteria for PMA are described by Pierre-Jerome *et al.*^[7] as a well-defined circular-shaped artery that is adjacent to the median nerve, reflecting a higher signal intensity than the median nerve and presenting a linear flow void artifact. The median nerve was evaluated as one branch or bifid and trifid variations in the carpal tunnel. The position of the PMA to the median nerve (anterior, posterior, anterolateral, and anteromedial passing through the median nerve) was recorded.

The incidence of the PMA was evaluated according to gender, hand side (left-right), and age. The patients were divided into three groups according to age: (1) Group I (4–30 years), (2) Group II (31–55 years), and (3) Group III (56–86 years).

The images were evaluated by two radiologists and if a consensus was not reached, consultation with a third radiologist with 10 years of experience in musculoskeletal radiology was provided. The participating physicians were blind to the clinical information, gender, age, and hand side of patients during the evaluation of the images.

The present study was approved by the ethics committee of Gaziosmanpaşa Training and Research Hospital. Data were analyzed with the SPSS software package (Version 23.0, Chicago, Illinois, USA). The accepted limit of statistical significance was $P < 0.05$ at a 95% confidence interval. Continuous variables were assessed using the Student's *t*-test, and the categorical variables were assessed by the Chi-square test.

Results

Wrist MRI of 1504 patients (age between 4 and 86 years) was evaluated.

The patients were divided into three groups according to age. Groups I, II, and III consisted of 649, 712, and 143 patients, respectively. The demographic distribution of patients according to age is summarized in Table 1.

Within the carpal tunnel, the PMA was observed in 184 of 540 male patients (34.1%) and 195 of 964 female patients (20.2%) [Figure 1]. The incidence of PMA was significantly higher among males ($P < 0.001$).

Among 1504 patients, 725 of the images were of the left wrist and 779 were of the right wrist. The incidence of the PMA within the carpal tunnel was 22.9% for the left wrists and 27.3% for the right wrists. The difference was statistically significant ($P < 0.05$).

The presence of the PMA was also evaluated according to age. The incidence of the PMA within the carpal tunnel was 27.9% ($n = 181$) in Group I; 24.2% in Group II ($n = 172$), and 18.2% in Group III ($n = 26$). The differences between the groups were statistically significant ($P < 0.05$).

During the evaluation of the median nerve variations within the carpal tunnel, the bifid median nerve (BMN) was observed in 150 patients (9.9%) and three median nerve branches in one patient [Figure 2]. No statistically significant differences between the patients regarding age, hand side (left-right), and gender were found.

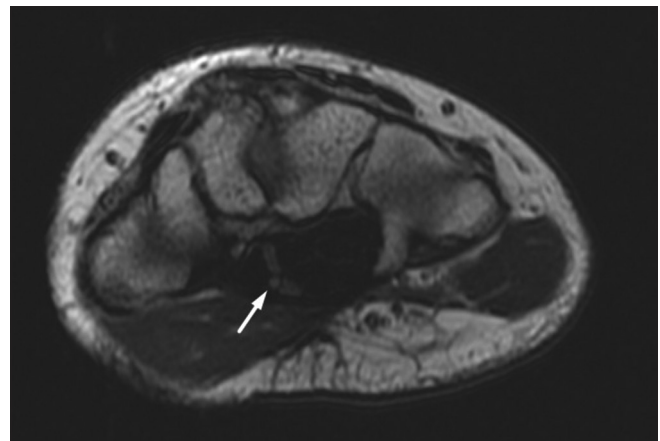


Figure 1: T2-weighted axial image displays persistent median artery (arrow) in carpal tunnel

Table 1: Demographics of the patient population

Groups	Age (years), mean	Gender (male/female)	Wrist (left/right)	Total patients
I	4-30 (22.53)	254/395	291/358	649
II	31-55 (40.58)	245/467	359/353	712
III	56-86 (62.52)	41/102	75/68	143
Total	4-86	540/964	725/779	1504

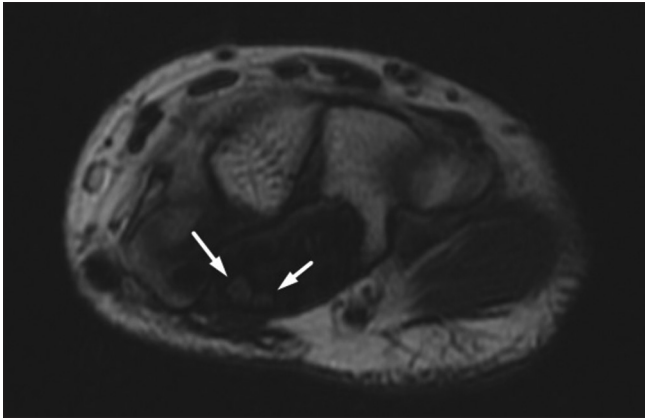


Figure 2: T2-weighted axial image shows the variation of median nerve with two nerves (arrows) in the carpal tunnel (bifid median nerve)

Ninety-four patients had PMA concomitant with BMN, and this occurrence was found to be statistically significant ($P < 0.001$). The prevalence of PMA and median nerve variations based on age groups, gender, and location are shown in Table 2

The position of the PMA to the median nerve was also evaluated. Of 379 patients with PMA in the carpal tunnel, the PMA was positioned at the anterolateral side of the median nerve (10.55%) in 40 patients, on the anterior side in 39 patients (10.29%), on the anteromedial side in 237 patients (62.5%), and on the posterior side in one patient (0.2%). In 61 patients, the PMA passed through the median nerve branches [Figure 3 and Table 3].

Discussion

Palmar-type PMA was observed in 379 wrists of the evaluated 1504 samples (25.1%). In previous studies, the reported incidence of palmar-type PMA was between 0.6% and 26%.^[4,5] The main difference among the reported results might depend on the number of evaluated wrists, bilaterality/unilaterality, use of different measurement techniques, and racial characteristics. Regarding the literature, most of the studies were conducted using ultrasonography and cadaver dissections. Particularly in ultrasonography, the evaluator's experience, patient compliance, and even probe compression differences may have led to conflicting results. Considering the cadaver studies, the limited number of samples may have affected the universality of the results. Both bilateral and unilateral wrists have been examined in the literature. Henneberg *et al.*^[8] determined that bilateral PMA was more common than unilateral PMA.

Recently, research similar to the present study, which has focused on the evaluation of PMA and the median nerve at the wrist level with MRI, has been published.^[7,9] The evaluation of MRI may provide different results depending on image quality, section thickness, and other factors. However, MR examination has certain advantages such as

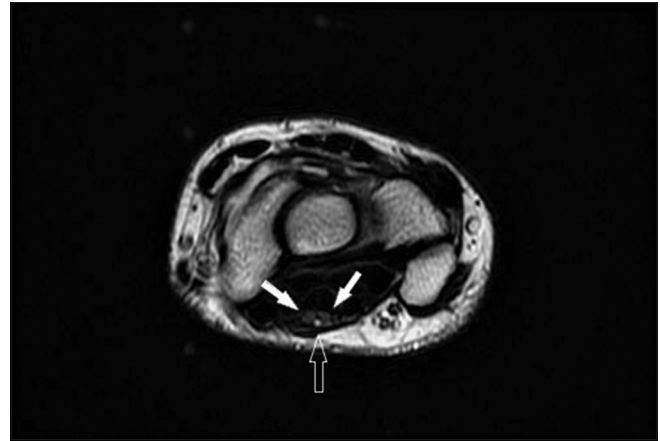


Figure 3: T2-weighted axial image represent a persistent median artery (open arrow) pierces through bifid median nerve (arrows)

noninvasive implementation, suitability for retrospective studies, and the evaluation of large sample sizes.

The evaluation of age groups showed a statistically significant difference between age and PMA incidence. This finding may depend on the regression of the artery or the inability to observe the artery due to calcification on the PMA that is found with increasing age or thrombosis. The findings of the present study are consistent with some studies in the literature. In a study conducted by Carry *et al.*^[10] in the pediatric population, it was found that the odds of a PMA decreased by 4.4% for every 1 year increase in age. Lucas *et al.*^[11] conducted a study on cadavers and reported that PMA incidence decreased with an increase in age. As the incidence of PMA has increased three-fold in the past 125 years, Lucas *et al.* suggested that the PMA may no longer be regarded as a variation 80 years later and may be considered a normal anatomic structure in humans.

In the present study, the incidence of PMA was 22.9% ($n = 166$) in the left wrists and 27.3% ($n = 213$) in the right wrists, and the difference between the two was statistically significant. Regarding the literature, right dominance was reported in most of the studies, which is consistent with this study. However, the differences reported in these studies were not statistically significant. In cadaver studies, Isaac *et al.*^[12] evaluated 62 wrists and found that the incidences of PMA in the right and left wrists were 12.9% and 6.5%, respectively, while the same incidences were 12% and 12.5% in a study conducted by Rodríguez-Niedenführ *et al.*,^[2] who evaluated 120 wrists. Carry *et al.*^[10] evaluated 270 wrists using ultrasonography in the pediatric population and detected PMA in 17% and 29.7% of the left and right wrists, respectively. In a study by Dag *et al.*,^[9] 300 wrists were evaluated with MR examination and it was found that the incidence of PMA was 10.5% and 14.6% in the left and right wrists, respectively.

Aragão *et al.*^[13] conducted a fetal dissection study on 32 wrists and found a higher PMA incidence in

Table 2: Prevalence of persistent median artery and median nerve variations based on age groups, gender, and location

	Group I (n=649), n (%)	Group II (n=712), n (%)	Group III (n=143), n (%)	Gender (male) (n=540), n (%)	Gender (female) (n=964), n (%)	Location (left hand) (n=725), n (%)	Location (right hand) (n=779), n (%)
PMA	181 (27.9)	172 (24.2)	26 (18.2)	184 (34.1)	195 (20.2)	166 (22.9)	213 (27.3)
Median nerve variations	67 (10.3)	69 (9.7)	14 (9.8)	60 (11.1)	90 (9.3)	64 (8.8)	86 (11)

PMA: Persistent median artery

Table 3: Position of persistent median artery based on gender and location

PMA position	Gender		Location	
	Male, n (%)	Female, n (%)	Right, n (%)	Left, n (%)
Anterolateral (n=40)	25 (62.5)	15 (37.5)	24 (60)	16 (40)
Anterior (n=39)	13 (33.3)	26 (66.7)	26 (66.7)	13 (33.3)
Anteromedial (n=237)	125 (52.7)	112 (47.3)	128 (54)	109 (46)
Posterior (n=1)	0	1 (100)	1 (100)	0
Between the median nerve (pierce) (n=61)	32 (52.5)	61 (47.5)	34 (55.7)	27 (44.3)

PMA: Persistent median artery

females. However, Pierre-Jerome *et al.*^[7] did not find a statistically significant difference between genders in MRI examinations of the wrists. In the present study, which had a considerably larger sample size, palmar PMA was observed in 195 females (20.2%) and 184 males (34.1%). The difference was statistically significant ($P < 0.001$).

In the present study, the position of the PMA in relation to the median nerve within the carpal tunnel was examined. The most frequent (62.5%) location of PMA was the anteromedial position of the median nerve. Furthermore, 10.55% and 10.29% of examined wrists had anterolateral and anterior positions, respectively. In 16% of the cases, the PMA passed through the median nerve branches. Haładaj *et al.*^[6] investigated 125 wrists and detected the PMA in only five patients. In their study, the PMA had anterolateral ($n = 2$), anterior ($n = 2$), and anteromedial positions ($n = 1$). The position of the PMA to the median nerve is particularly important with respect to performing carpal tunnel surgery and administering peripheral nerve blocks. In cases with a history of trauma of this region, the presence of a PMA should be cautiously examined in respect of the perfusion of the hand. In recent years, a considerable part of the cardiac, cerebral, and peripheral angiographic interventions have been performed through the radial artery. Before the intervention, the ulnar collateral flow of the arterial blood supply in the hand is evaluated using the Allen's test or the modified Allen's test.^[14] The possible presence of the median artery should be kept in mind during these interventions.

The PMA might be accompanied by median nerve variations, mostly bifid and trifid median nerve variations.^[15] In the present study, median nerve variations

in 151 patients (9.96%) were observed. One-hundred and fifty of them had bifid while only one patient had trifid median nerve variations. In 94 patients, the PMA was accompanied with BMN (6.25%), a finding that was found to be statistically significant. In 61 of these 94 wrists (64.8%), the PMA passed through the branches of the median nerve.

As this study had a retrospective design, bilateral variations could not be determined, which is considered one of the study limitations. Another limitation was the investigation of the PMA only at the wrist level. On the other hand, since this study has the largest sample size so far within the literature and includes a detailed description of the PMA with variations of the median nerve neighborhood, it is believed that it will be an important contribution to the literature.

Conclusion

The PMA is more common among young people and its incidence decreases as age increases. The PMA is more common in males and in the right wrist. It is located commonly at the anteromedial, anterolateral, and anterior sides of the median nerve. In patients with PMA, the incidence of median nerve variations is relatively higher. To avoid complications during wrist surgery, the presence and position of the PMA should be evaluated with imaging methods before performing any interventions, especially in young patients.

Financial support and sponsorship

Nil.

Conflicts of interest

There are no conflicts of interest.

References

1. Jones NF, Ming NL. Persistent median artery as a cause of pronator syndrome. *J Hand Surg Am* 1988;13:728-32.
2. Rodríguez-Niedenführ M, Sañudo JR, Vázquez T, Nearn L, Logan B, Parkin I. Median artery revisited. *J Anat* 1999;195:57-63.
3. Eid N, Ito Y, Shibata MA, Otsuki Y. Persistent median artery: Cadaveric study and review of the literature. *Clin Anat* 2011;24:627-33.
4. Ahn DS, Yoon ES, Koo SH, Park SH. A prospective study of the anatomic variations of the median nerve in the carpal tunnel in Asians. *Ann Plast Surg* 2000;44:282-7.

5. Gassner EM, Schocke M, Peer S, Schwabegger A, Jaschke W, Bodner G. Persistent median artery in the carpal tunnel: Color Doppler ultrasonographic findings. *J Ultrasound Med* 2002;21:455-61.
6. Haładaj R, Wyśiadecki G, Dudkiewicz Z, Polguj M, Topol M. Persistent median artery as an unusual finding in the carpal tunnel: Its contribution to the blood supply of the hand and clinical significance. *Med Sci Monit* 2019;25:32-9.
7. Pierre-Jerome C, Smitson RD Jr., Shah RK, Moncayo V, Abdelnoor M, Terk MR. MRI of the median nerve and median artery in the carpal tunnel: Prevalence of their anatomical variations and clinical significance. *Surg Radiol Anat* 2010;32:315-22.
8. George BJ, Henneberg M. High frequency of the median artery of the forearm in South African newborns and infants. *S Afr Med J* 1996;86:175-6.
9. Dag F, Dirim Mete B, Gursoy M, Uluc ME. Variations ignored in routine wrist MRI reports: Prevalence of the median nerve anatomical variations and persistent median artery. *Acta Radiol* 2022;63:76-83.
10. Carry PM, Nguyen AK, Merritt GR, Ciarallo C, Chatterjee D, Park J, *et al.* Prevalence of persistent median arteries in the pediatric population on ultrasonography. *J Ultrasound Med* 2018;37:2235-42.
11. Lucas T, Kumaratilake J, Henneberg M. Recently increased prevalence of the human median artery of the forearm: A microevolutionary change. *J Anat* 2020;237:623-31.
12. Cheruiyot I, Bundi B, Munguti J, Olabu B, Brian Ngure JO. Prevalence and anatomical pattern of the median artery among adult black Kenyans. *Anat J Afr* 2017;6:1015-23.
13. Aragão JA, da Silva AC, Anunciação CB, Reis FP. Median artery of the forearm in human fetuses in northeastern Brazil: Anatomical study and review of the literature. *Anat Sci Int* 2017;92:107-11.
14. Dietl CA, Benoit CH. Radial artery graft for coronary revascularization: Technical considerations. *Ann Thorac Surg* 1995;60:102-9.
15. Bayrak IK, Bayrak AO, Kale M, Turker H, Diren B. Bifid median nerve in patients with carpal tunnel syndrome. *J Ultrasound Med* 2008;27:1129-36.

Analysis of Workstation Posture in Diversified Professionals as a Tool to Enhance Better Understanding of Health Outcomes to Avoid Occupational Health Hazards

Abstract

Introduction: Wrong postures change the body mechanics, causing pressure on joint surfaces, strain to ligaments, and skeletal muscle disadvantage. Simple faulty posture is one of the main reasons for musculoskeletal pain, especially back pain and neck pain. Based on the understanding that aberrations in posture can cause pain and injury, training and education for posture correction through training have been used as treatment approaches. The intent of the present study was to analyze posture and the severity of postural abnormalities using plumb line and to identify if these abnormalities are associated with pain among professionals. **Material and Methods:** The posture of 120 participants from four occupational groups was analyzed using a plumb line in relation to anatomical landmark and categorized into four types. Data were recorded as the frequency of the posture types. To test the equality of means among more than two groups, the Kruskal–Wallis test was used. Posture frequency was then compared with musculoskeletal symptoms. **Results:** The major finding in this study is that a considerable proportion of the study sample displayed some degree of postural anomaly. Kyphosis was found to be highest among IT professionals (76.7%) compared to the other professional groups. Kypholordotic posture was more among the nurses. The frequency of pain increased in participants with more severe postural issues. It is hypothesized that the means of different groups compared are the same against the alternative that at least one group's mean is different from others. The difference observed difference was statistically significant ($P < 0.001$). **Discussion and Conclusion:** Postural abnormalities are a significant risk factor for musculoskeletal disorders. The ergonomics of the working environment have a direct impact on the well-being of professionals. Hence, the organizations employing them, and the professionals themselves need to be sensitized regarding the importance of correct working posture.

Keywords: *Kypholordosis, kyphosis, musculoskeletal symptoms, plumb line, posture*

Introduction

The word posture comes from the Latin verb “ponere,” which means “to put or place.”^[1] Posture refers to the position of the human body and its orientation in space. Posture is defined as a state of skeletal and muscular balance and alignment that protects the supporting structures of the body from progressive deformity and injury.^[2] In an ideal posture, the weight of the body is evenly distributed through the body so all joints are in their neutral zone and there will be minimal wear and tear on the structures. This will help maintain the natural balance and correct the length of the muscles. There is no restriction on the movement patterns and all vital organs are properly placed, and therefore can

function efficiently. The line of gravity passes through a point on a level with and immediately in front of the second sacral vertebra (the center of gravity).^[3]

Wrong postures change the body mechanics, causing pressure on joint surfaces, strain to ligaments, and skeletal muscle disadvantage. Soft tissue shortening associated with this may cause back pain. Another added problem is chronic pain, and that can worsen mood and decrease motivation. Stiffness and pain in the spine and ribs may hinder ventilation, and poor posture with low body weight may result in poor body image and diminished self-confidence. We wonder why it is so important to maintain correct posture. The answer is simple faulty posture is one of the main reasons for musculoskeletal pain, especially back pain

This is an open access journal, and articles are distributed under the terms of the Creative Commons Attribution-NonCommercial-ShareAlike 4.0 License, which allows others to remix, tweak, and build upon the work non-commercially, as long as appropriate credit is given and the new creations are licensed under the identical terms.

For reprints contact: WKHLRPMedknow_reprints@wolterskluwer.com

How to cite this article: Johnson WM, Koshy JM, Rajasundram A. Analysis of workstation posture in diversified professionals as a tool to enhance better understanding of health outcomes to avoid occupational health hazards. *J Anat Soc India* 2022;71:114-8.

**W M S Johnson,
Jinu Merlin Koshy,
Archana
Rajasundram**

*Departments of Anatomy, Sree
Balaji Medical College and
Hospital, (BIHER), Chennai,
Tamil Nadu, India*

Article Info

Received: 09 April 2020
Revised: 08 September 2021
Accepted: 18 April 2022
Available online: 30 June 2022

Address for correspondence:

*Dr. Jinu Merlin Koshy,
Department of Anatomy, Sree
Balaji Medical College and
Hospital, 7, Works Road,
Chromepet, Chennai - 600 044,
Tamil Nadu, India.
E-mail: jinumerlinkoshy@gmail.
com*

Access this article online

Website: www.jasi.org.in

DOI:
10.4103/JASI.JASI_60_20

Quick Response Code:



and neck pain. Based on the understanding that aberrations in posture can cause pain and injury, training and education for posture correction through training have been used as treatment approaches.^[4-11]

While there are many studies that have documented a high incidence of postural anomalies in a given population, the methods of measurement were not defined accurately.^[9-14]

The resting position and the lumbar spine are having a strong correlation. Kendall *et al.*^[6] explained the optimal posture using the plumb line assessment.

The spine has three natural curvatures, which can become exaggerated in one direction or the other.^[6-16] Four posture types are commonly seen in Figure 1; A is the optimal or neutral posture and exaggerated postures are B, C, and D.

Optimal posture

This posture has a vertical line passing through the midline of the knee, lumbar vertebrae, shoulder joint, cervical vertebrae, and earlobe.

Kypholordotic posture

An increased thoracic and lordotic curvature can be observed in this posture. The head is held slightly forward, often becoming the most anterior segment of the body. The pelvis tends to tilt anteriorly with an increase in lumbar lordosis (inward curve).

Swayback posture

In this posture, the pelvis becomes the most anterior segment of the body, and there is an increase in the inward curve. The knee joints tend to get hyperextended. Abdominal obesity worsens this posture.

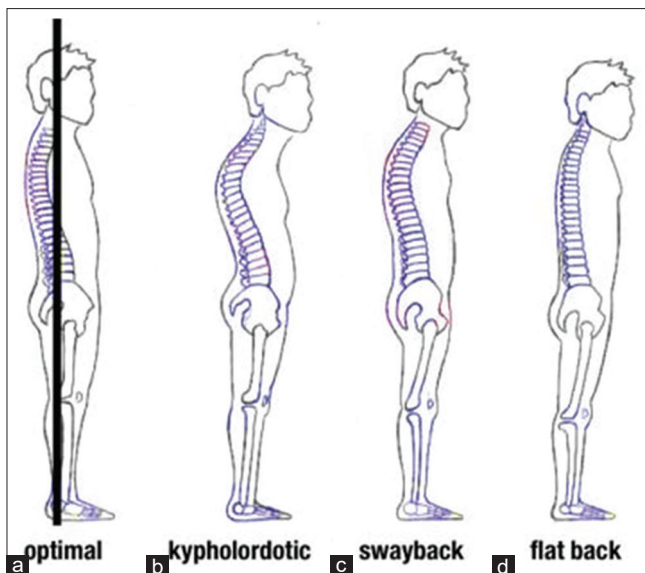


Figure 1: Comparison of common posture types. a)Optimal, b)Kypholordotic c)Swayback d) Flat back

Flat-back posture

A posterior tilt is observed in the pelvis with very little normal inward curvature of the lumbar spine. The knee joints are hyperextended. Sometimes the head is tilted slightly forward. The thoracic spine may be flexed forward a bit.

This study was designed to assess the severity of postural abnormalities among professionals and to determine whether these abnormalities are associated with pain.

Aim and objective

The aim of the present study was to analyze posture and the severity of postural abnormalities using a plumb line and to identify if these abnormalities are associated with pain among professionals.

Material and Methods

The study was designed to assess the posture using plumb line. The screenings were conducted in four occupational groups: the banking sector (Group 1), computer professionals (Group 2), dentists (Group 3), and nurses (Group 4). Thirty people from each group participated in the study.

The proposal was submitted to the institutional ethics committee and due clearance was obtained from the same.

Inclusion criteria:

Inclusion criteria was not based on presence or absence of pain. The participants were asked about the presence or absence of pain and noted it. They were also assessed using Nordic Questionnaire too.

- Bank employees, IT professionals, nurses, and dentists with a minimum of 3 years of work experience and a maximum of 25 years
- Age ranging from 25 to 55 years
- Both sexes.

Exclusion criteria:

- Individuals with any acute ailments or systemic diseases
- Pregnant women
- Those who were not willing.

Informed written consent was obtained from each of the participants.

Armamentarium:

- Weighing scale
- Freemans measuring tape
- Tailor's tape
- Plumb line.

The participants who fulfill the inclusion criteria were included based on their willingness and not based on the presence or absence of musculoskeletal pain they were having. Anthropometric measurements were recorded.

Participants were positioned with their lateral malleolus 6 cm behind the plumb line. Participants were asked to take 10 steps leading with their right leg and then to stop and remain in the resulting postural position was noted then.

The plumb line position was noted in relation to anatomical landmark and posture was determined. The participant was viewed from 3 aspects:

1. Anterior–posterior (A–P): The plumb line runs through the center of the forehead, middle of the sternum, navel, and midpoint between feet
2. Posterior–anterior (P–A): The plumb line runs through the occipital protuberance, spinous processes C7, T12, L5, coccyx, and between the feet
3. Lateral: The plumb line runs through the acromion, midpoint of the iliac crest, greater trochanter, and in front of the ankle.

Data were entered into Microsoft Excel spreadsheets after thorough screening and analysis were carried out using IBM SPSS Software Version 16: IBM, Technology company American multinational technology corporation headquartered in (Armonk, NewYork, USA). Descriptive statistics such as mean with standard deviation and proportions were reported. Posture was categorized into the four types and data were recorded as the frequency of the posture types. To test the equality of means among more than two groups, Kruskal–Wallis test was being used. Posture frequency was then compared with musculoskeletal symptoms.

Results

Data collected from the 120 participants in the study group (53 males and 67 females) were analyzed. There were 30 participants in each group. The general characteristics of the study participants are given in Table 1.

Posture was categorized as one of the four standard types and frequency was recorded for both males and females among the four professional groups. Table 2 represents the posture frequency of the four professional groups. Combinations of posture types were also seen. The nurses who were having swayback posture with anterior pelvic shift were having thoracic kyphosis which is extended to the upper part of the lumbar spine. The three dentists, four nurses, and one IT employee who were having kyphotic postures were exhibiting kypholordosis also.

To test the equality of means among more than two groups, Kruskal–Wallis test was used. It is hypothesized that the means of different groups compared are the same against

the alternative that at least one group’s mean is different from others.

The observed difference was found to be statistically significant ($P < 0.001$). In Figure 2 Incidence of postural abnormalities in the Plumb line analysis of the four professional groups can be viewed.

Participants having optimal posture and deviated posture are given in Table 3. All the participants who were having Kyphotic or Kypholordotic posture experienced pain in their back or neck. The pain among the participants was directly proportional with the age of the. One participant who was having optimal posture experienced pain in the neck.

Discussion

The major finding in this study is that a substantial proportion of the study population exhibited some degree of postural abnormality. Kyphosis was found to be highest among IT Professionals (76.7%) compared to other professional groups. Kypholordotic posture was more among the nurses.

The incidence of pain increased in the participants with severe postural abnormalities in the present study which is contrary to the study which reported no relationship was found between the severity of postural abnormality and the severity and frequency of pain.^[15-17] The severity of postural anomalies would be greater in an older population as compared to a younger population.^[18] Habits of “falling into gravity” are proposed to aggravate with advancing age.

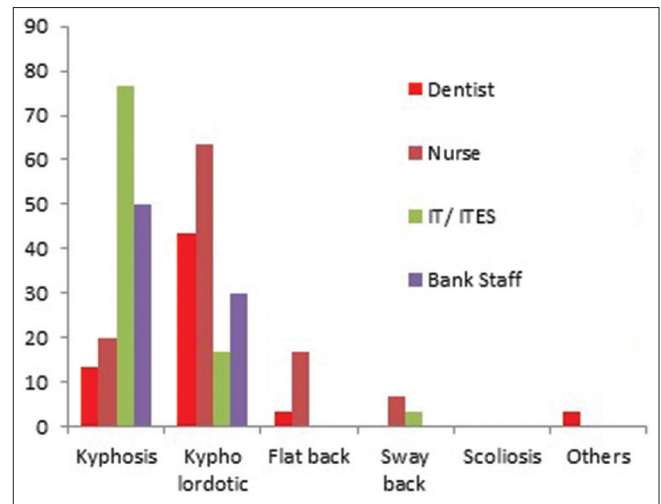


Figure 2: Incidence of postural abnormalities in plumb line analysis

Table 1: Physical characteristics of participants (mean±standard deviation)

???	Bank employees (Group 1)		IT professionals (Group 2)		Dentists (Group 3)		Nurses (Group 4)	
	Male (18)	Female (12)	Male (16)	Female (14)	Male (16)	Female (14)	Male (3)	Female (27)
Age	44±7.78	40±7.6	36±5.207	34±4.92	35±4.68	33±6.7	28±2.07	31±3.43
Height	164±3.38	151±5.2	172±8.201	159±5.13	168±6.76	160±4.6	164±6.09	154±4.73
Weight	84±4.44	60±6.76	79±7.67	58±7.69	75±5.37	65±8.17	72±3.19	58±6.24

Table 2: Association between the plumb line scores and the occupation groups

Characteristics	Dentist, n (%)	Nurses, n (%)	IT employee, n (%)	Bank employee, n (%)	χ^2	P
Kyphosis	4 (13.33)	6 (20)	23 (76.7)	5 (50)	31.2	0.0001
Kypholordotic	13 (43.3)	19 (63.3)	5 (16.7)	3 (30)	14.02	0.003
Flat back	1 (3.3)	5 (16.7)	0	0	8.89	0.031
Swayback	0	2 (6.7)	1 (3.3)	0	2.61	0.456
Scoliosis	1 (3.3)	0	0	0	0	1

Table 3 : Participants having optimal posture and deviated posture

Profession	Deviated posture	Optimal posture
Dentist	16	14
Nurses	26	4
IT employee	28	2
Bank employee	8	22

Swayback posture was found to be the predominant among the participants and the flat-back posture had the least occurrence in previous studies whereas the present study findings show that kypholordotic and kyphotic posture is more common in the study participants.^[16] This may be due to the difference in the age group in both studies, In the present study, the mean age of the study participants was 35 years and that of the previous one was adolescent participants. The participants in the present study were professionals and deviation from the standard working posture and extended working hours were also a reason for the musculoskeletal symptoms. Females were having less postural deviation compared to males, but the incidence of pain was more among females. Physiological factors contribute to the higher prevalence of musculoskeletal disorders (MSDs) in women. One of them is the presence of more type one fibers in the trapezius muscle in women than in men, and others include sexual dimorphism of the spine and the high incidence of dysmenorrhea, which sometimes is confounded with mechanical low back pain. Multitasking also accredited to the higher MSDs among women.^[19]

The most common risk factor for work-related musculoskeletal disorders (WMSDs) is bad posture which is a deviation from the ideal posture. Awkward, restrictive, uneven, repetitive, and prolonged postures; overstressing movements, and force can overload the tissues and exceed their threshold of tolerable stress, causing injury due to overexertion or imbalance.^[20] A person working in an or awkward posture will have to use more force to accomplish the same amount of work compared to using a neutral posture, which in turn affects muscle loading and compressive forces on the intervertebral disc.^[21]

In poor, or faulty posture there is a flawed relationship among various skeletal structures of the body, and this may produce strain on the body's supporting framework.^[21] With faulty posture, the body is balanced less efficiently over its base of support. The plumb line

analysis revealed that kyphosis was found to be highest among IT professionals (76.7%), compared to the other occupation groups. The observed difference was found to be statistically significant ($P < 0.001$).

An in-depth assessment of posture among IT employees was made due to their prolonged duration of work (mean working hours 8.6 h per day). An increased prevalence of abnormal positioning of the employees was observed which could potentially increase the risk of WMSD. The most common risk factor is sloppy posture which is a deviance from the ideal working posture of arms at the side of the torso, elbows bent, with the wrists straight and it typically includes reaching behind, twisting, working overhead, kneeling, forward or backward bending, and squatting. Awkward, restrictive, uneven, repetitive, and prolonged postures; overstressing movements and force can overload the tissues and exceed their threshold of tolerable stress, causing injury due to overexertion, or imbalance.^[20,22]

Conclusion

Postural abnormalities are a significant risk factor for MSD. Although all individuals are vulnerable in this regard, certain specific occupation groups are at increased risk of developing these postural problems, owing to the nature of their job and working environment. Our study was carried out to compare the prevalence of postural problems and MSD among select four occupations, namely dentists, nurses, IT professionals, and bank employees. In conformity with the research objectives, the following conclusions are derived: nearly three-fourths of the professionals we studied had mentioned having some health problems. The ergonomics of the working environment of the professionals have a direct impact on their level of well-being. Hence, the organizations employing them, as well as the professionals themselves need to be sensitized regarding the importance of correct working posture.

Financial support and sponsorship

Nil.

Conflicts of interest

There are no conflicts of interest.

References

1. Definition of Posture. Available from: <https://www.medicinenet.com/script/main/art.asp?articlekey=9731>. [Last accessed on 2020 Apr 06].

2. Britnell SJ, Cole JV, Isherwood L, Sran MM, Britnell N, Burgi S, *et al.* Postural health in women: The role of physiotherapy. *J Obstet Gynaecol Can* 2005;27:493-510.
3. Karhu O, Kansi P, Kuorinka I. Correcting working postures in industry: A practical method for analysis. *Appl Ergon* 1977;8:199-201.
4. Forrester-Brown MF. Posture as a factor in health and disease. *Br Med J* 1926;1:690-3.
5. Turner M. Posture and pain. *Physiotherapy* 1956;42:235-8.
6. Kendall FP, McCreary EK, Provance PG. *Muscles, Testing and Functions*. 4th ed. Baltimore: Williams and Wilkins; 1993.
7. Index-Catalogue of the Library of the Surgeon-General's Office, United-National Library of Medicine (U.S.) – Google Books. Available from: https://books.google.co.in/books?id=X3PPyAEACAAJ&printsec=frontcover&redir_esc=y#v=onepage&q&f=false. [Last accessed on 2020 Apr 06].
8. Posture of the Head: Its Relevance to the Conservative Treatment of Cervicobrachial Radiculitis | Physical Therapy | Oxford Academic. Available from: <https://academic.oup.com/ptj/article/46/9/953/4637970>. [Last accessed on 2020 Apr 07].
9. Mannheimer JS, Rosenthal RM. Acute and chronic postural abnormalities as related to craniofacial pain and temporomandibular disorders. *Dent Clin North Am* 1991;35:185-208.
10. Braun BL. Postural differences between asymptomatic men and women and craniofacial pain patients. *Arch Phys Med Rehabil* 1991;72:653-6.
11. Borstad JD, Ludewig PM. Comparison of three stretches for the pectoralis minor muscle. *J Shoulder Elbow Surg* 2006;15:324-30.
12. Sandra F, Lezberg BS. Clinical posture of the head. Its Relevance to the Conservative Treatment of Cervicobrachial Radiculitis, *Physical Therapy*, 1966;46:953-57. <https://doi.org/10.1093/ptj/46.9.953>.
13. Bullock-Saxton J. Normal and abnormal postures in the sagittal plane and their relationship to low back pain. *Physioth Theory Pract* 1988;4:94-104.
14. Singer KP. A new musculoskeletal assessment in a student population. *J Orthop Sports Phys Ther* 1986;8:34-41.
15. Mahmoud NF, Hassan KA, Abdelmajeed SF, Moustafa IM, Silva AG. The relationship between forward head posture and neck pain: A systematic review and meta-analysis. *Curr Rev Musculoskelet Med* 2019;12:562-77.
16. Norris CM, Berry SD. Occurrence of common lumbar posture types in the student sporting population: An initial investigation. *Sports Exercise and Injury* 1998;4:15-18.
17. Mani S, Sharma S, Omar B, Ahmad K, Muniandy Y, Singh DK. Quantitative measurements of forward head posture in a clinical settings: A technical feasibility study. *Eur J Physiother* 2017;19:119-23.
18. Russek AS. Diagnosis and treatment of scapulothoracic syndrome. *J Am Med Assoc* 1952;150:25-7.
19. Dahlberg R, Karlqvist L, Bildt C, Nykvist K. Do work technique and musculoskeletal symptoms differ between men and women performing the same type of work tasks? *Appl Ergon* 2004;35:521-9.
20. Kumar S. Theories of musculoskeletal injury causation. *Ergonomics* 2001;44:17-47.
21. Anderson CK, Chaffin DB, Herrin GD. A study of lumbosacral orientation under varied static loads. *Spine (Phila Pa)* 1976;11:456-62.
22. Senthil P, Sudhakar S, Porcelvan S, Francis TG, Rathnamala D, Radhakrishnan R. Implication of posture analysing software to evaluate the postural changes after corrective exercise strategy on subjects with upper body dysfunction – A Randomized Controlled Trial. *J Clin Diagn Res* 2017;11:YC01-4.

Morphometric Evaluation of Sacrum Volume in Healthy Women

Abstract

Introduction: The aim of this study was to calculate volume of the sacrum, sacral canal, caudal part of the epidural space, and dural sac volumes using stereological methods on magnetic resonance images (MRIs). **Material and Methods:** We used MRI series of 50 healthy women (the mean age; 44.0) in the study, retrospectively. Point counting and planimetry methods were used to calculate the volumetric parameters on MRIs. Volume calculation was performed by placing the dotted field ruler on MRI sections for point counting method, whereas ImageJ software was used for planimetry method. **Results:** Sacrum volume was measured as $135.38 \pm 24.12 \text{ cm}^3$ using point counting method, whereas it was $136.87 \pm 24.76 \text{ cm}^3$ in planimetry method. The mean volume of sacral canal was determined as $10.11 \pm 2.64 \text{ cm}^3$ and $10.30 \pm 2.73 \text{ cm}^3$ using point counting and planimetry methods, respectively. The mean volume of the caudal portion of the epidural space was $6.54 \pm 2.04 \text{ cm}^3$ in point counting method, whereas it was $6.53 \pm 1.89 \text{ cm}^3$ in planimetry method. **Discussion and Conclusion:** Knowing the volume of sacrum would contribute to minimization of complications during surgical approaches and anesthesia procedures in that region. Our results showed that sacrum volume can be calculated accurately using stereological methods such as point counting and planimetry.

Keywords: Anatomy, caudal epidural block, sacrum, stereology

Introduction

In degenerative diseases, lumbosacral instabilities and during surgical approaches targeting sacral region, preservation of anatomical structures are crucial. Therefore, a good knowledge of anatomic organization and morphometric values of the sacrum would be useful to prevent unexpected complications during surgical procedures in this region.^[1]

Dural and arachnoid sheaths of spinal cord terminate at the level of S2 vertebra. Adipose tissue, venous plexus, filum terminale, and coccygeal nerve are located in caudal part of the epidural space under dural sheath of S2 vertebra. Caudal part of epidural space is commonly used for caudal epidural block (CEB) and epidural analgesia.^[2] CEB is performed by administering local anesthetic into caudal part of epidural space. CEB is frequently used for treating lumbar spinal disorders and prevention of chronic low back pain, as well.^[1]

Epidural analgesia or commonly known as “painless delivery,” is a special form

of local anesthesia used to eliminate pain during labor or cesarean section. The difference of epidural analgesia from general anesthesia is that the expectant mother is awake during the procedure and completely perceives what is going on around her. It is a very safe method in terms of undesirable effects compared to general anesthesia.^[3,4]

If volume of caudal portion of the sacrum and epidural space is not known, it does not only increase the risk of perforation of the dural sac but also increases the probability of cardiac arrest due to overdosing of anesthetic or analgesic drug during CEB and epidural analgesia applications.^[3-7] Therefore, to prevent unexpected complications, volume of caudal part of the sacrum and epidural space should be carefully evaluated before surgical approaches.^[6]

The recent studies about epidural analgesia and CEB approaches demonstrated the importance of knowing anatomical organization of sacral region. Therefore, the main aim of this study was to morphometric evaluation of the sacrum, sacral canal, caudal part of the epidural space, and

**Emrah Özcan,
Ömür Karaca,
Mine İslimye
Taşkın¹,
Ramazan Çetin,
Aycan Büyükmert,
Alper Vatanserver,
İlter Kuş**

*Departments of Anatomy and
¹Obstetrics and Gynecology,
Faculty of Medicine, Balikesir
University, Balikesir, Turkey*

Article Info

Received: 22 February 2021

Revised: 10 July 2021

Accepted: 31 October 2021

Available online: 30 June 2022

Address for correspondence:

*Dr. Emrah Özcan,
Department of Anatomy,
Faculty of Medicine, Balikesir
University, Balikesir, Turkey.
E-mail: emrahozcan@balikesir.
edu.tr*

Access this article online

Website: www.jasi.org.in

DOI:
10.4103/jasi.jasi_33_21

Quick Response Code:



How to cite this article: Özcan E, Karaca Ö, Taşkın Mİ, Çetin R, Büyükmert A, Vatanserver A, *et al.* Morphometric evaluation of sacrum volume in healthy women. *J Anat Soc India* 2022;71:119-22.

This is an open access journal, and articles are distributed under the terms of the Creative Commons Attribution-NonCommercial-ShareAlike 4.0 License, which allows others to remix, tweak, and build upon the work non-commercially, as long as appropriate credit is given and the new creations are licensed under the identical terms.

For reprints contact: WKHLRPMedknow_reprints@wolterskluwer.com

dural sac volume using stereological methods on magnetic resonance image (MRI) series of healthy women.

Material and Methods

Ethical approval

Our study was begun after received ethical approval by Balikesir University's NonInterventional Clinical Research Ethics Committee (2018/108).

Participants

Fifty healthy women's (the mean age; 44.0, range; 16–71) MRI series were evaluated, retrospectively. MRI series of participants admitted to Obstetrics and Gynecology Department of Balikesir University Hospital for an another reasons than sacral region disorders between 2015 and 2018 and underwent lower abdominal MRI were retrospectively obtained from picture archiving and communication system. MRI series was evaluated by an obstetrics and gynecology and anatomy specialists.

Women that did not have any pathology or disorder in the sacrum and sacral region were included in the study. Women who had a sacral tumor history, sacrum anomaly, spina bifida, spinal surgery, osteoporosis, or related disorders were excluded.

Magnetic resonance image protocol

Pelvic MRI series was obtained from a 1.5 Tesla MRI unit (Philips, Ingenia, 2013). T1-weighted repetition time for volume measurements: 4500 ms, echo time: 80 ms, field of view: 170 × 170, matrix size: 172 × 119, voxel size: 1 × 1 × 1, flip angle: 90, and the images in the sagittal plane with a section thickness of 3 mm were used.

Morphometric measurements

The volume of sacrum, sacral canal, caudal epidural space and dural sac and termination of the dural sac were calculated using stereological methods such as Cavalieri and planimetry methods on MRI series.

Point counting method (Cavalieri method)

The point counting method used in our study is based on Cavalieri principle. Transverse-sectional images with 3 mm thickness were used to calculate the volume of the region of interest (ROI). First, MRIs in digital imaging and communications in medicine (DICOM) format imported to the RadiAnt DICOM viewer, and then sagittal sections were opened. Principally, preliminary study was needed to be performed with different point area measurement scales to calculate the coefficient of error for selecting an accurate scale. As a result of our preliminary study, 0.3 cm point area measurement scale was used, with the lowest error coefficient (0.05 and less). The dotted area measurement chart was randomly plotted onto the MRI and this procedure was repeated for each section [Figure 1]. The number of points on the ROI was noted. In the

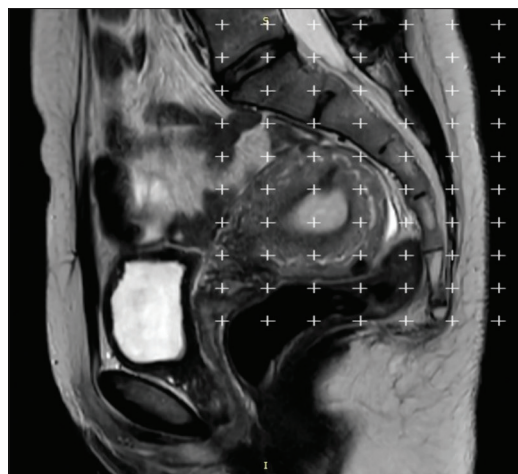


Figure 1: Disposal of the dotted area measurement ruler on the magnetic resonance image

MRIs of participants, sacrum's volume was calculated on 59 sections, sacral canal's volume in 13 sections, volume of caudal part of epidural space in 11 sections, and dural sac volume in 10 sections. The mean number of points was 578 for the sacrum, 99 for the sacral canal, 81 for the caudal part of the epidural space, and 64 for the dural sac. Once point counting process was completed, the volume was calculated according to the previously stated formula.^[8]

Planimetry method

For volumetric calculations using the planimetry method, Image J (Image Processing and Analysis in Java, Version 1.53), National Institutes of Health, Maryland, USA. which was developed by the American National Institute of Health and obtained free of charge^[9] was used. Images were displayed using a standard image and display levels on a monitor with constant contrast settings. In the ImageJ software, boundaries of the ROI were manually drawn on each MRI section [Figure 2]. The software automatically calculated the number of pixels covered within the ROI boundaries, and this process was repeated for each section. The ROI volume was calculated based on the pixel size and section thickness using the following formula:

$$\text{Volume} = \text{Sum of areas (cm}^2\text{)} \times \text{Section thickness (cm)}$$

Statistical analysis

Statistical analysis was completed using the SPSS (Statistical Package for the Social Sciences, Version 22), IBM Incorporated, New York, USA. The suitability of the variables to normal distribution was evaluated by applying Shapiro-Wilk test. Descriptive tests were performed to determine the volume of sacrum, sacral canal, caudal portion of epidural space, and dural sac. To determine statistically significant differences between Cavalieri and planimetry methods, intraclass correlation analysis was performed. Summary of data were stated as mean ± standard deviation. "Pearson correlation" test was used to evaluate the relationship between volumetric data

and normal distribution age. The cases where the $P < 0.05$ were evaluated as statistically significant.

Results

Volume of sacrum was $135.38 \pm 24.12 \text{ cm}^3$ in Cavalieri method, whereas it was $136.87 \pm 24.76 \text{ cm}^3$ in planimetry method. The mean volume of sacral canal was $10.11 \pm 2.64 \text{ cm}^3$ and $10.30 \pm 2.73 \text{ cm}^3$ in Cavalieri and planimetry methods, respectively. The mean volume of caudal portion of epidural space was $6.54 \pm 2.04 \text{ cm}^3$ by Cavalieri method and $6.53 \pm 1.89 \text{ cm}^3$ by planimetry method. Volume of the dural sac was measured as $3.57 \pm 1.85 \text{ cm}^3$ with Cavalieri method and $3.78 \pm 1.96 \text{ cm}^3$ with planimetry method. Intraclass correlation analysis showed no difference between the two methods [Table 1]. The closure site of the dural sac was found to be S2 vertebrae level in 82.0% (n = 41), S1 vertebrae level in 16.0% (n = 8), and S3 vertebrae level in 2.0% (n = 1) of participants. As a result of Pearson correlation analysis, there was a negative weak correlation between sacral canal volume and caudal part of epidural space with age, but no statistically significant correlation was found between other parameters and age [Table 2].

Discussion

Epidural analgesia and CEB have recently been performed by physicians in female patients. Thus, it is crucial to know

the sacrum morphometry to prevent unexpected injuries during epidural analgesia and CEB. Therefore, in this study, we aimed to determine termination of the dural sac by calculating volumetric values of sacrum, sacral canal, caudal portion of the epidural space, and sacral sac using the Cavalieri and planimetry methods on MRIs of healthy women.

The advantage of Cavalieri method is that it is easy to apply and economical and this method does not require extra accessories. This method can be applied on the MRI printed sections, and it is also a suitable method for prospective and retrospective studies. The advantages of the planimetry method are that it gives more accurate results and ImageJ software is free of charge and easy to use. Although this method requires a high degree of hand-eye coordination and skill in defining boundaries of the structure of interest, higher sensitivity, and higher standard deviation are among the advantages.^[8-10]

In the literature review, it is observed that morphometric studies of sacrum are generally performed on dry bones and radiographs directly, but there was not any study about the sacrum morphometry using MRIs of healthy individuals.^[6,11,12] These studies were completed using dry bones; thus, gender discrimination and individual’s medical history were not known. Therefore, the results of recent studies remain insufficient to determine the sacrum morphometry.

The studies indicated that decreased volume of caudal part of the epidural space with age.^[6,13] Similarly, in our study, a negative correlation was found between age and volume of caudal portion of the sacral canal and epidural space. Our findings showed that volume of the sacral canal and caudal portion of the epidural space located in the canal decreased with age.

The mean volume of sacral canal was $10.11 \pm 2.64 \text{ cm}^3$ with Cavalieri method and $10.30 \pm 2.73 \text{ cm}^3$ with planimetry method in healthy women. On the other hand, Crighton *et al.*^[14] performed a study on MRIs of 22 female and 13 male patients who suffering from low back pain. They found that the mean volume of sacral canal in women was $13.2 \pm 2.68 \text{ cm}^3$ that was different from our results. This difference may be caused due to their study was completed with patients with low back pain.^[11]

In a study conducted by Asghar and Naaz^[4] on 77 dry sacrum (42 females and 30 males), volume of the sacral canal was measured as $34.86 \pm 6.86 \text{ cm}^3$ in women, and

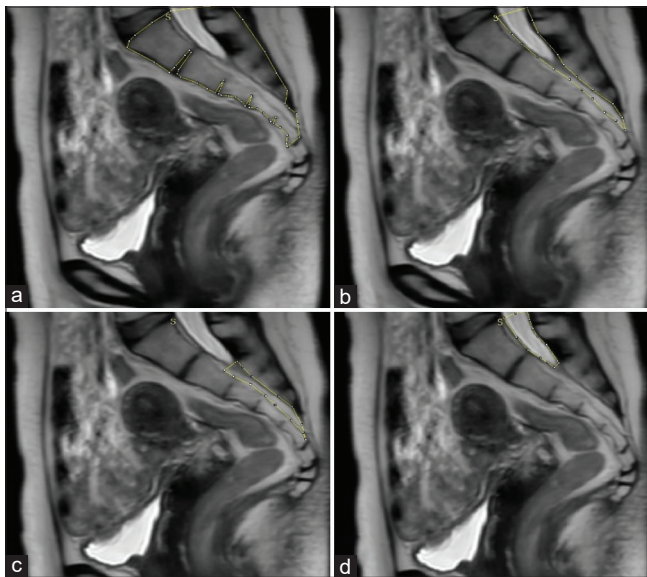


Figure 2: Volume calculation using the planimetry method. (a) sacrum volume, (b) sacral canal volume, (c) caudal portion of epidural space volume, and (d) dural sac volume

Table 1: Intraclass correlation coefficient

	Intraclass correlation	95% CI (lower bound–upper bound)	F test with true value 0			
			Value	df1	df2	Significance
Single measures	0.993	0.987-0.996	273.287	49	49	0.000
Average measures	0.996	0.994-0.998	273.287	49	49	0.000

CI: Confidence interval

Table 2: Pearson correlation analysis

Volume (cm ³)	Age			
	Cavalieri method		Planimetri method	
	P	r	P	r
Sacrum	0.219	-0.177	0.169	-0.197
Caudal portion of epidural space	0.079	-0.251	0.023	-0.321
Dural sac	0.342	-0.137	0.272	-0.158
Sacral canal	0.041	-0.289	0.017	-0.335

caudal volume of the epidural space was measured as $12.46 \pm 3.52 \text{ cm}^3$. They found that volumes of the caudal portion of the sacral canal and epidural space were very high compared with the results of our study. The fact that the study was carried out on dry bone, and the disease resumes belonging to the owners of the measured bones explain the difference between the results obtained and our findings.

Senoglu *et al.*^[7] completed a study using MRIs of 641 women to determine the termination level of the dural sac. According to their results, this level was found at the S2 vertebra in 72.0% of women (n = 460). Furthermore, the termination level of dural sac was found at S3 vertebra in only one participant in our study.

Many previous studies mainly used dry bones and radiographic images for morphometric evaluation of sacrum and its contents in patients suffering from any clinical history. Meanwhile, our study especially focused on anatomical properties of these structures in healthy individuals. Our results may be useful as a preoperative guide for physicians. Therefore, postoperative quality of life of patients suffering from any pathology may be increased.

Conclusion

Knowing the sacrum morphometry well is very important for surgical approaches and anesthesia procedures to this region. Each patient should be evaluated individually to select a proper surgical method with regard to anatomical properties. Knowing volume of the sacrum may reduce risks of unexpected complications by preserving the anatomical structures (especially dural sac) in this region.

Limitations of the study

Due to the retrospective nature of our study, the limitations were the fact that the cross-sectional thickness of the MRIs was 3 mm and the number of participants was low.

Acknowledgments

Authors would like to thank to staff of the Radiology Department for their support.

Financial support and sponsorship

Nil.

Conflicts of interest

There are no conflicts of interest.

References

1. Standring S. Gray's Anatomy: The Anatomical Basis of Clinical Practice. 41st ed. New York: Elsevier Limited; 2019.
2. Moore KL, Dalley AF, Agur AM. Clinically Oriented Anatomy. 7th ed. Philadelphia: Wolters Kluwer/Lippincott Williams & Wilkins Health; 2014.
3. Park GY, Kwon DR, Cho HK. Anatomic differences in the sacral hiatus during caudal epidural injection using ultrasound guidance. *J Ultras Med* 2015;34:2143-8.
4. Asghar A, Naaz S. The volume of the caudal space and sacral canal in human sacrum. *J Clin Diagn Res* 2013;7:2659-60.
5. Moralar GD, Turkmens UA, Altan A. Dogum aneljezisi. *Okmeydani Tip Derg* 2011;27:5-11.
6. Cheng JS, Song JK. Anatomy of the sacrum. *Neurosurg Focus* 2003;15:E3.
7. Senoglu N, Senoglu M, Ozkan F, Kesilmez C, Kızıldağ B, Celik M. The level of termination of the dural sac by MRI and its clinical relevance in caudal epidural block in adults. *Surg Radiol Anat* 2013;35:579-84.
8. Başaloğlu H, Turgut M, Taşer FA, Ceylan T, Başaloğlu HK, Ceylan AA. Morphometry of the sacrum for clinical use. *Surg Radiol Anat* 2005;27:467-71.
9. Aggarwal A, Aggarwal A, Harjeet, Sahni D. Morphometry of sacral hiatus and its clinical relevance in caudal epidural block. *Surg Radiol Anat* 2009;31:793-800.
10. Gundersen HJ, Bendtsen TF, Korbo L, Marcussen N, Møller A, Nielsen K, *et al.* Some new, simple and efficient stereological methods and their use in pathological research and diagnosis – Review article. *APMIS* 1988;96:379-94.
11. Abramoff M, Magalhães P, Ram SJ. Image processing with ImageJ. *Biophotonics Int* 2004;11:36-42.
12. Acer N, Sahin B, Usanmaz M, Tatoğlu H, Irmak Z. Comparison of point counting and planimetry methods for the assessment of cerebellar volume in human using magnetic resonance imaging: A stereological study. *Surg Radiol Anat* 2008;30:335-9.
13. Polat KT, Ertekin T, Acer N, Cınar S. Sakrum kemiginin morfometrik değerlendirilmesi ve eklem yuzey alanlarının hesaplanması. *Erciyes Univ Sağlık Bilimleri Derg* 2014;26:67-73.
14. Crighton IM, Barry BP, Hobbs GJ. A study of the anatomy of the caudal space using magnetic resonance imaging. *Br J Anaesth* 1997;78:391-5.

Demonstration of the Epigastric Vessels Surface Anatomy with Equation Model: An Anatomical Feasibility Study

Abstract

Introduction: The objective of this study is to design a patient-specific model to predict the location of epigastric vessels on the abdominal surface and to show clinicians safe areas before surgical intervention. **Material and Methods:** A total of 200 patients who underwent color Doppler ultrasound evaluation of the deep epigastric vessel before gynecological laparoscopic surgery were recruited in the study. The deep epigastric vessels were identified at three equal levels between the xiphoid and umbilicus, and five equal levels between the umbilicus and the symphysis pubis. The distance between the epigastric vessels and the midline was measured bilaterally at each level. Linear mixed effect modeling was used to assess the anatomical location of the epigastric vessels. **Results:** The model with waist circumference term was found to be the model with best performance metric. This model included waist circumferences as a covariate, the region of the epigastric vessel as a categorical variable, and random effects for patients. The model that calculates the expected distance from the midline of the epigastric vessels for different regions and waist circumferences are presented as “Distance to midline (cm) = 2.57 + Region A + Region B × Waist Circumference.” **Discussion and Conclusion:** With the equation model, we proposed, the location of the epigastric vessels can be determined specifically for the patient and the abdominopelvic regions. This model can be a guide to prevent vascular injury.

Keywords: Epigastric vessels, laparoscopy, obesity, ultrasound

Introduction

Epigastric arteries are at risk of injury during abdominal procedures close to the artery, such as laparoscopic trocar placement, intra-abdominal drain placement, and paracentesis due to their anatomical position.^[1] Abdominal wall vascular injuries during surgical procedures have been reported in 0.2%–2% of cases.^[2] These vessels include the superficial epigastric vessels, the superficial circumflex iliac vessels, the superior epigastric vessels, and the inferior epigastric vessels.

Unlike the superficial vessels, the superior and inferior epigastric vessels are larger and their injury can cause significant morbidity and mortality.^[3] The inferior epigastric artery (IEA) arises from the external iliac artery just above the inguinal ligament.^[4] It rises along the medial edge of the inguinal ring, pierces the transversalis fascia, and lies anterior to the arcuate line between the rectus abdominis and the posterior rectus sheath.^[4] Above the umbilicus, it

anastomoses with the superior epigastric artery. The superior epigastric artery is the terminal continuation of the internal thoracic artery. It begins at the level of the sixth rib and runs down between the costal and xiphoid muscle slips of the diaphragm. The artery then reaches the anterior surface of the abdomen and runs over the transversus thoracis and transversus abdominis muscles.^[4] It enters the rectus sheath and descends toward the umbilicus.^[4]

Although the transillumination method in laparoscopic surgery largely defines the superficial vessels, transperitoneal imaging of the deep epigastric vessels is difficult, especially in obese patients.^[5] Various studies have been conducted in the literature to map the location of the deep epigastric vessel.^[5-8] These studies evaluated the distance from the midline of the epigastric arteries in different several abdominal segments and suggested a more lateral location of the deep epigastric vessels in obese patients. Although the previous studies show lateralization of epigastric vessels in obese patients, patient-specific

This is an open access journal, and articles are distributed under the terms of the Creative Commons Attribution-NonCommercial-ShareAlike 4.0 License, which allows others to remix, tweak, and build upon the work non-commercially, as long as appropriate credit is given and the new creations are licensed under the identical terms.

For reprints contact: WKHLRPMedknow_reprints@wolterskluwer.com

How to cite this article: Karaca SY, Ince O, Adiyeye M, İleri A, Vural T, Töz E, *et al.* Demonstration of the epigastric vessels surface anatomy with equation model: An anatomical feasibility study. *J Anat Soc India* 2022;71:123-7.

Suna Yıldırım Karaca^{1,2},
Onur Ince³,
Mehmet Adiyeye¹,
Alper İleri¹,
Tayfun Vural¹,
Emrah Töz¹,
Ahmet Demir¹,
İbrahim Karaca¹,
Alparslan Pulur⁴,
İbrahim Egemen Ertaş¹

¹Department of Obstetrics and Gynaecology, Health Sciences University Tepecik Education and Research Hospital, ²Department of Stemcell, Institute of Health Sciences, Ege University, Izmir, ³Department of Obstetrics and Gynaecology, Kutahya Health Sciences University, Kutahya, ⁴Department of Obstetrics and Gynaecology, Yozgat City Hospital, Yozgat, Turkey

Article Info

Received: 20 December 2021

Accepted: 25 March 2022

Available online: 30 June 2022

Address for correspondence:

Dr. Alper İleri,
Health Sciences University
Tepecik Education and Research
Hospital, Gaziler Caddesi,
No: 468, 35020, İzmir, Turkey.
E-mail: alper_ileri@hotmail.com

Access this article online

Website: www.jasi.org.in

DOI:
10.4103/jasi.jasi_207_21

Quick Response Code:



localization is far from estimating. The most important reason for this situation was the anatomical variations and the inability to show the body mass index (BMI) and waist circumference changes between patients.

The aim of this study is to create a patient-specific model to predict the location of epigastric vessels on the abdominal surface and to show clinicians safe areas before surgical intervention.

Material and Methods

This study was conducted with patients scheduled for laparoscopic surgery for benign gynecological indications at Health Sciences University Tepecik Education and Research Hospital between July 2021 and October 2021. Following the approval of the study protocol by the local ethics committee of Health Sciences University Tepecik Education and Research Hospital, the patients were included in the study.

Since the superficial epigastric vessels were interrupted during the pfannenstiell incision and both the superficial and lower epigastric vessels were interrupted during the Maylard incision, patients who had undergone previous transverse lower abdominal incisions, including cesarean section, were excluded from the study. In addition, patients with large skeletal deformities that may displace the epigastric vessels, large abdominal tumors, tense ascites, incisional hernia, or any condition such as diastasis recti were not included in the study.

The location of the deep epigastric vessels was mapped across the abdomen at three equal levels between the xiphoid and umbilicus, and five equal levels between the umbilicus and the symphysis pubis, for a total of eight levels with Doppler ultrasound. The reliability of Doppler ultrasonography to measure the distance of epigastric vessels has been demonstrated in previous studies.^[9] The distance between the epigastric vessels and the midline was measured bilaterally at each level. A total of 16 measurements were made from the right and left abdominal region from the xiphoid line to the symphysis line for each patient. L1-R1; xiphoid line measuring point, L4-R4; the umbilical line represents the measurement point, and the L8-R8 the symphysis pubis line measurement points. To control for interoperator variability, localization of the vessels was performed by a single-experienced ultrasonographer (M. A) using the Voluson 750 Pro ultrasound machine [Figure 1]. After determining the short and long axes of the vessels with Doppler, their projections to the abdominal skin were marked. At each level, the most lateral branch of the IEA and vein or superior epigastric artery and vein was marked. The data set consisted of the epigastric vessel ($200 \times 16 = 3200$) localization obtained by Doppler ultrasound of a total of 200 patients.

Afterward, patients' waist circumference, weight, and height were measured. Waist circumference was measured at the

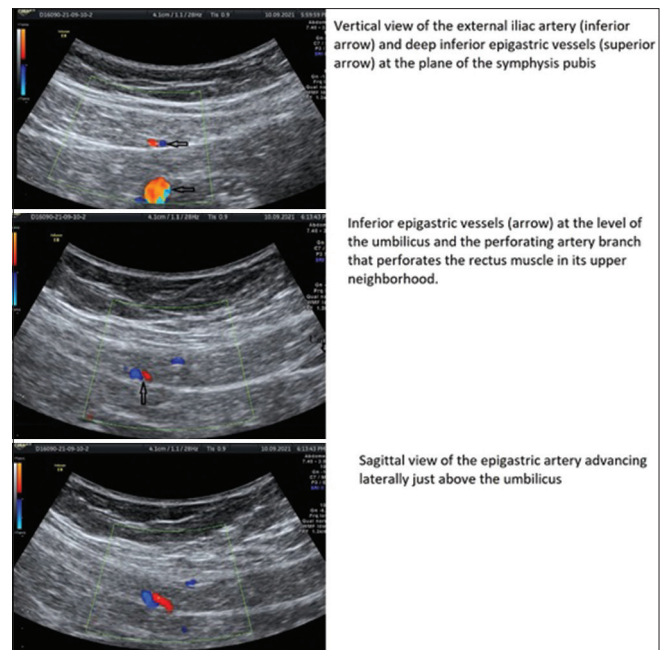


Figure 1: Demonstration of epigastric vessels by Doppler ultrasound in different abdominal planes

horizontal plane between the inferior costal margin and the iliac crest on the midaxillary line. Height and weight were measured in the standing position while the participants were barefoot and in light clothing. Demographic data, including age, gravidity, and parity, were collected from the patients and their electronic medical records.

Statistics

The primary outcome of the study is the distance of the epigastric vessels to the midline of the abdomen which passes through the umbilicus. For predicting the distance, linear mixed model analysis and maximum likelihood estimation were used. The independent variables were gravida, parity, age, weight, height, BMI, and waist circumference. In the model, random effect for patients was included, based on their identification. Linearity, normality of the residuals, homogeneity of residual variance (homoscedasticity), and no autocorrelation assumptions were verified. The intercepts for different patients were assumed to be normally distributed. A concern for the statistical analysis is potential multicollinearity between the predictor variables. In this respect, gravida, parity, age, weight, height, BMI, and waist circumference were found to be highly correlated, with most pairwise Pearson correlation coefficients > 0.75 . Therefore, these predictors are not included in the multivariate model together. The literature does not indicate direct effects of gravida parity and age on the anatomical location of the epigastric vessels. Hence, only the effects of weight, height, BMI, and waist circumference were analyzed. Since weight, BMI, and waist circumference have Pearson correlation coefficients of around 0.90 with

each other, we estimate three separate candidate models each including only one of the three as fixed effects. For each of these three models, we estimate hierarchical and nonhierarchical versions, resulting in a total of six models. The six candidate models and their performance metric are presented in Table 1. For all three models, hierarchical and nonhierarchical versions had same log-likelihood and same number of parameters, therefore, the same Bayesian information criterion (BIC) value. The two models with waist circumference as the fixed effect have the lowest BIC value. The Wald test of waist circumference as the main effect is not statistically significant. The model that includes only waist circumference as the interaction term has the same likelihood and BIC as the model that includes waist circumference both as the main effect and in the interaction term. Therefore, the former nonhierarchical model was chosen as the best predictor model. To present the results of the linear mixed model, the marginal and conditional R^2 values are used.^[10] Ninety-five percent confidence intervals for the distance of epigastric vessels in different regions were calculated by taking the uncertainty due to random effect variance in addition to uncertainty of variance due to fixed effects into account [Figure 1]. A two-tailed $P < 0.05$ was considered statistically significant. Statistical analyses were performed using R is available as Free Software under the terms of the Free Software Foundation's GNU General Public License.

Results

Linear mixed effect modeling was used to assess the anatomical location of the epigastric vessels. The distance of the artery to the midline is defined as the response variable. Compared to models including weight and height or BMI, the model with waist circumference term was found to be the model with best performance metric [Table 1]. This model included waist circumferences as a covariate, the region of the epigastric vessel as a categorical variable, and random effects for patients. The model used was nonhierarchical and did not include waist circumference as main effect but only in the interaction term. The marginal R^2 value of the linear mixed model was 69.3% and the conditional R^2 value was 87.6%. Therefore, 69.3% of the variability in the distance to the midline (dependent variable) is explained by the region of the

vessel and waist circumference, and the 18.3% variability (87.6% - 69.3%) is explained by the random effects of the patients. The standard deviation of the random effects due to the patients was 0.6532. The remaining 12.4% variability is due to model error. The model to calculate the expected distance of epigastric vessels to the midline for different regions and waist circumferences is presented in Table 1. The 95% confidence interval for the location of IEA of a woman with a waist circumference of 85.3 is presented in Figure 2.

Discussion

To the best of our knowledge, this study is the first equation model to make a patient-specific topographic marking of deep epigastric vessels. Our findings showed that lateralization of vessels from the midline increased in correlation with the increase in the values of weight, BMI, and waist circumference variables. A patient-specific equation was created to predict the localization of epigastric vessels by analyzing the inter-patient variations. In this equation, the best metric performance was achieved with waist circumference. A safe entry point could be determined to prevent epigastric vessel damage by placing the patient's waist circumference measurement and the Region A and Region B values of the abdominal region where the surgical intervention will be performed into this equation.

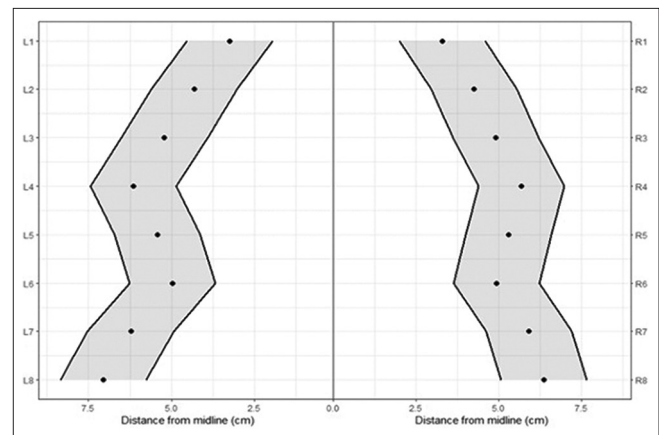


Figure 2: The estimated anatomical trace of the inferior epigastric artery in a woman with waist circumference of 85.3 with 95% confidence interval for different height levels (1–8) and sides (the left or right) using the formula in Table 2

Table 1: Comparison of the models including waist circumference, body mass index, and weight plus height

Model type	Main effects	Interaction terms	BIC
Hierarchical models	Region + weight + height	Weight × region + height × region	2448.7
	Region + BMI	BMI × region	2406.5
	Region + WC	WC × region	2371.5
Nonhierarchical models	Region	Weight × region + height × region	2448.7
	Region	BMI × region	2406.5
	Region	WC × region	2371.5

Hierarchical models include main effect terms for weight, height, BMI, and WC in addition to the variables in nonhierarchical models, The model with the lowest BIC value is the best model. BMI: Body mass index, WC: Waist circumference, BIC: Bayesian information criterion

Table 2: The formula for calculating the distance of the epigastric artery from the midline in different regions (height level: 1-8, sides: L for left and R for right)

The mean value of the distance of the inferior epigastric artery to midline can be calculated by the formula below

$$\text{Distance to the midline (cm)} = 2.57 + \text{Region_A} + \text{Region_B} \times \text{WC}$$

Find below the relevant region for which you want to calculate the distance of the epigastric artery to the midline. Put the corresponding values in the Region_A and Region_B terms in the formula. The WC measurement to be multiplied by the Region_B expression in the formula is in cm

Equation coefficients of the left abdominal region	L1	L2	L3	L4	L5	L6	L7	L8
Region_A	0	-1.485	-2.155	-1.339	-1.517	-1.401	-0.169	-0.484
Region_B	0.008	0.038	0.056	0.058	0.051	0.045	0.045	0.058
Equation coefficients of the right abdominal region	R1	R2	R3	R4	R5	R6	R7	R8
Region_A	-0.080	-2.115	-2.688	-1.356	-1.338	-1.449	-0.034	-0.400
Region_B	0.009	0.045	0.059	0.052	0.048	0.045	0.039	0.049

WC: Waist circumference, R: Right, L: Left

The topographic definitions of deep epigastric vessels have been studied in many previous studies. However, the results of these studies could not provide a consensus to explain how far the vessels are from the midline. For example, Saber *et al.* found that the mean distance of the epigastric vessels from the midline at the level of the symphysis pubis was 7.5 cm.^[11] Rao *et al.* reported that the farthest distance from the midline of the epigastric vessels at this level was 6.9 cm.^[12] Rao *et al.* reported that the average distance from the midline of the epigastric vessels at the umbilicus was 3.5 cm,^[12] whereas Epstein *et al.* reported an average of 4.8 cm.^[13] Some authors, who suggested that the reason for this anatomical inconsistency in the studies was the disregard of obesity, reported that the vessels were located more laterally in obese patients.^[6,11] The most important deficiency in these studies with a limited number of patients was the categorical classification of patients as obese or nonobese. However, BMI is a continuous variable. As expected, the studies in the literature were insufficient to evaluate the effect of the degree of obesity on the lateralization of the epigastric artery. For example, if a patient with a BMI of 40 kg/m² and a patient of 30 kg/m² are in the same group, it may lead to the misconception that the epigastric vessel trace is more medial than it should be in patients with high BMI.

The main purpose of clinical studies in the literature is to define a safe zone to prevent possible epigastric vessel injuries. Pun *et al.* successfully detected epigastric vessels using color Doppler ultrasound and recommended sonographic localization of vessels before laparoscopic procedures, especially in obese patients, to avoid injury to these vessels.^[14] Tinelli *et al.* showed that the adipose subperitoneal tissue located in the lateral third of the line

between the anterior superior iliac spine and the umbilicus is the site for a safe auxiliary trocar port.^[5] We created a patient-based equation for a similar purpose, and we found that the model with the term waist circumference had a better performance metric than BMI. With the help of this equation, it was possible to determine the distance of the epigastric artery from the midline at different levels of the abdominal surface of a patient whose waist circumference was known. For example, in a patient with a waist circumference of 100 cm (BMI = 31 kg/m²), we found the distance of epigastric vessels from the midline (2.56 + [-0.4] + [0.049 × 100]) 7.06 cm at the level of the right symphysis pubis (R8). In another obese patient, whose abdominal circumference was 130 cm (BMI = 40.5 kg/m²) in our model, the distance of the epigastric vessels was 8.53 cm from the midline. This equation model can be of great value as a real-time guide for many interventions, such as port site placement for abdominopelvic surgeons, epigastric perforator flap breast reconstruction for plastic surgeons, and perforation of the anterior abdominal wall for anesthesiologists.

With this study, we performed an equation model showing epigastric vessel location, but we are aware of some limitations of our study. First, our study population consisted of women. Although some studies reported that epigastric vessel location did not differ according to gender, we think that our results should not be generalized to the entire population. Second, since ultrasonography is subjective and dynamic imaging, all measurements were performed by a single ultrasonographer to limit interobserver variability. In addition, we could not show the perforator branches of the epigastric vessels in the model.

Conclusion

We believe that this study is a model of equations that show the localization of epigastric vessels based on anthropometric and ultrasound imaging and is useful to prevent vessel damage in surgical procedures. Therefore, clinicians who follow the recommendations of this study should first measure their patients' abdominal circumference. They can determine the appropriate entry localization for each patient by inserting the constant values of the localization to be operated into the equation.

Financial support and sponsorship

Nil.

Conflicts of interest

There are no conflicts of interest.

References

1. Wong C, Merkur H. Inferior epigastric artery: Surface anatomy, prevention and management of injury. *Aust N Z J Obstet Gynaecol* 2016;56:137-41.
2. Vasquez JM, Demarque AM, Diamond MP. Vascular complications of laparoscopic surgery. *J Am Assoc Gynecol Laparosc* 1994;1:163-7.
3. Fuller J, Ashar BS, Carey-Corrado J. Trocar-associated injuries and fatalities: An analysis of 1399 reports to the FDA. *J Minim Invasive Gynecol* 2005;12:302-7.
4. Ireton JE, Lakhiani C, Saint-Cyr M. Vascular anatomy of the deep inferior epigastric artery perforator flap: A systematic review. *Plast Reconstr Surg* 2014;134:810e-21e.
5. Tinelli A, Gasbarro N, Lupo P, Malvasi A, Tsin DA, Davila F, *et al.* Safe introduction of ancillary trocars. *JSL* 2012;16:276-9.
6. Burnett TL, Garza-Cavazos A, Groesch K, Robbs R, Diaz-Sylvester P, Siddique SA. Location of the deep epigastric vessels in the resting and insufflated abdomen. *J Minim Invasive Gynecol* 2016;23:798-803.
7. Bowness J, Seeley J, Varsou O, McKinnie A, Zealley I, McLeod G, *et al.* Arterial anatomy of the anterior abdominal wall: Evidence-based safe sites for instrumentation based on radiological analysis of 100 patients. *Clin Anat* 2020;33:350-4.
8. Joy P, Simon B, Prithishkumar IJ, Isaac B. Topography of inferior epigastric artery relevant to laparoscopy: A CT angiographic study. *Surg Radiol Anat* 2016;38:279-83.
9. Sriprasad S, Yu DF, Muir GH, Poulsen J, Sidhu PS. Positional anatomy of vessels that may be damaged at laparoscopy: New access criteria based on CT and ultrasonography to avoid vascular injury. *J Endourol* 2006;20:498-503.
10. Nakagawa S, Schielzeth H. A general and simple method for obtaining R2 from generalized linear mixed-effects models. *Methods Ecol Evol* 2013;4:133-42.
11. Saber AA, Meslemani AM, Davis R, Pimentel R. Safety zones for anterior abdominal wall entry during laparoscopy: A CT scan mapping of epigastric vessels. *Ann Surg* 2004;239:182-5.
12. Rao MP, Swamy V, Arole V, Mishra P. Study of the course of inferior epigastric artery with reference to laparoscopic portal. *J Minim Access Surg* 2013;9:154-8.
13. Epstein J, Arora A, Ellis H. Surface anatomy of the inferior epigastric artery in relation to laparoscopic injury. *Clin Anat* 2004;17:400-8.
14. Pun TC, Chau MT, Lam C, Tang G, Leong L. Sonographic localization of abdominal vessels in Chinese women: Its role in laparoscopic surgery. *Ultrasound Obstet Gynecol* 1998;11:59-61.

Analysis of Anatomical Variations of the Main Arteries Branching from the Abdominal Aorta by Multidetector Computed Tomography: A Prospective Study of 500 Patients in a Tertiary Center

Abstract

Introduction: Embryological development of the aorta being a complex process can lead to a variety of congenital variants. It may result in complications during abdominal laparoscopic and radiological interventions. Prior knowledge can identify the anatomy, which may require special attention at the time of surgery/interventions. Diagnostic imaging with multidetector computed tomography (MDCT) allows accurate and noninvasive preoperative evaluation. To identify and to evaluate the anatomical variation of major arteries branching from the abdominal aorta using MDCT. **Material and Methods:** Five hundred patients of different age groups referred to the Department of Radiodiagnosis, Dayanand Medical College and Hospital, Ludhiana, for MDCT abdomen were included in the study. It was performed on 128-slice MDCT Siemens Somatom Definition AS scan machine. **Results:** The results showed that anatomical variation occurs in a high percentage of patients. In the celiac axis, it occurred in 34.6% of cases, out of which the most common variant was a replaced right hepatic artery (3.7%). Celiacomesenteric trunk was observed in 0.2% of patient. Single renal artery was observed (43.2%) while accessory renal artery in 41.6% and early branching in 15.2%. **Discussion and Conclusion:** Prior knowledge of variations of these vessels can prevent iatrogenic injuries.

Keywords: Anatomical variations, celiac axis, multidetector computed tomography, renal arteries, superior mesenteric artery

Navneet Dabria,
Anisha Galhotra¹,
Ritu Dhawan
Galhotra,
Arnav Galhotra²,
Isha Sharma,
Chandan Kakkar,
Kamini Gupta,
Kavita Saggur

Department of
Radiodiagnosis, DMCH,
Ludhiana, Punjab, ²DMCH,
Ludhiana, Punjab, ¹GMCH,
Chandigarh, India

Introduction

Embryological development of the aorta being a complex process can lead to a variety of congenital variants.^[1] It may result in complications during abdominal laparoscopic and radiological interventions. Recent trends are more toward minimally invasive surgeries, hence, raising the demand of detecting anatomical variations preoperatively. Diagnostic imaging with multidetector computed tomography (MDCT) allows accurate and noninvasive preoperative evaluation.^[2,3] The aim of our study is to analyze the prevalence of anatomical variations of the major branches of the abdominal aorta in regional population and to compare the results with the ones presented in the literature.^[4,5] In our study, we analyzed the variations in anatomy of celiac axis and its branches, superior mesenteric artery (SMA), and renal arteries as these are the most important

branches of abdominal aorta due to their vascularization field.^[6]

MDCT with the added value of postprocessed images may allow accurate identification of areas at risk for venous congestion or devascularization, potentially influencing surgical planning with regard to the extent of resection, or the need for vascular reconstructions.^[7] If the variant anatomy remains unrecognized before surgery, it could prolong operative time, increase blood loss, cause iatrogenic injury, and/or increase morbidity.

Aims and objectives

To identify and to analyze anatomical variation of main arteries branching from the abdominal aorta using MDCT.

Material and Methods

Method of collection of data

A prospective study was conducted in 500 patients of different age groups referred

How to cite this article: Dabria N, Galhotra A, Galhotra RD, Galhotra A, Sharma I, Kakkar C, *et al*. Analysis of anatomical variations of the main arteries branching from the abdominal aorta by multidetector computed tomography: A prospective study of 500 patients in a tertiary center. *J Anat Soc India* 2022;71:128-34.

This is an open access journal, and articles are distributed under the terms of the Creative Commons Attribution-NonCommercial-ShareAlike 4.0 License, which allows others to remix, tweak, and build upon the work non-commercially, as long as appropriate credit is given and the new creations are licensed under the identical terms.

For reprints contact: WKHLRPMedknow_reprints@wolterskluwer.com

Article Info

Received: 12 August 2021

Revised: 13 April 2022

Accepted: 18 April 2022

Available online: 30 June 2022

Address for correspondence:

Dr. Ritu Dhawan Galhotra,
96, Lal Bagh, Near Rajguru
Nagar, Ludhiana, Punjab, India.
E-mail: ritugalhotra96@gmail.
com

Access this article online

Website: www.jasi.org.in

DOI:
10.4103/jasi.jasi_137_21

Quick Response Code:



to the Department of Radiodiagnosis, Dayanand Medical College and Hospital, Ludhiana, for MDCT abdomen for different reasons.

Informed consent was obtained from all the subjects/guardians before the study. The clinical history and the spectrum of findings were recorded as per the pro forma. The study was performed on 128-slice MDCT Siemens Somatom Definition AS scan machine.

MDCT was performed with the patient positioned supine with the area of interest from diaphragm to symphysis pubis. 80–100 ml of nonionic contrast was injected at the rate of 3–3.5 ml/sec followed by saline flush through the antecubital vein. Arterial phase study was analyzed to look for the arterial variations. Patients with vascular diseases (thrombosis, stenosis, strictures, and collaterals), major abdominal surgery/trauma, were not included in the study.

Observations and Results

This study was conducted in Dayanand Medical College and Hospital, Ludhiana. A total of 500 cases who underwent MDCT abdomen with arterial phase study were included in the study.

In our study, most of the cases were aged between 51 and 60 years (28.8%). The mean age was observed to be 53.20 ± 14.8 years.

Out of 500 cases, there were 287 (57.4%) male and 213 (42.6%) female. A total of 327 (65.4%) cases of the 500 cases had a normal celiac axis anatomy, which appeared as a hepato-gastrosplenic trunk and SMA originating separately from the aorta [Figure 1 and Table 1].

Ten specific types of celiac axis anatomical variations were observed in our study. The most frequent variation was a replaced right hepatic artery (RHA) from the SMA, which was seen in 68 (13.4%) cases [Figure 2]. The next variation according to frequency was accessory left hepatic artery (LHA), originating from the left gastric artery (LGA) seen in 48 (9.6%) cases [Figure 3]. Replaced LHA was observed in 25 (5.0%) cases, and accessory RHA was observed in 7 (1.4%) cases [Figure 4]. Variations in the origin of the common hepatic (CHA) (from the aorta) were observed in 8 (1.6%) cases [Figure 5]. The RHA originated from the celiac axis in 5 (1.0%) cases and from the aorta in 1 (0.2%) patient [Figure 6]. LGA from the aorta was observed in 9 (1.8%) cases [Figure 7]. Splenic artery originating from the aorta was observed in 1 (0.2%) patient [Figure 8]. The common trunk of the celiac trunk and SMA is a rare variation in this research, it was observed in 1 (0.2%) patient [Figure 9]. In this study, the mean diameter of celiac axis orifice was observed to be 5.6 ± 1.0 . The mean distance between celiac axis and SMA was observed to be 10.4 ± 2.1 [Table 2].

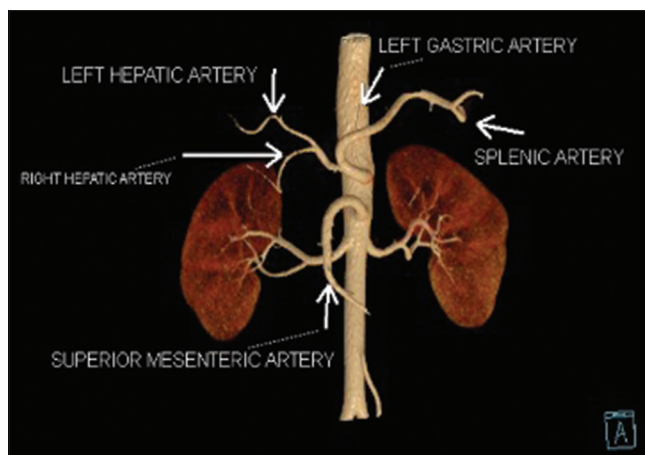


Figure 1: Normal celiac axis anatomy and normal origin of SMA. SMA: superior mesenteric artery

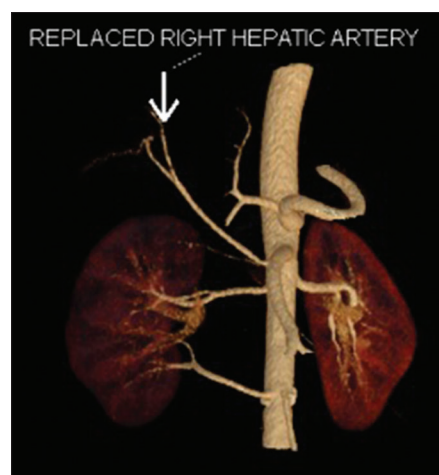


Figure 2: Image showing replaced right hepatic artery

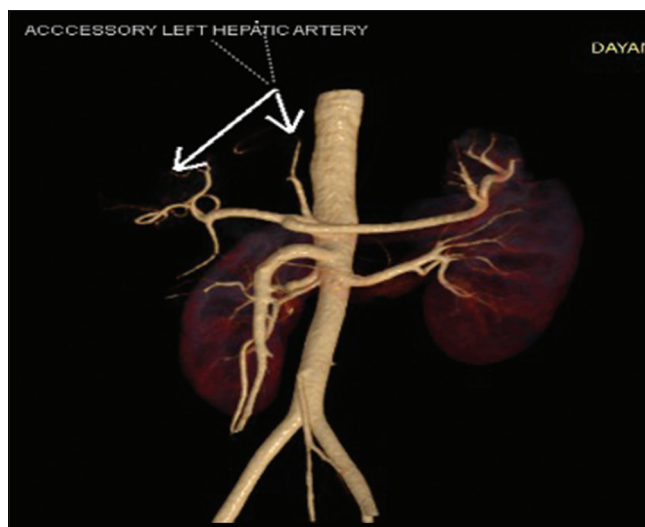


Figure 3: Image showing accessory left hepatic artery

A total of 499 cases showed normal anatomical origin of SMA. The common trunk of the celiac trunk and SMA is a rare variation in this study, it was observed in 1 (0.2%)

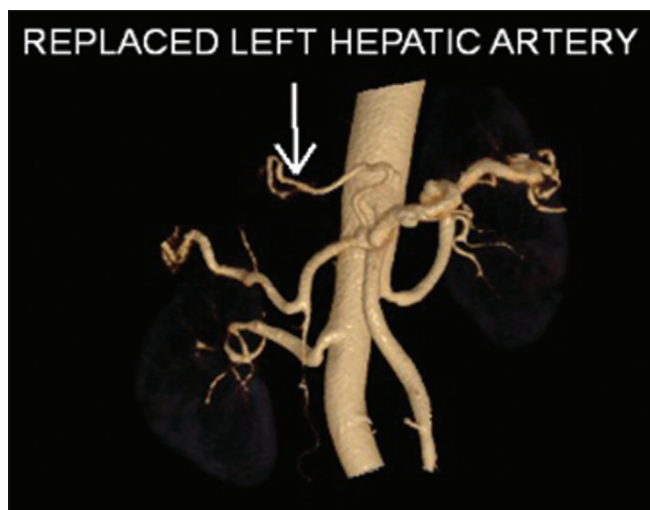


Figure 4: Image showing replaced left hepatic artery



Figure 5: Image showing common hepatic from the aorta

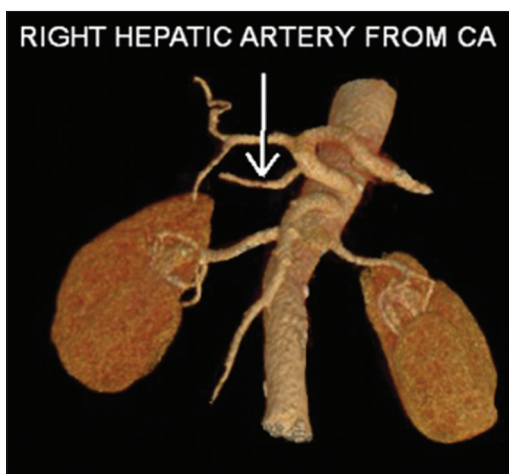


Figure 6: Image showing the right hepatic artery from the celiac axis

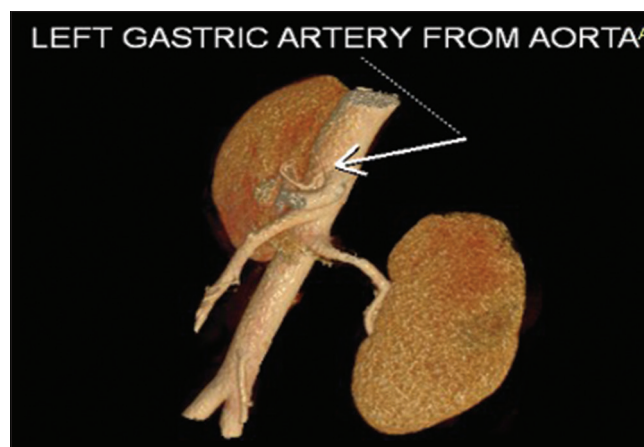


Figure 7: Image showing the left gastric artery from the aorta

Table 1: Types of the celiac trunk observed in the cases included in the study

Celiac trunk	Number of cases, n (%)
Classical	327 (65.4)
Variant	173 (34.6)
Total	500 (100.0)

patient [Table 3]. No case showing hepatomesenteric trunk or absence of SMA was observed in our study. In this study, the mean diameter of SMA at orifice was observed to be 6 ± 1.0 .

Out of 500 study cases, on evaluation for renal arteries, single renal artery was observed in 292/500 (58.4%) cases, while there was presence of accessory renal artery in 208/500 (41.6%) cases. The mean diameter of the orifice of the renal arteries was found to be 4 ± 0.9 mm [Table 4].

There was presence of accessory renal artery in 208/500 (41.6%) cases. Early branching was observed in

76/500 (15.2%) cases, while there was no accessory renal artery or early branching in 216/500 (43.2%) cases.

Renal arteries with early branching were observed in 76/500 (15.2%) cases, while in rest of the 424/500 (84.8%) cases, there was no early branching. The cases with accessory renal artery 208/500 were further categorized into [Table 5]:

1. Additional hilar artery: Right/left/bilateral
2. Superior renal polar artery: Right/left/bilateral
3. Inferior renal polar artery: Right/left/bilateral.

Additional hilar artery was seen in 83/208 (39.9%) cases on the right side, 58/208 (27.9%) cases on the left side and 25/208 (12%) cases on both the sides.

Superior renal polar artery was seen in 19/208 (9.2%) cases on the right side, 14/208 (6.8%) cases on the left side and 3/208 (1.4%) cases on both the sides. Inferior renal polar artery was seen in 3/208 (1.4%) cases on the right side, 3/208 (1.4%) cases on the left side, while there was no single case with bilateral inferior polar artery.

The polar arteries were seen in total 42 cases. In 36/42 cases, there was superior renal polar artery [Figure 10]. In 6/42 cases, there was inferior renal polar artery [Figure 11].

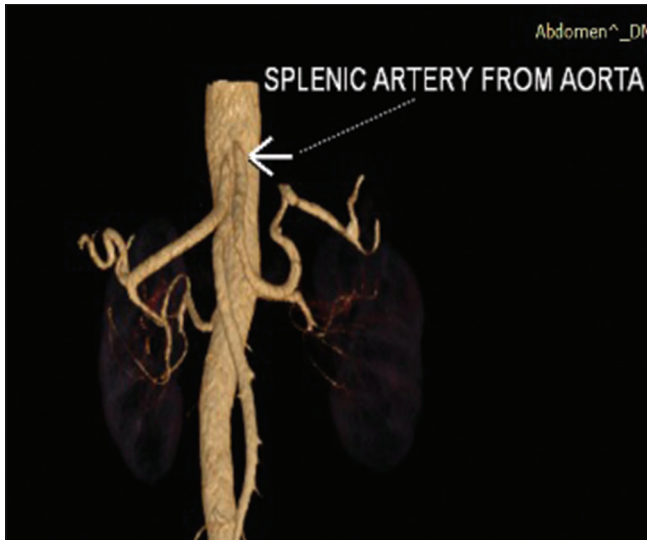


Figure 8: Image showing splenic artery from the aorta

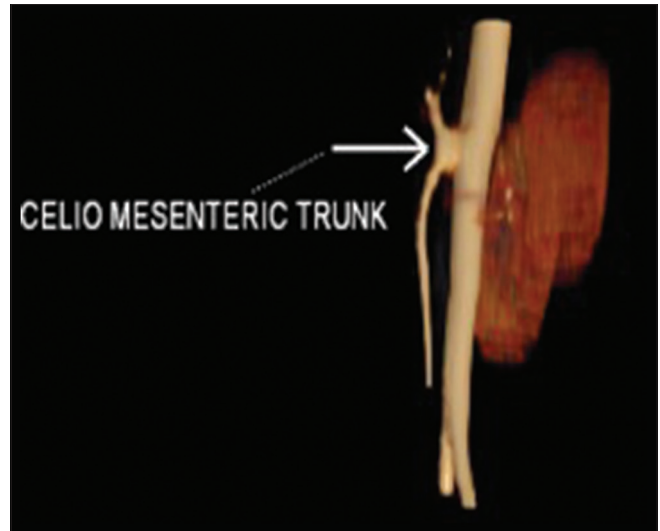


Figure 9: Image showing celiac- Mesenteric Trunk

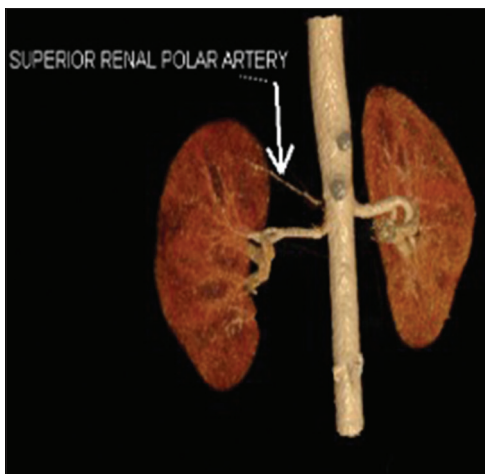


Figure 10: Image showing superior renal polar artery

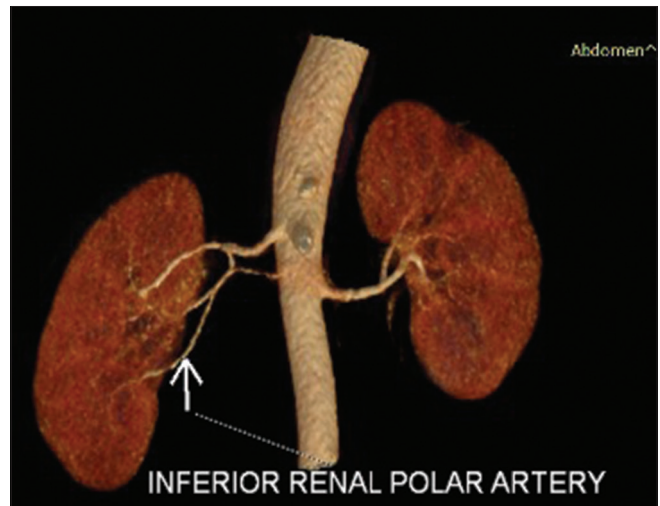


Figure 11: Image showing inferior renal polar artery

Table 2: Types of the variants of the celiac trunk observed in the cases included in the study

Variant celiac axis anatomy	Number of cases, <i>n</i> (%)
Replaced RHA	68 (13.7)
Accessory LHA	48 (9.5)
Replaced LHA	25 (5)
LGA from aorta	9 (1.8)
CHA from aorta	8 (1.6)
Accessory RHA	7 (1.4)
RHA from CA	5 (1)
RHA from aorta	1 (0.2)
Splenic artery from aorta	1 (0.2)
Common origin of celiac axis and SMA	1 (0.2)
Total	173 (34.6)

RHA: Right hepatic artery, LHA: Left hepatic artery, CHA: Common hepatic artery, LGA: Left gastric artery, SMA: Superior mesenteric artery, CA: Coronary artery

The cases with early branching were further divided into three categories: early branching on the right side

seen in 43/500 (8.6%) cases and on the left side seen in 29/500 (5.8%) cases and on both the sides in 4/500 (0.8%) cases [Table 6].

Discussion

During human embryogenesis, four roots of omphalomesenteric artery arise from abdominal aorta and are interconnected by a ventral longitudinal anastomosis. Two central roots of these four aortic branches disappear during embryogenesis, and the first and fourth roots connect to each other with longitudinal anastomosis. The splenic, left gastric, and CHA will come from this longitudinal anastomosis and the SMA from the fourth roots of the omphalomesenteric artery. Remain or regression of any of these arteries leads to the development of vascular variations of the celiac trunk or SMA.^[8] In the past, preoperative evaluation of hepatic resection candidates consisted of both noninvasive and invasive studies,

Table 3: Types of origin of superior mesenteric artery

SMA	Number of cases, n (%)
Normal origin	499 (99.8)
Variant origin	1 (0.2)
Total	500 (100.0)

SMA: Superior mesenteric artery

Table 4: Types of renal artery in the study group

Renal artery in the study group	Cases (%)
Single	292 (58.4)
Accessory renal artery	208 (41.6)
Total	500 (100)

Table 5: Types of accessory renal artery and their further distribution

Accessory renal artery	n (%)
Additional hilar artery	
Right	83 (39.9)
Left	58 (27.9)
Both	25 (12)
Superior renal polar artery	
Right	19 (9.2)
Left	14 (6.8)
Both	3 (1.4)
Inferior renal polar artery	
Right	3 (1.4)
Left	3 (1.4)
Both	0
Total	208 (100)

Table 6: Distribution of the cases with single renal artery and with early branching

Types of renal arteries	n (%)
Single	424 (84.8)
Single with early branching	
Right	43 (8.6)
Left	29 (5.8)
Both	4 (0.8)
Total	500 (100)

including computed tomography (CT), MRI, CT arterial portography, and conventional angiography.^[9-11] More recently, CT has been combined with three-dimensional CT angiography for the depiction of the vascular anatomy. Preoperative knowledge of variant arterial anatomy may reduce extensive exploration during surgery and consequently decrease the risk of vascular damage. In the classic anatomy, the celiac trunk was divided into three branches, LGA and then CHA and splenic artery. The CHA artery bifurcates into the gastroduodenal artery and the proper hepatic artery. Hepatic artery proper divides into RHA and LHA. In this study, classical hepatic arterial anatomy was seen in 327 (65.4%) of the patients who

underwent CT abdomen, while the previous studies showed different results, i.e., 89% by Michel,^[12] 51% by Winston *et al.*,^[13] 66% by De Cecco *et al.*,^[11] 89% by Song *et al.*,^[14] and 91% by Sureka *et al.*^[15] The most common frequent variant in this study was a replaced RHA originating from SMA, seen in 68 (13.6%) of patients. It was found in 15% and 9.2% of patients in a study of Winston and Cecco, respectively. Accessory arteries provide an additional source of blood supply to the hepatic lobes. These accessory arteries needed to be occluded separately when surgeons want to control inflow to hepatic lobes. Replaced LHA was observed in 25 (5.0%) of patients. The prevalence of this variation in Cecco *et al.*'s study was 5.2%, and it was observed in 8% of patients in the study of both Winston and Michel. Before the left hepatectomy, this variant should be identified and ligated.^[11-13,16,17] Accessory RHA was observed in 7 (1.4%) patients. On the other hands, variant arterial anatomy has an important role in chemotherapy as an adjuvant to resection in controlling hepatic disease. The hepatic variant artery can result in a nonuniform perfusion of the chemotherapeutic agent through the liver so a replaced or accessory artery should be ligated during chemotherapy.^[18-21] The common trunk of the celiac artery and the SMA is a rare variation and according to the earlier studies, it has been observed in <2% of patients.^[22,23] In our research, it was observed in 1 (0.2%) of patients. In 5 (1.0%) patients, the RHA was seen to arise directly from the celiac trunk. In 1 (0.2%) patient, the RHA was seen to arise directly from aorta. An unusual course of RHA that originates from the celiac axis or aorta may result in iatrogenic injury to this vessel if the location of the vessel is unknown for the surgeon. Eight (1.6%) patients had CHA artery from the aorta and 9 (1.8%) patients had LGA directly from the aorta. Splenic artery arising directly from the aorta was observed in 1 (0.2%) patient in our study.

Among all abdominal aorta ramifications, renal arteries show the highest anatomical variability. In our study, variants of the renal arteries were significantly more frequent (56.8%) than the variants of the celiac trunk (34.6%) of patients or of the variant origin of SMA (0.2%).

There are a few theories about the embryonic origin of the renal vasculature.^[24,25] Vasculature development is strictly dependent on the cephalic migration of the kidneys during embryogenesis. If their final location is atypical, renal vasculature may also be atypical, which can be explained by arterial vasculature adjustments to the location of the kidneys.^[26] In our study group, the atypical kidney location was not observed, and thus, the additional renal arteries were probably the remains of the mesonephric blood vessels, giving rise to the renal artery.^[27] Renal vessel variations are not contraindications for transplant surgery, but having knowledge about the presence of these vessels and their courses will prevent the possible injuries or bleedings and prolonged ischemia of graft. Therefore, all

accessory or polar arteries must be anastomosed in order to reduce surgery duration and risk of graft ischemia.

In our study, including 500 patients, the prevalence of accessory renal artery was observed in 208 (41.6%) patients with additional hilar artery observed in 166 patients, superior renal polar arteries observed in 36 patients, and inferior renal polar arteries observed in 6 patients. We observed more accessory RAs on the right side, studies done by Ozkan *et al.*,^[28] Holden *et al.*,^[29] and Ugurel *et al.*^[30] reported that accessory renal arteries were more frequently observed on the right side.

Most of the studies that have investigated the prevalence of accessory renal arteries were based on autopsy or digital subtraction angiography (DSA) findings. The prevalence of accessory renal arteries varies between 9% and 76% in the literature, and the general average in postmortem studies is 28%–30%.^[31,32] In the study by Ozkan *et al.*, including DSA examinations obtained in 855 patients, the prevalence of accessory renal artery was 24%. In a study by Ugurel *et al.*, the incidence of the accessory renal artery was 42% and accessory renal arteries were on the right side in the majority of patients.^[30]

Although Khamanarong *et al.*^[31] detected higher polar arteries than hilar arteries in their study, we detected higher frequency for hilar arteries than for polar arteries.

In our study, the pattern of early branching was observed in 76 (15.2%) patients with early branching on the right was in 43 cases, on the left in 29 cases. In the literature, the prevalences reported for early branching in the main renal artery vary between 4.3% and 13%.^[33,34] In the study by Raman *et al.*,^[35] the early branching frequency on the right side was 15% and 21% on the left side. The rate of early branching we determined is slightly higher than the rate specified in the literature for early branching.

To provide an easier hemorrhage control, the renal artery incision should be done 1.5–2 cm distal from the aortic origin. Therefore, it is very important to determine early branching of the main renal artery. It is also essential to measure the length and caliber of hilar and polar arteries (though not done in our study) and look for branches arising from these arteries as anomalous origin of testicular arteries can be seen from polar arteries in rare cases.^[36]

Hence, anatomical variations in the origin, number, and branching of renal arteries are very useful for planning and performing endovascular and laparoscopic surgeries for urological pathologies and can be helpful for the development of new medical devices for future treatment strategies.^[37]

Conclusion

The results of the present study showed that anatomical variation occurs in a high percentage of patients. In the

celiac axis, it occurred in 34.6% of cases out of which most common variant was a replaced RHA in 3.7% cases. The second most common was an accessory LHA arising from LGA 9.5%. Replaced LHA was observed in 5.0% of patients, and accessory RHA was observed in 1.4% of patients. Origin of the CHA (from the aorta) was observed in 1.6% of patients. RHA originated from the celiac axis in 1.0% of patients and from the aorta in 0.2% of patient. LGA from the aorta was observed in 1.8% of patients. Splenic artery originating from the aorta was observed in 0.2% of patient.

Celiaco-mesenteric trunk was observed in 0.2% of patients.

Out of 500 cases, on evaluation for renal arteries, single renal artery was observed in 43.2% cases, while there was presence of accessory renal artery in 41.6% cases and early branching in 15.2% cases. The accessory hilar artery was observed in 39.9% cases on the right side, 27.9% cases on the left side and 12% on both the sides.

The superior renal polar artery was observed in 9.2% of cases on the right side, 6.8% of cases on the left side and 1.4% of cases on both the sides.

Inferior renal polar artery was observed in 1.4% of cases on the right side, 1.4% of cases on the left side, while there was no single case with bilateral inferior polar artery.

Early branching on the right side was observed in 8.6% of cases, early branching on the left side seen in 5.8% cases, and early branching on both the sides in 0.8% cases.

Financial support and sponsorship

Nil.

Conflicts of interest

There are no conflicts of interest.

References

1. Kau T, Sinzig M, Gasser J, Lesnik G, Rabitsch E, Celedin S, *et al.* Aortic development and anomalies. *Semin Intervent Radiol* 2007;24:141-52.
2. Osman AM, Abdrabou A. Celiac trunk and hepatic artery variants: A retrospective preliminary MSCT report among Egyptian patients. *Egypt J Radiol Nucl Med* 2016;47:1451-8.
3. Sahani D, Mehta A, Blake M, Prasad S, Harris G, Saini S. Preoperative hepatic vascular evaluation with CT and MR angiography: Implications for surgery. *Radiographics* 2004;24:1367-80.
4. Kornafel O, Baran B, Pawlikowska I, Laszczyński P, Guziński M, Sasiadek M. Analysis of anatomical variations of the main arteries branching from the abdominal aorta, with 64-detector computed tomography. *Pol J Radiol* 2010;75:38-45.
5. Prakash, Mokhasi V, Rajini T, Shashirekha M. The abdominal aorta and its branches: Anatomical variations and clinical implications. *Folia Morphol (Warsz)* 2011;70:282-6.
6. Pennington N, Soames RW. The anterior visceral branches of the abdominal aorta and their relationship to the renal arteries. *Surgical and radiologic anatomy* 2005;27:395-403.
7. Fiorello B, Corsetti R. Splenic artery originating from the

- superior mesenteric artery: An unusual but important anatomic variant. *Ochsner J* 2015;15:476-8.
8. Farghadani M, Momeni M, Hekmatnia A, Momeni F, Baradaran Mahdavi MM. Anatomical variation of celiac axis, superior mesenteric artery, and hepatic artery: Evaluation with multidetector computed tomography angiography. *J Res Med Sci* 2016;21:129.
 9. Saba L, Mallarini G. Multidetector row CT angiography in the evaluation of the hepatic artery and its anatomical variants. *Clin Radiol* 2008;63:312-21.
 10. Prabhasavat K, Homgade C. Variation of hepatic artery by 3-D reconstruction MDCT scan of liver in Siriraj Hospital. *J Med Assoc Thai* 2008;91:1748-53.
 11. De Cecco CN, Ferrari R, Rengo M, Paolantonio P, Vecchiotti F, Laghi A. Anatomic variations of the hepatic arteries in 250 patients studied with 64-row CT angiography. *Eur Radiol* 2009;19:2765-70.
 12. Michels NA. Blood Supply and Anatomy of the Upper Abdominal Organs with a Descriptive Atlas. Philadelphia, PA: Lippincott; 1955.
 13. Winston CB, Lee NA, Jarnagin WR, Teitcher J, DeMatteo RP, Fong Y, *et al.* CT angiography for delineation of celiac and superior mesenteric artery variants in patients undergoing hepatobiliary and pancreatic surgery. *AJR Am J Roentgenol* 2007;189:W13-9.
 14. Song SY, Chung JW, Yin YH, Jae HJ, Kim HC, Jeon UB, *et al.* Celiac axis and common hepatic artery variations in 5002 patients: Systematic analysis with spiral CT and DSA. *Radiology* 2010;255:278-88.
 15. Sureka B, Mittal MK, Mittal A, Sinha M, Bhambri NK, Thukral BB. Variations of celiac axis, common hepatic artery and its branches in 600 patients. *Indian J Radiol Imaging* 2013;23:223-33.
 16. Blumgart LH, Fong Y. *Surgery of the Liver and Biliary Tract*. New York: Saunders; 2000. p. 10-4.
 17. Kapoor V, Brancatelli G, Federle MP, Katyal S, Marsh JW, Geller DA. Multidetector CT arteriography with volumetric three-dimensional rendering to evaluate patients with metastatic colorectal disease for placement of a floxuridine infusion pump. *AJR Am J Roentgenol* 2003;181:455-63.
 18. Allen PJ, Stojadinovic A, Ben-Porat L, Gonen M, Kooby D, Blumgart L, *et al.* The management of variant arterial anatomy during hepatic arterial infusion pump placement. *Ann Surg Oncol* 2002;9:875-80.
 19. Hazirolan T, Metin Y, Karaosmanoglu AD, Canyigit M, Turkbey B, Oguz BS, *et al.* Mesenteric arterial variations detected at MDCT angiography of abdominal aorta. *AJR Am J Roentgenol* 2009;192:1097-102.
 20. Yi SQ, Terayama H, Naito M, Hayashi S, Moriyama H, Tsuchida A, *et al.* A common celiacomesenteric trunk, and a brief review of the literature. *Ann Anat* 2007;189:482-8.
 21. Yilmaz MT, Tezer M, Cicekcibasi AE, Aydin AD, Salbacak A. A case report of coeliacomesenteric trunk. *Biomed Res* 2013;24:150-2.
 22. Nebesar RA, Kornblith PL, Pollard JJ, Michels NA. *Celiac and Superior Mesenteric Arteries: A Correlation of Angiograms with Dissections*. Boston Little: Brown; 1969.
 23. Tandler J. About the varieties of the celiac artery and their development. *Anat Hefte* 1904;25:473-500.
 24. Saldarriaga B, Pérez AF, Ballesteros LE. A direct anatomical study of additional renal arteries in a Colombian mestizo population. *Folia Morphol (Warsz)* 2008;67:129-34.
 25. Sykes D. The arterial supply of the human kidney with special reference to accessory renal arteries. *Br J Surg* 1963;50:368-74.
 26. Satyapal KS, Haffeejee AA, Singh B, Ramsaroop L, Robbs JV, Kalideen JM. Additional renal arteries: Incidence and morphometry. *Surg Radiol Anat* 2001;23:33-8.
 27. Bochenek A, Reicher M. *Anatomia Człowieka*. Vol. 2. Warszawa: PZWL; 2006. p. 512-5, 3:284-9, 272-93.
 28. Ozkan U, Oguzkurt L, Tercan F, Kizilkiliç O, Koç Z, Koca N. Renal artery origins and variations: Angiographic evaluation of 855 consecutive patients. *Diagn Interv Radiol* 2006;12:183-6.
 29. Holden A, Smith A, Dukes P, Pilmore H, Yasutomi M. Assessment of 100 live potential renal donors for laparoscopic nephrectomy with multi-detector row helical CT. *Radiology* 2005;237:973-80.
 30. Ugurel MS, Battal B, Bozlar U, Nural MS, Tasar M, Ors F, *et al.* Anatomical variations of hepatic arterial system, coeliac trunk and renal arteries: An analysis with multidetector CT angiography. *Br J Radiol* 2010;83:661-7.
 31. Khamanarong K, Prachaney P, Utraravichien A, Tong-Un T, Sripaoraya K. Anatomy of renal arterial supply. *Clin Anat* 2004;17:334-6.
 32. Ollivier R, Boulmier D, Veillard D, Leurent G, Mock S, Bedossa M, *et al.* Frequency and predictors of renal artery stenosis in patients with coronary artery disease. *Cardiovasc Revasc Med* 2009;10:23-9.
 33. Rydberg J, Kopecky KK, Tann M, Persohn SA, Leapman SB, Filo RS, *et al.* Evaluation of prospective living renal donors for laparoscopic nephrectomy with multisection CT: The marriage of minimally invasive imaging with minimally invasive surgery. *Radiographics* 2001;21:S223-36.
 34. Kim JK, Park SY, Kim HJ, Kim CS, Ahn HJ, Ahn TY, *et al.* Living donor kidneys: Usefulness of multi-detector row CT for comprehensive evaluation. *Radiology* 2003;229:869-76.
 35. Raman SS, Pojchamarnwiputh S, Muangsomboon K, Schulam PG, Gritsch HA, Lu DS. Surgically relevant normal and variant renal parenchymal and vascular anatomy in preoperative 16-MDCT evaluation of potential laparoscopic renal donors. *AJR Am J Roentgenol* 2007;188:105-14.
 36. Ganapathy A, Banerjee A, Jhajhria SK, Singh S. A rare case of anomalous origin of bilateral testicular arteries: An anatomical and developmental overview. *J Anat Soc India* 2021;70:173.
 37. Patil RA, Chowki PA. Comparison of human renal arteries in cadavers and in computed tomography scans – A morphometric study. *J Anat Soc India* 2021;70:233.

Sternalis Muscle in Living Individuals Identified with Computed Tomography

Abstract

Introduction: The sternalis muscle is a rare muscular variation of the anterior thoracic wall. When present, it can confuse the radiologists as a breast mass on mammograms and pose as a challenge and opportunity at the same time for surgeons during mastectomies or breast augmentation procedures. This study aims to investigate the frequency and anatomy of the sternalis muscle on a large Turkish sample. **Material and Methods:** Following ethical approval, the presence and anatomy of the sternalis muscle was investigated on thoracic computed tomography (CT) scans of 8408 patients. **Results:** The sternalis muscle was present in 263 (3.1%) patients. The presence of the muscle was unilateral on the right side in 104 (39.5%), unilateral on the left side in 96 (36.5%), and bilateral in 63 (24%) patients. In 326 hemithoraces, Type 1, Type 2, and Type 3 sternalis muscles were observed in 79.2%, 14.4%, and 6.4% of the patients, respectively. **Discussion and Conclusion:** The frequency of the sternalis muscle among the Turkish population was relatively lower compared to the previous studies on different ethnicities. In addition, CT provides a detailed evaluation of the muscle.

Keywords: Anatomy, computed tomography, sternalis muscle

Introduction

The sternalis muscle is an infrequent musculoskeletal variation at the anterior thoracic wall.^[1] Its presence is relevant for radiologists because it might appear as a mass at medial breast during routine mammograms and could be misdiagnosed as a breast mass lesion.^[2] Similarly, an unrecognized sternalis muscle before breast augmentation surgery may lead to confusion.^[3] These cases identified during surgery may cause complications, prolong surgery time, or result in asymmetric implants with poor esthetic outcomes.^[3-5] Conversely, a sternalis muscle identified before surgery could be used as a muscular flap in reconstructive breast surgery as well as neck surgery.^[5,6]

The frequency of the sternalis muscle varies among studies with different methodologies. The lowest frequencies were reported by mammography studies with an average frequency of 0.02%.^[7] These low frequencies were attributed to the limited imaging field in mammograms.^[8] Similarly, surgical studies underreport the presence of the sternalis muscle with an average frequency of 0.48%.^[7] Lack of surgeon's

knowledge on sternalis muscle or surgical removal of the muscle along with the breast tissue was proposed for the low frequencies in these studies.^[7,9]

In contrast to X-ray and surgical studies, cadaveric studies and studies performed with computed tomography (CT) report higher frequencies of sternalis muscles with similar results.^[7] For cadaveric studies, the overall frequency of sternalis muscle is around 7.8% (1%–23.5%), while CT studies report an average frequency of 6.4% (0.87%–10.5%).^[1,7,10,11]

The previous CT studies evaluated the sternalis muscle in large samples and provided the frequencies for the Chilean, Japanese, Korean, and Chinese populations.^[10-13] CT also could provide detailed information on sternalis muscle anatomy.^[13]

This study aims to investigate the frequency and morphology of the sternalis muscle in a large-scale Turkish population using CT images.

Material and Methods

Patient population

This retrospective study was performed at Haseki Research and Training Hospital

How to cite this article: Türkay R, Özdemir S, Göçgün N, Can TS, Yılmaz BK, İkizceli T, *et al.* Sternalis muscle in living individuals identified with computed tomography. *J Anat Soc India* 2022;71:135-9.

**Rüstü Türkay,
Sevim Özdemir,
Nurdan Göçgün,
Tuba S. Can,
Behice K. Yılmaz,
Türkan İkizceli,
Ilke Ali Gürses¹**

*Department of Radiology,
University of Health Science,
Haseki Training and Research
Hospital, ¹Department of
Anatomy, Istanbul Faculty of
Medicine, Istanbul University,
Istanbul, Turkey*

Article Info

Received: 11 December 2021

Revised: 08 April 2022

Accepted: 18 April 2022

Available online: 30 June 2022

Address for correspondence:

*Dr. Sevim Özdemir,
Department of Radiology,
University of Health Science,
Haseki Training and Research
Hospital, Istanbul, Turkey.
E-mail: sevimozdemir76@
yahoo.com*

Access this article online

Website: www.jasi.org.in

DOI:
10.4103/jasi.jasi_204_21

Quick Response Code:



This is an open access journal, and articles are distributed under the terms of the Creative Commons Attribution-NonCommercial-ShareAlike 4.0 License, which allows others to remix, tweak, and build upon the work non-commercially, as long as appropriate credit is given and the new creations are licensed under the identical terms.

For reprints contact: WKHLRPMedknow_reprints@wolterskluwer.com

between June and September of 2020. Institutional review board approval was obtained before the study (Date: August 19, 2020; Number: 2020-136). Thorax CT scans of 8552 individuals aged between 3 and 94 years who were admitted to the radiology department with various indications between January 2019 and April 2020 were evaluated.

Patients with suboptimal images (images with artifacts due to motion, implants, etc.), breast implants, and prior thoracotomy were excluded from the study. Patients with more than one thoracic examinations were evaluated only once, and the first scans of these patients were used for the evaluation. Therefore, 8408 (4656 men, 3752 women; mean age 42 years) patients were included in the study. In addition, patients were grouped according to age intervals of 10 years. Although the patients who were 19 and younger were appointed into the same group due to the small sample size of patients younger than 10 ($n = 40$). Similarly, patients older than 90 ($n = 5$) were appointed into the group over 80 years of age.

Computed tomography protocol

CT data were acquired using a 128 detector CT scanner (PHILIPS Ingenuity, Netherlands). The parameters used for the scanning protocol were as follows: the patient was in the supine position and end inspiratory acquisition tube voltage, 120 kV; tube current–exposure time product, 200–300 mAs and section thickness after reconstruction, 1.25 mm. CT scans were obtained without contrast material administration.

Image analysis

A local workstation (Syngo Via, Siemens Medical Solution, Erlanger, Germany) was used to evaluate all images. Multiplanar reformation reconstructions were obtained with Synapse Picture Archiving and Communication Systems, (Panathes Medical systems, Turkey) in order to evaluate images on axial, sagittal, and coronal planes. In addition, maximum intensity projections (MIP) were used to evaluate the anterior thoracic wall in detail.

A muscle with a craniocaudal course that is located superficial to the pectoralis major was accepted as the sternalis muscle. Images of the patients who had a sternalis muscle were further evaluated with MIP in order to outline the shape and location of the muscles. The morphology of the muscles was classified regarding the number of heads and bellies.^[13]

Statistical analysis

The SPSS statistical package, version 21 (IBM Corp., Armonk, NY, USA) was used to perform the statistical analyses. The one-way analysis of variance test was used to compare the mean ages for different sternalis muscle morphologies. The Chi-square test was used to compare sternalis frequencies between sexes and age groups. $P < 0.05$ was accepted as statistically significant.

Results

The sternalis muscle was identified in 263 (3.1%) patients. The presence of a sternalis muscle had a similar frequency for females (121/3752, 3.2%) and males (142/4656, 3%), which did not reach statistical significance ($X^2 = 0.21$, $P = 0.65$). The patients with and without sternalis muscles had an average age of 41.4 ± 13.3 and 42.1 ± 15.2 , respectively. The average age did not show significant differences between two groups ($t = 0.763$, $P = 0.45$). The frequency of the sternalis muscle did not change with increasing age ($X^2 = 8.81$, $P = 0.27$). Similarly, the presence of bilateral sternalis muscles did not change over the decades ($X^2 = 11.77$, $P = 0.62$) [Table 1].

Among the 263 patients who had sternalis muscle, 104 (39.5%) had a right sternalis muscle, 96 (36.5%) had a left sternalis muscle, and 63 (24%) had bilateral sternalis muscles. The presence of bilateral sternalis muscles was more frequent in females (33/121, 27.3% vs. 30/142, 21.1%), but this difference did not reach statistical significance ($X^2 = 1.572$, $P = 0.46$) [Table 2].

The sternalis muscle was located superficial to the pectoralis major muscle coursing longitudinally at the anterior thoracic wall [Figure 1], sometimes exceeding medially over the sternum [Figure 1]. Multiplanar and MIP images revealed that the muscle had three morphological types. Type 1 muscles had a single head and belly, Type 2 muscles were double or multiheaded, and Type 3 muscles were double or multi bellied [Figure 2]. The

Table 1: Frequency of sternalis muscle presence among age groups

Age groups	Absence of sternalis muscle (%)	Unilateral presence of sternalis muscle (%)	Bilateral presence of sternalis muscle (%)	P
0-19	411 (97.6)	6 (1.4)	4 (1)	0.62
20-29	1472 (97.0)	35 (2.3)	10 (0.7)	
40-49	1990 (96.3)	61 (3)	16 (0.8)	
50-59	1348 (96.8)	34 (2.4)	10 (0.7)	
60-69	734 (97.6)	14 (1.9)	4 (0.5)	
70-79	272 (98.9)	3 (1.1)	0 (0)	
>80	103 (97.2)	2 (1.9)	1 (0.9)	

Values are presented as number of cases - frequency within age group

Table 2: Frequency of sternalis muscles among sexes

Sexes	Absence of sternalis muscle (%)	Unilateral presence of sternalis muscle (%)	Bilateral presence of sternalis muscle (%)	Total (%)
Females	3631 (96.8)	88 (2.3)	33 (0.9)	121 (3.2)
Males	4514 (97)	112 (2.4)	30 (0.6)	142 (3)

Values are presented as number of cases - frequency within age group

sternalis muscle had a lower thoracic or upper abdominal wall origin. Identifying the termination of the muscle in all patients was not possible; therefore, these data were excluded from the study.

Among the study population (263 cases), the sternalis muscle was observed in 326 hemithoraces. The frequency for Type 1, Type 2, and Type 3 sternalis muscles within all hemithoraces were 79.2%, 14.4%, and 6.4%, respectively [Table 3].

Discussion

The sternalis muscle is a rare band-shaped muscle variant of the anterior thoracic wall with a highly variable morphology.^[14] Its upper attachment includes the sternum, clavicle, and upper ribs and their costal cartilages, while its lower attachment includes the rectus sheath, external oblique aponeurosis, and lower ribs and their costal cartilages.^[1,7,13-18] Similarly, the morphology of the belly of the muscle could range from a few muscle fibers to

a large strap muscle easily recognized during gross dissections.^[1,7]

Despite its variable anatomy, the sternalis muscle has a relevant clinical significance for diagnostic and surgical procedures involving the anterior chest wall.^[4-6,8,19] Especially, during routine mammographic evaluation, it could be seen as an asymmetric opacity at the medial posterior edge of craniocaudal mammograms, mimicking mass lesions of the breast.^[2,8] Rarely, it could be seen as a longitudinally running opacity in mediolateral oblique views as well.^[8] In such cases, it is noteworthy that an obtuse angle on craniocaudal mammograms usually indicates a muscular structure.^[20] Similarly, it usually is surrounded with fat, which could be confirmed with ultrasonography,^[21] magnetic resonance imaging,^[22] or CT^[12,13] as the underlying fatty tissue separating the sternalis from the pectoralis major muscle.

Unlike radiology practice, the presence of a sternalis muscle in surgical practice could be advantageous and disadvantageous in different situations. For example, the sternalis and pectoralis major muscles could be used as a conjoint muscle flap in reconstructing the breast following mastectomy or soft-tissue defects following head-and-neck carcinomas.^[5,6] Although the presence of sternalis muscle results in a smaller pocket for breast implants with a submuscular approach, including the sternalis to submuscular dissection is advised for expanding the inadequate medial dissection.^[5] In addition, a submuscular approach is reported to provide more cover for the breast implant at the lower parasternal region in thin individuals, resulting in a more satisfactory outcome.^[4] Schulman and



Figure 1: The anatomy of the sternalis muscle is shown on images of 22-year-old male (a), 56-year-old male (b and c), and 39-year-old male (d) patients. The sternalis muscle has an oblique course (a and b) on the anterior thoracic wall that gets closer to the midline as it ascends (a). The muscle lies superficial to the pectoralis major muscle and is separated from the pectoralis major muscle with a thin fatty layer (c) which is more prominent in some individuals. Despite its oblique course, some sternalis muscles course more medially and cover the sternal body (d)

Table 3: Frequencies for sternalis muscle morphological types

	Sternalis muscle morphological types (%)			
	Type 1	Type 2	Type 3	Total
Unilateral right	86 (82.7)	13 (12.5)	5 (4.8)	104 (100)
Unilateral left	78 (81.3)	15 (15.6)	3 (3.1)	96 (100)
Bilateral	94 (74.6)	19 (15.1)	13 (10.3)	126 (100)
Total	258 (79.2)	47 (14.4)	21 (6.4)	326 (100)

Values are presented as the number of cases - frequency within the group



Figure 2: Types of sternalis muscles are shown on images of 43-year-old male (a), 22-year-old male (b), and 51-year-old female (c) patients. Muscles with a single head and belly were classified as Type 1 (a), muscles with double or multi heads were classified as Type 2 (b), and muscles with double or multi bellies were classified as Type 3 (c)

Chun emphasized the inclusion of the sternalis muscle in conjoint muscle flap because it provided additional coverage due to the smaller nature of accompanying pectoralis major muscle.^[5,7] Nevertheless, the presence of a sternalis muscle might hinder the detection of the dissection plane due to its superficial location and prolong surgery time.^[3,5]

During modified radical mastectomy, the pectoralis fascia is excised along with the breast tissue.^[23] The sternalis muscle which lies superficial to the pectoralis fascia when present might pose as a challenge during breast cancer surgery. Incidental detection of the muscle during surgery usually causes an expanded dissection for complete identification of the muscle, thus prolonging surgery time.^[3,23,24] In addition, the decision of removing or sparing the muscle might cost more time during the surgery. Removal of the sternalis muscle was advised if it had a proximity to the primary breast tumor or presence of additional breast tissue underneath it.^[23] On the other hand, the muscle could be spared since the resection of muscle tissue during modified radical mastectomy does not improve patient survival.^[24] Nevertheless, recording this decision and informing the radiologists for future follow-ups is highly recommended.^[24]

There is a distinct discrepancy between reported frequencies for the sternalis muscle. Mammographic studies especially provide frequencies as low as 0.02%.^[2,7,8,18] Similarly, incidental identification of sternalis muscles in patients who underwent modified radical mastectomy or augmentation mammoplasty is around 0.3%–0.7%.^[4,9] This clinical underreporting had been associated with improper patient positioning, low-quality image resolution, or lack knowledge and awareness of this muscle among surgeons, radiologists, residents, and medical students.^[7,25] Although cadaveric studies report the highest frequencies as up to 23.5%, only a few cadaveric studies report reliable big samples.^[1,7] In addition, slender muscles might be overlooked during routine dissection practices resulting in improper reporting of its frequency.^[7]

Conversely, modern modalities, such as CT and magnetic resonance imaging, are highly sensitive for identifying this muscle variant.^[7] They provide detailed information, including the superficial location of the muscle to the pectoralis major muscle and the thin fat tissue between them.^[13,21] Investigations on sternalis muscle performed with CT report a frequency of 0.87% for the Chilean, 5.8% for the Chinese, 6.2% for the Korean, and 10.5% for the Japanese populations.^[10-13] Moreover, these studies evaluated large samples ranging from 948 to 6000. A previous Turkish study reported a sternalis muscle frequency of 0.02%. The study of Demirpolat G *et al.* investigated 52,930 mammographies and was limited to female patients only and by its methodology with low sensitivity.^[8] Furthermore, there are no cadaveric studies other than case reports among the Turkish population.^[26] Although the results of this study report a relatively low

frequency of 3.1% for the Turkish population, it provides a higher frequency for the sternalis muscle, similar to cadaveric and previous tomographic studies.

Conclusion

This study reported the frequency of the sternalis muscle in a big Turkish sample of 8408 patients. Despite its low recognition among surgeons, radiologists, and students and current discrepancies between radiologic and surgical studies, knowledge on the anatomy of the sternalis muscle has clinical impact.

Financial support and sponsorship

Nil.

Conflicts of interest

There are no conflicts of interest.

References

1. Jelev L, Georgiev G, Surchev L. The sternalis muscle in the Bulgarian population: Classification of sternales. *J Anat* 2001;199:359-63.
2. Bradley FM, Hoover HC Jr., Hulka CA, Whitman GJ, McCarthy KA, Hall DA, *et al.* The sternalis muscle: An unusual normal finding seen on mammography. *AJR Am J Roentgenol* 1996;166:33-6.
3. Salval A, Scevola A, Baruffaldi Preis FW. Sternalis muscle: An uncommon finding during aesthetic breast surgery. *Aesthet Surg J* 2012;32:903-5.
4. Khan UD. Use of the rectus sternalis in augmentation mammoplasty: Case report and literature search. *Aesthetic Plast Surg* 2008;32:21-4.
5. Schulman MR, Chun JK. The conjoined sternalis-pectoralis muscle flap in immediate tissue expander reconstruction after mastectomy. *Ann Plast Surg* 2005;55:672-5.
6. Sari E, Oktem HF, Durgun M, Ozakpinar HR, Tellioglu AT. The sternalis muscle: An unusual finding during the reconstruction of the soft tissue defect of mouth floor and neck, a case report. *J Curr Surg* 2014;4:49-51.
7. Snosek M, Tubbs RS, Loukas M. Sternalis muscle, what every anatomist and clinician should know. *Clin Anat* 2014;27:866-84.
8. Demirpolat G, Oktay A, Bilgen I, Isayev H. Mammographic features of the sternalis muscle. *Diagn Interv Radiol* 2010;16:276-8.
9. Harish K, Gopinath KS. Sternalis muscle: Importance in surgery of the breast. *Surg Radiol Anat* 2003;25:311-4.
10. Molina CR, Pinochet JA, Heras AA, Taunton MJ, Letelier RG, Letelier RF. Prevalence of the sternalis muscle in Chilean population: A computed tomography study. *Ital J Anat Embryol* 2017;122:173-8.
11. Shiotani M, Higuchi T, Yoshimura N, Kiguchi T, Takahashi N, Maeda H, *et al.* The sternalis muscle: Radiologic findings on MDCT. *Jpn J Radiol* 2012;30:729-34.
12. Young Lee B, Young Byun J, Hee Kim H, Sook Kim H, Mee Cho S, Hoon Lee K, *et al.* The sternalis muscles: Incidence and imaging findings on MDCT. *J Thorac Imaging* 2006;21:179-83.
13. Ge Z, Tong Y, Zhu S, Fang X, Zhuo L, Gong X. Prevalence and variance of the sternalis muscle: A study in the Chinese population using multi-detector CT. *Surg Radiol Anat* 2014;36:219-24.

14. Snosek M, Loukas M. Thoracic wall muscles. In: Tubbs RS, Shoja MM, Loukas M, editors. *Bergman's Comprehensive Encyclopedia of Human Anatomic Variation*. New Jersey: Wiley Blackwell; 2016. p. 335-68.
15. Douvatzemis S, Natsis K, Piagkou M, Kostares M, Demesticha T, Troupis T. Accessory muscles of the anterior thoracic wall and axilla. Cadaveric, surgical and radiological incidence and clinical significance during breast and axillary surgery. *Folia Morphol (Warsz)* 2019;78:606-16.
16. Plakornkul V, Viravud Y. Sternalis muscle: Anatomical variations in Thais. *Siriraj Med J* 2012;64 Suppl 1:S19-21.
17. Raikos A, Paraskevas GK, Yusuf F, Kordali P, Ioannidis O, Brand-Saberi B. Sternalis muscle: A new crossed subtype, classification, and surgical applications. *Ann Plast Surg* 2011;67:646-8.
18. Saeed M, Murshid KR, Rufai AA, Elsayed SE, Sadiq MS. Sternalis. An anatomic variant of chest wall musculature. *Saudi Med J* 2002;23:1214-21.
19. Vaida MA, Damen NS, Jianu AM, Grigorita L. Sternalis and transversus thoracis muscles: An anatomical variation and its clinical implications. *J Anat Soc India* 2021;70:113-5.
20. De Parades ES. *Atlas of Mammography*. 3rd ed. Philadelphia: Lippincott, Williams & Wilkins; 2007. p. 8.
21. Nuthakki S, Gross M, Fessell D. Sonography and helical computed tomography of the sternalis muscle. *J Ultrasound Med* 2007;26:247-50.
22. Goktan C, Orguc S, Serter S, Ovali GY. Musculus sternalis: A normal but rare mammographic finding and magnetic resonance imaging demonstration. *Breast J* 2006;12:488-9.
23. Kabay B, Akdogan I, Ozdemir B, Adiguzel E. The left sternalis muscle variation detected during mastectomy. *Folia Morphol (Warsz)* 2005;64:338-40.
24. Kocaay F, Basceken SI, Akyol C, Sari T, Celik U, Oztanaci S, *et al.* The importance of sternalis muscle in breast surgery. *Anat Physiol* 2014;4:4. [Doi: 10.4172/2161-0940.1000160].
25. Bailey PM, Tzarnas CD. The sternalis muscle: A normal finding encountered during breast surgery. *Plast Reconstr Surg* 1999;103:1189-90.
26. Üçerler H, İkiz ZA, Bilge O, Orhan M. The sternalis muscle in a cadaver and an overview to its significance in clinical approaches. *Ege J Med* 2008;47:51-3.

Sub-Acromion Impingement Syndrome: Scapular Morphometric Analysis: A Study On Dry Bones among Eastern Indian Population

Abstract

Introduction: Among various factors responsible for the development of chronic shoulder pain worldwide, the role of scapula, as a bony factor, is very important. This study focuses on evaluating the scapular shape and contour as a determinant of sub-acromion impingement syndrome. This was a cross-sectional observational study conducted on dry bones. **Material and Methods:** Dry scapulae (42 right sided and 38 left sided) were studied by taking digital photographs in different views and analyzing various parameters (critical shoulder angle (CSA), glenoid inclination, shape of acromion process, etc.) using ImageJ analyzer. Results were analyzed using measures of central tendency, and statistical significance was analyzed by measuring *P* values with the help of SPSS software (v25). **Results:** There were 40% Type I, 38.75% Type II, and 21.25% Type III scapulae, respectively. The Type I and III scapulae showed significant variations on the basis of various acromion overhangs (anterior overhang was 9.03 mm and 11.08 mm in Types I and III, respectively, while for the lateral overhang, the values were 9.73 mm and 6.25 mm in Types I and III, respectively) and angles (lateral acromion angle was 79.5° and 71.9° for Types I and III, respectively, whereas the coraco-acromion angle was 37° and 30.8° in Types I and III, respectively). The glenoid inclination and CSA were also significantly variable between all three types of scapulae. **Discussion and Conclusion:** The scapular morphology plays a pivotal role which can be extrapolated on a radiological basis in pertinent patients to determine the chances of developing pathological shoulders in future.

Keywords: Acromion overhangs, critical shoulder angle, glenoid inclination, rotator cuff, scapula, sub-acromion impingement syndrome

Introduction

Rotator cuff (RC) injury is a predominant disease affecting multiple persons globally. The prevalence of the disease among US population was 33.8% unilaterally and 30.1% bilaterally.^[1] In Japanese population, the prevalence was 20.7%.^[2] Subacromial impingement syndrome (SIS) includes a spectrum of pathologies involving the subacromial space.^[3-5] Neer describes the subacromial space, bounded inferiorly by the humeral head and superiorly by the coraco-acromial arch.^[6] Both intrinsic (intra-tendinous) and extrinsic (extra-tendinous) factors play an important role in SIS.^[7-11] Most of the studies relating the scapular angles (critical shoulder angle [CSA] and glenoid inclination) were based on radiological imaging previously. These two parameters were mostly related to pathologies around

the shoulder including osteoarthritis, SIS, and RC tears of various degrees.^[12-14] The focus of this study is on the assessment of bony factors of scapula, which can contribute significantly in development of SIS.

Material and Methods

Eighty dry scapulae (42 right sided and 38 left sided) were collected from the museum of Kolkata-based medical college for purpose of the morphometric study. Bones with any morphological deformity or breakage were excluded from the study. The scapulae were divided into three groups following Bigliani *et al.*'s classification: Type I – flat acromion, Type II – curved acromion, and Type III – hooked acromion.^[15] For each scapula, four views were obtained with digital camera: lateral, anterior, posterior, and superior (with each scapula being held in anatomical position by a tripod). With the help of image

This is an open access journal, and articles are distributed under the terms of the Creative Commons Attribution-NonCommercial-ShareAlike 4.0 License, which allows others to remix, tweak, and build upon the work non-commercially, as long as appropriate credit is given and the new creations are licensed under the identical terms.

For reprints contact: WKHLRPMedknow_reprints@wolterskluwer.com

How to cite this article: Dutta M, Poddar R. Sub-acromion impingement syndrome: Scapular morphometric analysis: A study on dry bones among Eastern Indian population. *J Anat Soc India* 2022;71:140-5.

Madhumita Dutta, Ratnadeep Poddar¹

Department of Anatomy, Murshidabad Government Medical College and Hospital, Berhampore, ¹Department of Anatomy, Rampurhat Government Medical College and Hospital, Rampurhat, West Bengal, India

Article Info

Received: 01 August 2020

Revised: 19 October 2021

Accepted: 03 April 2022

Available online: 30 June 2022

Address for correspondence:

Dr. Ratnadeep Poddar,
Flat-2A, Gungun Apartment,
229/1, Maharani Indira Devi
Road, Behala Parnasree,
Kolkata - 700 060, West Bengal,
India.

E-mail: ratno.dp@gmail.com

Access this article online

Website: www.jasi.org.in

DOI:
10.4103/JASI.JASI_143_20

Quick Response Code:



analyzer (ImageJ), the following parameters were studied and analyzed.

Glenoid inclination

On posterior view, four points were marked. The angle formed at superolateral quadrant by intersection of two lines was considered glenoid inclination. This is shown in Figure 1.

Critical shoulder angle

This defines the position of glenoid fossa relative to the lateral-most point of acromion process. This angle is very much important from radiological point of view, as it determines the translation of humeral head against the scapula. This parameter was studied radiologically on multiple occasions previously.^[12,13] Figure 2 depicts the CSA.

Acromion overhangs

The extensions of acromion process over the sub-acromion space were represented by the anterior, posterior, and lateral acromion overhangs. They were determined in the superior view in relation to the posterior margin of the glenoid fossa, as shown in Figure 3. The posterior acromial overhang was the distance between the posterior edge of the glenoid and the anterior edge of the acromion on a line passing through the anterior and the posterior edges of the glenoid. The lateral acromial overhang was the distance between the posterior edge of the glenoid and the medial edge of the acromion on a line perpendicular to the glenoid surface. The anterior acromial overhang was the distance between the posterior edge of the glenoid and the intersection of lines passing through the anterior and posterior edges of the glenoid and a perpendicular line passing through the anterior end of the acromion.

Lateral acromion angle

This is the angle formed at the intersection of two lines – one drawn along the undersurface of acromion process and the other along the surface of glenoid fossa. This is shown in Figure 4.

Coraco-acromion angle

The coraco-acromial angle was the angle formed between a line passing through the axis of the coracoid process and a line perpendicular to the glenoid surface, joining the anterior end of the acromion on a superior view. This angle also indicates indirectly the shape and volume of sub-acromion space. It is calculated in the superior view, as shown in Figure 5.

Lateral coracoid angle

The lateral coracoid angle was measured on the lateral view. It was the angle between a line passing through the axis of the base of the coracoid process and a line passing through the vertical axis of the glenoid. This is again an

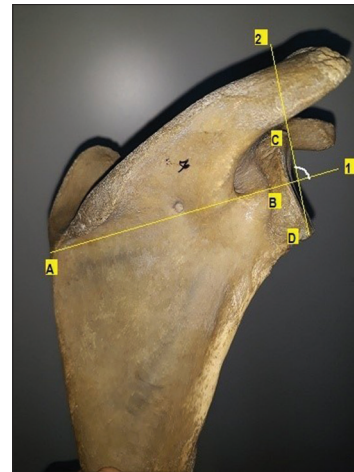


Figure 1: Glenoid inclination angle was calculated as the angle formed between line 1 and line 2. Line 1 was defined as connecting (A) the intersection of the scapular spine with the scapula's medial border and (B) the middle of the spinoglenoid notch. Line 2 was defined as connecting (C) the superior-most point on the glenoid rim and (D) the inferior-most point on the glenoid rim

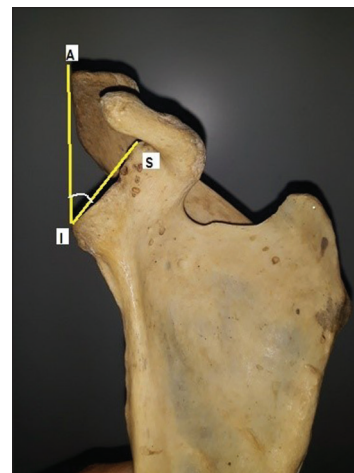


Figure 2: S – Supraglenoid tubercle; I – Infraglenoid tubercle; A – Lateral-most point on Acromion process

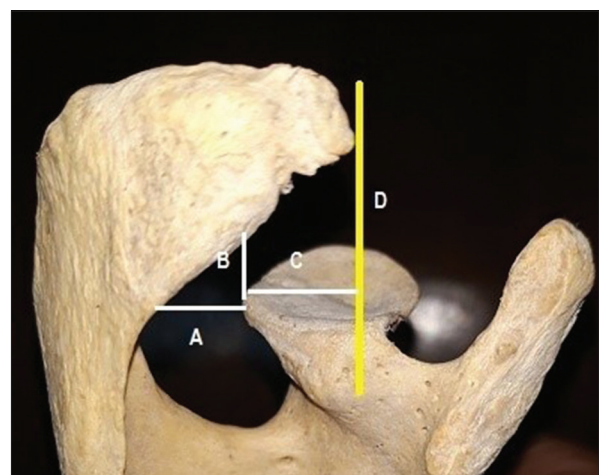


Figure 3: The posterior (A), lateral (B), and anterior (C) acromial overhangs were all measured on the superior view. Acromial overhangs, (D) reference line perpendicular to glenoid fossa for measuring Anterior Acromion Overhang, passing through anterior end of acromion process

indirect measure of the sub-acromion space, as evident from Figure 6.

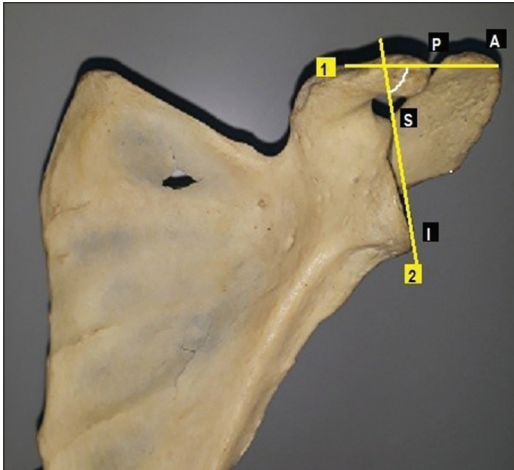


Figure 4: (A and P) Anterior-most point and posterior-most point of tip of acromion process, respectively; S and I: Supraglenoid and infraglenoid tubercles, respectively. Line 1 joins A and P along undersurface of acromion, while line 2 joins S and I along surface of glenoid fossa. Lateral acromial angle



Figure 5: Coraco-acromion angle (shown in red) on superior view

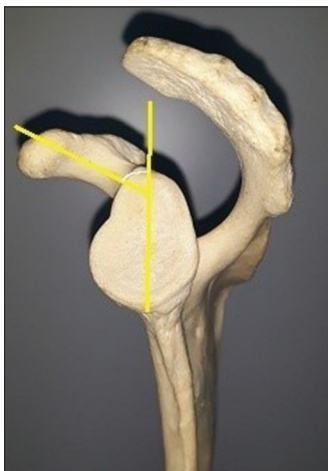


Figure 6: Lateral coracoid angle (shown in white line) on lateral view

Results

The scapulae were primarily divided into three categories, on the basis of shapes of their acromion processes: Type I (40%), Type II (38.75%), and Type III (21.25%), respectively. When laterality was taken into consideration, around 50% of the scapulae of either side fell into each subtype, as shown in Table 1.

The mean overhang readings, based on the type of acromion process, noted in our study are depicted in Table 2. The measurements were also categorized according to laterality, as shown in Table 3.

As evident from the Table 2, lateral overhang measurements varied significantly between the acromion types, the maximum being in Type II (10.2 ± 3.5 mm) and minimum being in Type III (6.25 ± 2.4 mm). Similarly, the anterior overhang measurements varied significantly between Type I and III acromion processes. There was no significant variation of the overhang measurements on scapulae of either side.

The different angles in relation to the acromion process were compared between different types of scapulae, as shown in Table 4. The mean lateral coracoid angle measurements were 53.5° , 50.7° , and 55.1° in Types I, II, and III, whereas the mean lateral acromion angle measurements were 79.5° , 78.4° , and 71.9° , respectively.

Type III scapulae varied from both Types I and II with respect to the lateral acromion angle while the lateral coracoid angle did not vary significantly between the three types of scapulae. On the other hand, the type I scapulae was varying significantly from both the other types in respect to the coraco-acromion angle. Between the right and left scapulae, only the coraco-acromion angle varied significantly while others had no significant variation. This is evident from Table 5.

Apart from the acromion process, another two important angles were measured in relation to the glenoid cavity. The mean glenoid inclination was measured to be $92.48^\circ (\pm 5.2^\circ)$, $88.9^\circ (\pm 3.9^\circ)$, and $96^\circ (\pm 3.3^\circ)$, respectively, in Type I, II, and III scapulae, whereas the mean CSA was noted to be $31.5^\circ (\pm 3.8^\circ)$, $34.3^\circ (\pm 3.8^\circ)$, and $37.7^\circ (\pm 7.1^\circ)$, respectively. These are evident from Table 6. Laterality-wise variation in these angles was also analyzed on the basis of measurements obtained, and they are reflected in Table 7.

Both the glenoid inclination and CSA showed significant variations between different types of scapulae, as shown

Table 1: Prevalence of different types of scapulae (based on their shapes) in either side

Type I (n=32)		Type II (n=31)		Type III (n=17)	
Right, n (%)	Left, n (%)	Right, n (%)	Left, n (%)	Right, n (%)	Left, n (%)
17 (53.1)	15 (46.9)	16 (51.6)	15 (48.4)	9 (52.9)	8 (47.1)

Table 2: Comparison of the acromion overhangs of various types of scapulae among themselves

Type of acromion	Type I (mm) (mean±SD)	Type I-II (P)	Type II (mm) (mean±SD)	Type II-III (P)	Type III (mm) (mean±SD)	Type I-III (P)
Overhangs						
AOH	9.03±2.5	0.46	9.53±2.13	0.1	11.08±3.3	0.043*
POH	9.2±2.1	0.69	9.47±2.6	0.09	7.99±2.3	0.12
LOH	9.73±2.4	0.6	10.2±3.5	0.001*	6.25±2.4	<0.001*

*Asterisks showing significant result. AOH: Anterior overhang, POH: Posterior overhang, LOH: Lateral overhang, SD: Standard deviation

Table 3: Variations in measurements of acromion overhangs of either side, without considering the individual types of scapula

Side (laterality)	Mean±SD		
	AOH (mm)	POH (mm)	LOH (mm)
Right	9.72±3.1	9.2±2.8	9.7±3.4
Left	9.6±2.1	9.7±1.9	8.5±2.9
P	0.86	0.46	0.17

AOH: Anterior overhang, POH: Posterior overhang, LOH: Lateral overhang, SD: Standard deviation

Table 4: Comparative data regarding variations in angles with respect to the acromion process in scapulae of different types

Angles around acromion	Type I (mean±SD)	Type I-II (P)	Type II (mean±SD)	Type II-III (P)	Type III (mean±SD)	Type I-III (P)
LCA (°)	53.5±8.4	0.23	50.7±7.5	0.15	55.1±10.2	0.61
LAA (°)	79.5±12.5	0.72	78.4±5.9	0.003*	71.9±5.6	0.046*
CAA (°)	37±8.9	0.047*	32.3±6.6	0.052	30.8±6.8	0.036*

*Asterisks showing significant results. LCA: Lateral coracoid angle, LAA: Lateral acromion angle, CAA: Coraco-acromion angle, SD: Standard deviation

Table 5: Variations in angles around acromion process among scapulae of either side

Side (laterality)	Mean±SD		
	LCA	LAA	CAA
Right (°)	51.4±7.3	76.1±11.8	37.43±7.6
Left (°)	54.4±9.5	78.9±6.9	29.8±6.5
P	0.17	0.23	<0.0001*

*Asterisks showing significant results. LCA: Lateral coracoid angle, LAA: Lateral acromion angle, CAA: Coraco-acromion angle, SD: Standard deviation

Table 6: Differences in angles around glenoid fossa among various types of scapulae

Angles around glenoid fossa	Type I (mean±SD)	Type I-II (P)	Type II (mean±SD)	Type II-III (P)	Type III (mean±SD)	Type I-III (P)
GI (°)	92.48±5.2	0.011*	88.9±3.9	<0.0001*	96±3.3	0.032*
CSA (°)	31.5±3.8	0.017*	34.3±3.8	0.061	37.7±7.1	0.001*

*Asterisks showing significant results. GI: Glenoid inclination, CSA: Critical shoulder angle, SD: Standard deviation

in the above Table 6. However, the angles in relation to glenoid fossa did not vary significantly between the right and left sides.

Discussion

Bigliani *et al.* in their study argued that due to the shape and resultant damage, the Type II and Type III acromion had a greater predisposition to a RC tear and hence SIS.^[15] Multiple anatomical factors including trauma or overuse of Rotator Cuff and allied structures can lead to Sub-acromion Impingement Syndrome.^[16] Anatomical

factors include acromial morphology variations such as shape of acromion process, lateral extension of acromion and coracoid processes, and degenerative changes at the inferior surface of the acromion, acromio-clavicular joint (ACJ), or coraco-acromial ligament (CAL). However, due to poor inter-observer reliability, this theory has been widely criticized.^[17]

In our study, the incidence of Type I acromion was more on the right side which coincides with Penni *et al.* (1996) and Schippinger *et al.* (1997).^[18,19] On the left side, the incidence of Type II acromion was more than the other two

types, which is similar to the findings of Bigliani *et al.*, Paraskevas *et al.*, and many more.^[20] Table 8 shows the incidence of acromial types in previous studies.^[15,18-27]

Analyzing the relationship between the acromial shapes and acromial overhang, significantly greater anterior acromial overhang was found in Type III than Type I and Type II. On the other hand, lateral acromial overhang was significantly less in Type III acromion than Type I and Type II. No significant relationship was found between posterior acromial overhang and types of acromion process. This study result was similar to that of Le Reun *et al.*^[28]

Glenoid inclination angle varies significantly between the three types of acromion processes in our study. Glenoid inclination angles were 92.48°, 88.9°, and 96°, respectively, in Types I, II, and III in this study. Hughes *et al.* in their study found that glenoid inclination was greater in cadaver shoulders having full-thickness RC tears (98.6°) than in shoulders without tears (91.0°).^[29]

The presence of degenerative shoulder pathologies may be indicated in a new radiographic measurement which is CSA. This parameter is not only associated with degenerative RC tears but also with the presence of glenohumeral osteoarthritis. Degenerative RC tear is associated with CSA greater than 35° while angle below 30° is common in osteoarthritis.^[30,31] In this study, CSA

of Type I scapula varies significantly from Types II and III, the maximum being in Type III (37.7°) and minimum being in Type I (31.5°).

Conclusion

The CSA and glenoid inclinations, in addition to the shapes of scapular acromion processes and overhangs, can be early predictors for the SIS and other shoulder pathologies. This anatomical study on dry bones can be used for extending the results upon patients based on their clinical presentations, which might be a cornerstone for orthopedicians and radiologists while dealing with shoulder pathologies, particularly the SIS.

Acknowledgment

The study has been possible due to the immense co-operation of Prof. (Dr.) Asis Kumar Ghosal, Head of the Department (Anatomy), IPGME and R, Kolkata, as well as the support and guidance of Prof. (Dr.) Avijit Hazra, Professor, Department of Pharmacology, IPGME and R, Kolkata. Furthermore, the Department of Anatomy of Murshidabad Government College and Hospital has played an important role for the support.

Financial support and sponsorship

This study was financially supported by the Department of Anatomy of Murshidabad Government College and Hospital as well as Rampurhat Government Medical College and Hospital.

Conflicts of interest

There are no conflicts of interest.

References

1. Yamaguchi K, Ditsios K, Middleton WD, Hildebolt CF, Galatz LM, Teefey SA. The demographic and morphological features of rotator cuff disease. A comparison of asymptomatic and symptomatic shoulders. *J Bone Joint Surg Am* 2006;88:1699-704.
2. Yamamoto A, Takagishi K, Osawa T, Yanagawa T, Nakajima D, Shitara H, *et al.* Prevalence and risk factors of a rotator cuff tear in the general population. *J Shoulder Elbow Surg* 2010;19:116-20.
3. Koester MC, George MS, Kuhn JE. Shoulder impingement syndrome. *Am J Med* 2005;118:452-5.
4. Lehman C, Cuomo F, Kummer FJ, Zuckerman JD. The incidence of full thickness rotator cuff tears in a large cadaveric population. *Bull Hosp Jt Dis* 1995;54:30-1.
5. Reilly P, Macleod I, Macfarlane R, Windley J, Emery RJ. Dead men and radiologists don't lie: A review of cadaveric and radiological studies of rotator cuff tear prevalence. *Ann R Coll Surg Engl* 2006;88:116-21.
6. Neer CS 2nd. Anterior acromioplasty for the chronic impingement syndrome in the shoulder: A preliminary report. *J Bone Joint Surg Am* 1972;54:41-50.
7. Sarkisian GC. Current concepts review. Subacromial impingement syndrome (79-A: 1854-1868, Dec. 1997). *J Bone Joint Surg Am* 1998;80:1851.

Table 7: Comparison between scapulae of either side, with respect to the angles around glenoid fossa

Side (laterality)	Mean±SD	
	GI	CSA
Right (°)	33.2±4.2	91.3±5.6
Left (°)	34.7±6.1	92.5±4.4
<i>P</i>	0.28	0.37

GI: Glenoid inclination, CSA: Critical shoulder angle, SD: Standard deviation

Table 8: Comparison between previous studies showing different types of scapulae

Author (year)	Sample size	Incidence (%)		
		Type I	Type II	Type III
Bigliani <i>et al.</i> (1986) ^[15]	140	17.1	42.9	39.3
Getz <i>et al.</i> (1996) ^[25]	394	22.8	68.5	8.6
Panni <i>et al.</i> (1996) ^[18]	80	42.5	25	32.5
Schippinger <i>et al.</i> (1997) ^[19]	31	67.7	32.3	0
Hirano <i>et al.</i> (2002) ^[26]	91	36.3	24.2	39.6
Paraskevas <i>et al.</i> (2008) ^[20]	88	26.1	55.6	18.1
Gupta <i>et al.</i> (2014) ^[27]	50	32	22	46
Singroha <i>et al.</i> (2017) ^[28]	100	9	48	43
Vinay and Sivan (2017) ^[29]	164	37.1	47.5	15.2
Sinha <i>et al.</i> (2018) ^[30]	164	24.5	49.1	26.4
Prasad <i>et al.</i> (2019) ^[31]	70	57.1	40	2.8
Present study (2020)	80	40	38.75	21.25

8. Terrier A, Reist A, Nyffeler RW. Influence of the shape of the acromion on joint reaction force and humeral head translation during abduction in the scapular plane. *J Biomech* 2006;39:S82.
9. Daggett M, Werner B, Gauci MO, Chaoui J, Walch G. Comparison of glenoid inclination angle using different clinical imaging modalities. *J Shoulder Elbow Surg* 2016;25:180-5.
10. Kandemir U, Allaire RB, Jolly JT, Debski RE, McMahon PJ. The relationship between the orientation of the glenoid and tears of the rotator cuff. *J Bone Joint Surg Br* 2006;88:1105-9.
11. Bishop JL, Kline SK, Aalderink KJ, Zuel R, Bey MJ. Glenoid inclination: *In vivo* measures in rotator cuff tear patients and associations with superior glenohumeral joint translation. *J Shoulder Elbow Surg* 2009;18:231-6.
12. Engelhardt C, Farron A, Becce F, Place N, Pioletti DP, Terrier A. Effects of glenoid inclination and acromion index on humeral head translation and glenoid articular cartilage strain. *J Shoulder Elbow Surg* 2017;26:157-64.
13. Moor BK, Kuster R, Osterhoff G, Baumgartner D, Werner CM, Zumstein MA, *et al.* Inclination-dependent changes of the critical shoulder angle significantly influence superior glenohumeral joint stability. *Clin Biomech (Bristol, Avon)* 2016;32:268-73.
14. Altintas B, Kääh M, Greiner S. Arthroscopic lateral acromion resection (ALAR) optimizes rotator cuff tear relevant scapula parameters. *Arch Orthop Trauma Surg* 2016;136:799-804.
15. Bigliani LU, Morrison DS, April EW. The morphology of the acromion and its relationship to rotator cuff tears. *Orthop Trans* 1986;10:228.
16. Michener LA, McClure PW, Karduna AR. Anatomical and biomechanical mechanisms of subacromial impingement syndrome. *Clin Biomech (Bristol, Avon)* 2003;18:369-79.
17. Seitz AL, McClure PW, Finucane S, Boardman ND 3rd, Michener LA. Mechanisms of rotator cuff tendinopathy: Intrinsic, extrinsic or both? *Clin Biomech* 2011;26:1-12.
18. Panni AS, Milano G, Lucania L, Fabbriani C, Logroscino CA. Histological analysis of the coracoacromial arch: Correlation between age-related changes and rotator cuff tears. *Arthroscopy* 1996;12:531-40.
19. Schippinger G, Bailey D, McNally EG, Kiss J, Carr AJ. Anatomy of the normal acromion investigated using MRI. *Langenbecks Arch Chir* 1997;382:141-4.
20. Paraskevas G, Tzaveas A, Papaziogas B, Kitsoulis P, Natsis K, Spanidou S. Morphological parameters of the acromion. *Folia Morphol (Warsz)* 2008;67:255-60.
21. Getz JD, Recht MP, Piraino DW, Schils JP, Latimer BM, Jellema LM, *et al.* Acromial morphology: Relation to sex, age, symmetry, and subacromial enthesophytes. *Radiology* 1996;199:737-42.
22. Hirano M, Ide J, Takagi K. Acromial shapes and extension of rotator cuff tears: Magnetic resonance imaging evaluation. *J Shoulder Elbow Surg* 2002;11:576-8.
23. Gupta C, Priya A, Kalthur SG, D'Souza AS. A morphometric study of acromion process of scapula and its clinical significance. *CHRISMED J Health Res* 2014;1:164-9.
24. Singroha R, Verma U, Malik P, Kanta Rathee S. Morphometric study of acromion process in scapula of North Indian population. *Int J Res Med Sci* 2017;5:49-65.
25. Vinay G, Sivan S. Morphometric study of the acromion process of scapula and its clinical importance in South Indian population. *Int J Anat Res* 2017;5:4361-4.
26. Sinha MB, Sinha HP, Joy P. The acromial morphology and its implication in impingement syndrome: An anatomical study. *J Anat Soc India* 2018;67:30-4.
27. Prasad M, Rout S, Stephen PC. Acromion morphology and morphometry in the light of impingement syndrome and rotator cuff pathology. *J Anat Soc India* 2019;68:27-33.
28. Le Reun O, Lebhar J, Mateos F, Voisin JL, Thomazeau H, Ropars M. Anatomical and morphological study of the subcoracoacromial canal. *Orthop Traumatol Surg Res* 2016;102:S295-9.
29. Hughes RE, Bryant CR, Hall JM, Wening J, Huston LJ, Kuhn JE, *et al.* Glenoid inclination is associated with full-thickness rotator cuff tears. *Clin Orthop Relat Res* 2003;407:86-91.
30. Moor BK, Bouaicha S, Rothenfluh DA, Sukthankar A, Gerber C. Is there an association between the individual anatomy of the scapula and the development of rotator cuff tears or osteoarthritis of the glenohumeral joint?: A radiological study of the critical shoulder angle. *Bone Joint J* 2013;95-B: 935-41.
31. Moor BK, Wieser K, Slankamenac K, Gerber C, Bouaicha S. Relationship of individual scapular anatomy and degenerative rotator cuff tears. *J Shoulder Elbow Surg* 2014;23:536-41.

Coexisting Multiple and Complex Peritoneal Variations and Agenesis of Vermiform Appendix

Abstract

We have come across a series of variations on our cadaver during routine dissection of the abdominal viscera. The amount and extent of the variations were unexpected in one cadaver, and they were followed one after another as listed: a peritoneal cyst formed by the parietal peritoneum that was stuck to the anterior surface of the right kidney, intraperitoneal duodenum, intraperitoneal ascending colon, partially constricted transverse colon, and several peritoneal strings running in between the various parts of the visceral peritoneum and the parietal peritoneum covering the abdominal wall, unusual location and size of the root of mesentery, and agenesis of the vermiform appendix. Our cadaver's medical history has not shown any surgery; it never showed any scars on the abdominal wall that might have indicated surgical operations. Peritoneal variations and agenesis of vermiform appendix are of great importance during diagnostic monitoring as well as surgical interventions. Extensive peritoneal variations in one patient may cause some extremely critical complications during the peritoneal dialysis, as well as during the laparoscopic approaches. We present these multiple and complex variations in one cadaver with respect to serious clinical complications that may come out because of ignorance of such cases.

Keywords: Agenesis of vermiform appendix, malformation, peritoneal cyst, peritoneal adhesion, peritoneal band, parietal peritoneum, peritoneum, renal peritoneal sac

Introduction

The peritoneum is a double-layered serous membrane and the most extensive and complex structure within the abdominal cavity. It consists of mesoderm-derived squamous epithelium. It covers the free surfaces of the intra-abdominal organs and the abdominal cavity. The parietal peritoneum covers the abdominal walls, whereas the visceral peritoneum envelops the intraperitoneal abdominal viscera.^[1]

Development of the peritoneum and the digestive tube cannot be considered separately; the viscera grow to invaginate the mesodermal peritoneum. Once organs start growing and pushing, they change their positions, the peritoneum relocates accordingly. Differences in development and rotation of the primitive bowel tube are the main cause of the deviations in the peritoneal structure in adults; thus, a brief look at the embryological development of the peritoneum would be explanatory.^[2]

The early gastrointestinal tract is in the form of a tube suspended between

the anterior and posterior wall of the embryonic body cavity within two layers of mesoderm: the primary ventral and the primary dorsal mesenteries.^[1] As the gut tube starts rotating, the organs begin situating within the body cavity. The peritoneum also moves along; at the end of the midgut rotation, the parts of the peritoneum from one viscus to another and also between the abdominal wall and viscera are described differently. These anatomical terms include the peritoneal ligament, peritoneal fold, mesentery, and omentum.^[3] The mesentery is a double-layer visceral peritoneum suspending the intraperitoneal organs such as the small intestine and the transverse colon to the body wall, and the omentum is part of the visceral peritoneum connecting the stomach to the liver and transverse colon.^[3,4]

The peritoneum stretched between porta hepatis, duodenum, and lesser curvature of the stomach is known as the lesser omentum. Greater omentum is the greatest fold of the peritoneum and formed by the peritoneum covering the anterior and posterior sides of stomach extending downward like an apron and turning back

This is an open access journal, and articles are distributed under the terms of the Creative Commons Attribution-NonCommercial-ShareAlike 4.0 License, which allows others to remix, tweak, and build upon the work non-commercially, as long as appropriate credit is given and the new creations are licensed under the identical terms.

For reprints contact: WKHLRPMedknow_reprints@wolterskluwer.com

How to cite this article: Tiryakioglu M, Fahrioglu SL, Onderoglu S, Ilgi S. Coexisting multiple and complex peritoneal variations and agenesis of vermiform appendix. *J Anat Soc India* 2022;71:146-50.

**Mehtap Tiryakioglu,
Sevda Lafci
Fahrioglu¹,
Selda Onderoglu,
Sezgin Ilgi**

*Department of Anatomy,
Faculty of Medicine, Near East
University, ¹Department of
Anatomy, Faculty of Medicine,
Cyprus International University,
Nicosia, Cyprus*

Article Info

Received: 16 September 2020

Accepted: 26 January 2022

Available online: 30 June 2022

Address for correspondence:

*Prof. Mehtap Tiryakioglu,
Near East University, Faculty
of Medicine, Near East
Boulevard, 99138 Nicosia,
Cyprus (optional), Turkey.
E-mail: mehtap.tiryakioglu@
neu.edu.tr*

Access this article online

Website: www.jasi.org.in

DOI:
10.4103/jasi.jasi_188_20

Quick Response Code:



to form the transverse mesocolon. The peritoneal space located between the parietal and visceral layers of the peritoneum has two main portions as the greater and the lesser sacs that are connected by an epiploic foramen.^[4,5] Usually, the organs developed within the peritoneal layers remain intraperitoneal, while the organs developed connected to the abdominal wall remain retroperitoneal. Organs developed intraperitoneal during early stages of development, yet their dorsal mesenterium fused with the posterior abdominal wall is called secondary retroperitoneal organs. The ascending and descending colon, duodenum, and pancreas develop as secondary retroperitoneal organs.^[2]

Case Report

During routine abdominal dissection in the anatomy laboratory, we encountered a series of anatomical variations on a 72-year-old Caucasian male cadaver. His medical history did not show any significant disease or surgical information, and his body showed no scars on the abdominal wall.

The peritoneal cyst (sac) attached to the anterior surface of the right kidney was the first gross anatomical deviation observed during our dissection. The blind sac was full of peritoneal fluid about 150 cc and extending upward through the hepatorenal recess [Figure 1a]. It is formed by the parietal peritoneum of the right lumbar region by flapping over itself around the right kidney and sticking around its anterior surface and edges [Figure 1b and Supplementary Figure 1]. The upper end of the cyst was blended with the parietal peritoneum within the hepatorenal recess. The right kidney was not fixed to the posterior abdominal wall; instead, it was mobile and suspended by the peritoneal sac. The posterior aspect of the kidney had no adipose tissue when easily lifted [Supplementary Figure 2]; therefore, the fat tissue forming the renal bed was thought to be the perirenal fat that is stuck with the pararenal fat. The parietal peritoneum of the posterior abdominal wall was partially missing in the right lower part of the lumbar region, where it reminded the missing part was the part which flapped over and formed the sac in front of the right kidney [Figures 1b, 2, and 3]. The border of the missing peritoneum on the left side was tracing the inferior vena cava on its anterior surface while the right side was passing in front of the right iliac muscle and transversus abdominis fascia.

There was no vermiform appendix at the distal part of the cecum. It was palpated carefully to rule out the vermiform appendix intussusceptions within ileocecal and retrocecal areas, but could not be found. The cecum was much wider than ascending colon, and all three taeniae were observed at the distal part of the cecum without interruption [Figure 4].

Ascending colon was observed intraperitoneal within the same peritoneal layers with the cecum and transverse colon; it was running within the ascending mesocolon. It was difficult to distinguish the ascending colon from the

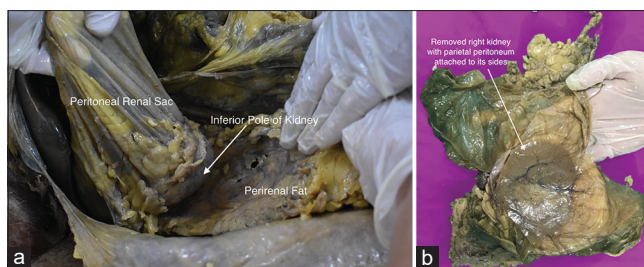


Figure 1: (a) Renal peritoneal sac formed by parietal peritoneum. (b) Removed right kidney with renal peritoneal sac (exposed)

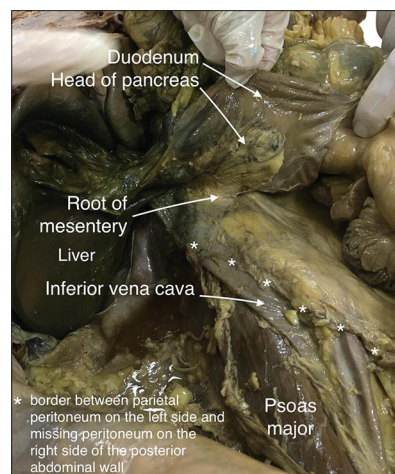


Figure 2: Missing part of parietal peritoneum after the removal of the right kidney

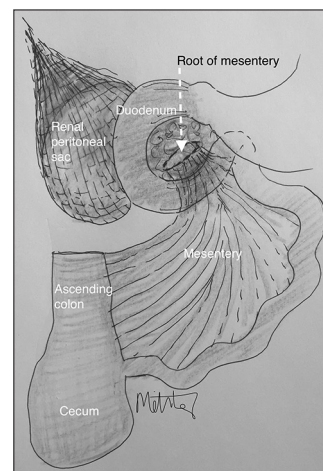


Figure 3: Illustration of the renal peritoneal sac, root of the mesentery, intraperitoneal ascending colon, duodenum, and head of pancreas representing our case report

transverse colon since a significant right colic flexure was not observed [Figures, 5a, b, and 6].

Transverse colon showed 12 cm long constriction at its distal end with extremely thickened wall; this part did not show any taenia or haustra and it was wrapped with a twisted mesocolon [Figure 7]; rest of transverse colon was not showing proper haustra or taenia coli, also and the lumen was wider than normal. There was another extreme

constriction in its proximal part that seemed to be caused by a peritoneal band.

The duodenum and head of pancreas were intraperitoneal and the root of the mesentery (RM) observed as being tucked behind the head of pancreas [Figure 8]; RM was forming the inferior boundary of the epiploic foramen, and it was only about 5 cm long; therefore, there were no supra- and infra-mesenteric peritoneal recesses. The proximal part of the jejunum was suspended on the posterior abdominal wall through some peritoneal bands attaching the transverse mesocolon. Similarly, some other peritoneal bands were observed from the jejunal mesentery that had a clear attachment to the parietal peritoneum in front of the sacral promontory [Figure 9].

The left side of the abdominal cavity showed no deviation from the normal peritoneal and/or intestinal anatomy.

Discussion

Considering embryological development of peritoneum and intestines, our case is clearly showing extensive

embryological variations on both dorsal and ventral mesenteries [Figure 6]. The parietal peritoneum appears to be separated from the posterior abdominal wall to form a peritoneal cyst in front of the right kidney and attached firmly to its edges and poles by leaving a wide peritoneal gap on the posterior abdominal wall in our case [Figures 1a, 1b and 3]. It is suggestive of a history of intra-abdominal surgery; however, there was no scar on the body, and his medical record showed no history of a surgery or a disease that might have caused it. The presence of the peritoneal mesothelial cysts could occur as a result of an inflammatory disease or a past intra-abdominal surgery.^[6] Our cadaver's history showed none of these implications, so we focused more on a congenital abnormality; however, an undiagnosed inflammatory disease should also be kept in mind for this particular case.

Agenesis of vermiform appendix is a very rare condition with a frequency of 1/100,000. It usually is encountered

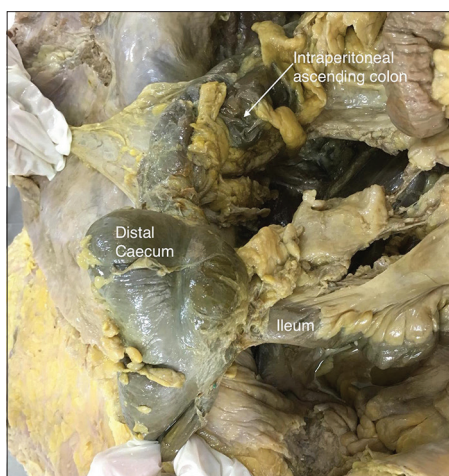


Figure 4: Agenesis of vermiform appendix

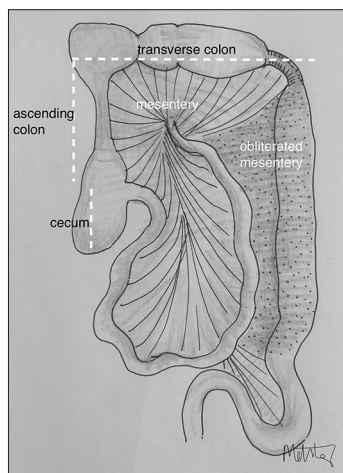


Figure 6: Illustration of the obliterated part of the embryological mesentery and intra-peritoneal ascending colon representing our case report

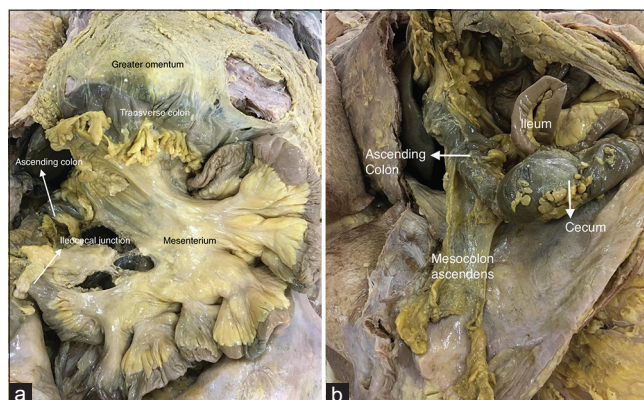


Figure 5: (a) Small intestines and ascending colon within the mesentery. (b) Intra-peritoneal ascending colon (was placed on the anterior abdominal wall for demonstration purpose)

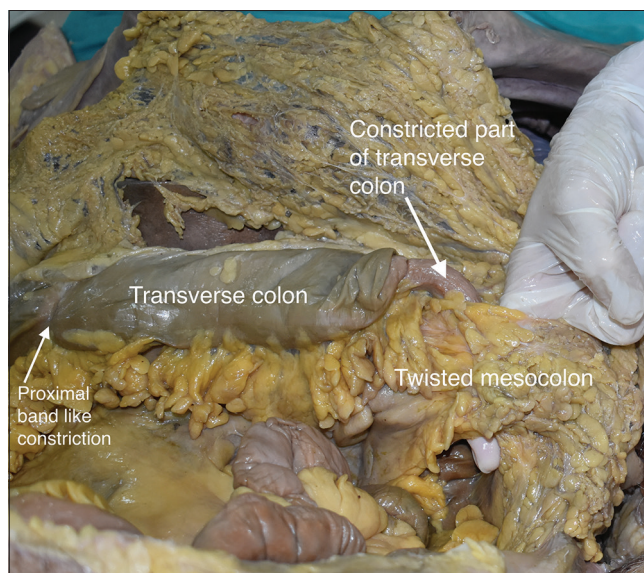


Figure 7: Transverse colon with its constrictions and twisted mesocolon

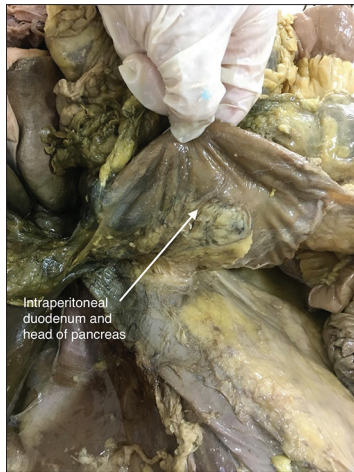


Figure 8: Intrapерitoneal duodenum and head of pancreas

incidentally in cases of suspected appendicitis.^[7] The vermiform appendix, a narrow diverticulum develops from the distal end of the cecal bud during the descent of the colon.^[3] The anomalies of the vermiform appendix may be associated with other congenital anomalies such as jejunal atresia or short bowel syndrome.^[7] Collins examined 71,000 vermiform appendices and classified cecum and appendix anomalies in five classes: Type I showed absence of both cecum and vermiform appendix; in type II, cecum is rudimentary and there is no vermiform appendix; in type III, there is normally developed cecum with an absence of vermiform appendix; and in type IV, normal cecum accompanies the rudimentary vermiform appendix. Type V shows an enlarged cecum and absence of appendix vermiformis,^[7] showing great similarity to our case [Figure 4].

The intraperitoneal ascending colon is usually formed by a failure of the dorsal mesentery to fuse to the posterior abdominal wall and remain as intraperitoneal [Figures 3, 5a, b, and 6]. When an incomplete fusion occurs, the long mesentery causes abnormal bowel movements that can lead to volvulus. This may also lead to a retrocolic hernia, which is caused by a compression of the small bowel folding in the retrocecal pocket.^[8] There is neither retrocecal recess nor right paracolic gutter in our case as both cecum and ascending colon continues intraperitoneal.

The intraperitoneal duodenum and head of pancreas in our cadaver also remind a congenital anomaly showing the rotated midgut has failed to fuse with the abdominal wall and left the duodenum intraperitoneal. The RM was 5 cm long located behind head of the pancreas; thus, the right paracolic gutter, right infracolic, and left infracolic spaces were united. This situation can clinically cause very serious consequences when considered the abdominal interventions such as peritoneal dialysis;^[4] however, furthermore, there is an extensive gap on the parietal peritoneum on the body cavity in our cadaver [Figure 2] that can cause even more serious conditions in the abdominal organs.

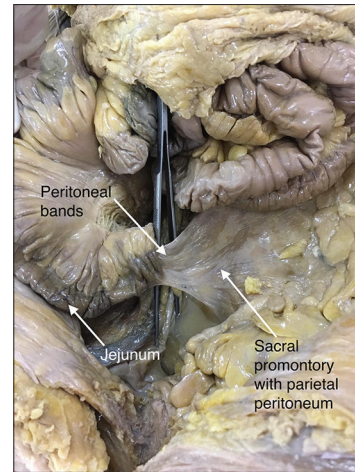


Figure 9: Peritoneal bands

Transverse colon had constricted part that was about 12 cm long at its distal 1/3rd [Figure 7]. The wall was thick enough to almost obstruct the lumen; taeniae and haustrae were interrupted. It reminded developmental intestinal stenosis that may occur from vascular accidents in the embryological period. Problems to expression of HOX genes and some receptors in the fibroblast growth factor family are held responsible as the reason for these vascular accidents during bowel differentiation. This is observed in 20% of intestinal atresia and stenosis cases. In our case, the part of the transverse colon before the constriction was wider than usual. Aganglionic megacolon or Hirschsprung disease is an intestinal disorder characterized by the failure of enteric ganglion cells to migrate completely during intestinal development; hence, the aganglionic segment of the colon fails to relax, causing intestinal stenosis as seen in our case. A rare type of the aganglionic colon named zonal segmental aganglionosis was first described by Tiffin *et al.* in 1940. In such cases, the presence of myenteric ganglionic cells can be detected proximal and distal to the aganglionic segment. Around 95% of the patients are diagnosed in early childhood; however, patients may remain undiagnosed until adulthood. To be accurate, our case needs to be examined histopathologically for the presence of aganglionic segment; however, a histopathological observation could not be done due to technical problems. The factors resulting in the intestinal obstructions can be several: adhesions from previous surgery, malrotation of midgut, tumors, hernias, inflammatory bowel disease, Crohn's disease, chronic constipation, volvulus, intussusception, etc.^[7,9] A volvulus is caused by a twisted colon and its mesentery and resulted with ischemia, yet the presented part of the transverse colon did not show any ischemia, although we observed twisted mesocolon which reminds a volvulus, particularly considering the transvers colon's increased volume caused its haustras to be disappeared [Figure 7].^[6]

Peritoneal bands or adhesions can cause compression within the abdominal cavity; they also are known as Ladd's

bands and found because of failure of the embryonic mesentery to be obliterated properly,^[10] so the persistence of the parts of embryonic mesentery remains as the peritoneal bands. Depending on their route and extent, they may cause serious intra-abdominal problems such as intestinal obstructions, volvulus, extensive intra-abdominal pressure and pain, herniation, strangulation, constipation, diarrhea, etc. According to Nyakirugumi and Nduhiu, congenital peritoneal bands are the main reason for 3% of intestinal obstructions.^[11] When we consider the amount of the observed peritoneal bands in our case, there is a high probability of them, leading to a possible transverse colon volvulus.

Conclusion

Peritoneal and intestinal variations may not cause any clinical symptoms, so the prevalence of them may not be accurate. Peritonitis caused by perforation, ischemia, pancreatitis, and/or anastomotic leakage are some of the surgical emergencies affecting the entire peritoneal cavity. If the patient's peritoneal course and relationship to the organs show similar variation/s, as in our case, infection can easily spread, and the clinical symptoms may be worse than expected. Peritoneal structures such as ligaments, mesenteries, omenta, and peritoneal recesses can be a boundary for the infection spread depending on their location and conditional situations; however, our case express a great potential for the strangulations, volvulus, extensive peritonitis as there were some missing recesses due to the lack of proper root of mesentery and existence of many peritoneal bands. Furthermore, the missing parietal peritoneum on the right side was a great threat to the kidney and ureters. The several peritoneal strings and the abnormal peritoneal recesses around the intestines are surgically important as they may strangulate the bowel parts causing internal abdominal hernias. Although there are reports on individual variations such as intraperitoneal ascending colon, intestinal volvulus, peritoneal bands, and agenesis of vermiform appendix, there are no reports in the literature on the co-occurrence of them all in the same individual. We could not find any report such as a renal peritoneal sac in the literature. The overwhelming amount of the variations and our cadaver's age is controversial, yet this might be considered as an undiagnosed case that strongly emphasizes the importance of being aware of these variations as each one of them may cause serious complications during

surgical interventions such as pancreaticoduodenectomy and distal/total pancreatectomy for an extensive tumor involvement throughout the entire pancreas/kidney or laparoscopic abdominal interventions. Atypical location of the RM may affect the way of cancer metastasis on related organs.^[5] Keeping the potential peritoneal variations in mind when going through an abdominal imaging process for any of the mentioned diseases and/or operations may prevent any possible misdiagnosis and/or mistreatment for such unfortunate case.

Financial support and sponsorship

Nil.

Conflicts of interest

There are no conflicts of interest.

References

1. Ashaolu JO, Ukwenya VO, Adenowo TK. Cystoduodenal ligament as an abnormal fold and the accompanying anatomical and clinical implications. *Surg Radiol Anat* 2011;33:171-4.
2. Sadler TW. *Langman's Medical Embryology*. 14th ed., Ch. 7. Printed in China: Wolters Kluwer; 2019. p. 236-41.
3. Sarkar A. Congenital absence of the vermiform appendix. *Singapore Med J* 2012;53:e189-91.
4. Healy JC, Reznick RH. The peritoneum, mesenteries and omenta: Normal anatomy and pathological processes. *Eur Radiol* 1998;8:886-900.
5. Capobianco A, Cottone L, Monno A, Manfredi AA, Rovere-Querini P. The peritoneum: Healing, immunity, and diseases. *J Pathol* 2017;243:137-47.
6. Erten EE, Çavuşoğlu YH, Arda N, Karaman A, Afşarlar ÇE, Karaman I, *et al.* A rare case of multiple skip segment Hirschsprung's disease in the ileum and colon. *Pediatr Surg Int* 2014;30:349-51.
7. Sozen S, Emir S, Yazar FM, Altinsoy HK, Topuz O, Vurdem UE, *et al.* Small bowel obstruction due to anomalous congenital peritoneal bands – Case series in adults. *Bratisl Lek Listy* 2012;113:186-9.
8. Blackburn SC, Stanton MP. Anatomy and physiology of the peritoneum. *Semin Pediatr Surg* 2014;23:326-30.
9. Beyene RT, Kavalukas SL, Barbul A. Intra-abdominal adhesions: Anatomy, physiology, pathophysiology, and treatment. *Curr Probl Surg* 2015;52:271-319.
10. Kassem MW, Patel M, Iwanaga J, Loukas M, Tubbs RS. Constriction of the stomach by an unusual peritoneal band. *Cureus* 2018;10:e2148.
11. Nyakirugumi S, Nduhiyu M. Anomalous vascular peritoneal bands causing small bowel obstruction in adult. *Ann Afr Surg* 2020;17:85-7.



Supplementary Figure 1: The boundary of the missing parietal peritoneum on the anterior abdominal wall



Supplementary Figure 2: Right kidney with peritoneal sac and missing parietal peritoneum on the posterior abdominal wall

Unilateral Absence of Round Ligament of Femur - Cadaveric Case Report

Abstract

Round ligament of femur is a pyramidal structure with apex attached to the fovea of the femoral head and its base blends with the transverse acetabular ligament. It is an intracapsular but extrasynovial structure. It is also called ligamentum teres femoris or foveal ligament. It transmits the acetabular branch of obturator artery and also acts as a secondary stabilizer of the hip joint by supplementing the other ligaments of the hip joint in extreme range of motion. Absence of round ligament of femur is a rare variation which can be unilateral or bilateral and prevalence is 2%–3%. It presents rarely as isolated entity or in association with congenital dysplasia of the hip. This report presents a rare variation of unilateral absence of round ligament of femur with minimal evidence of developmental dysplasia of the hip. During routine dissection of a middle-aged cadaver, on opening the hip joint cavity, the round ligament of femur was absent on the left side whereas, acetabular labrum and femoral head were normal. On the right side, the lower limb was normal in position and round ligament of femur was present in normal length and thickness. Awareness and knowledge of such a rare variation are important for radiologists and orthopedicians for better diagnosis and management of hip-related problems.

Keywords: Acetabular branch of obturator artery, fovea capitis, foveal ligament, hip joint, ligamentum teres femoris, total hip replacement

Introduction

Round ligament of femur was initially thought to be a vestigial structure but now its importance and interest have been increasing since it was found to be acting as a secondary stabilizer of the hip joint. With an increase in the use of arthroscopy in surgical management, recent studies have concluded that repairing ligamentum teres will provide more stability to the hip in case of any tears. In this background, knowledge about round ligament of femur is very important.

Round ligament of femur although very small, it is quite strong ligament. It is a pyramidal structure with apex attached to the fovea of the femur head and its base is blending with the transverse acetabular ligament. It is an intracapsular but extrasynovial structure. It is also called ligamentum teres femoris or foveal ligament. Its mean length is 30–35 mm.^[1] It transmits the acetabular branch of obturator artery, but now recent studies have proven that it also acts as a secondary stabilizer of the hip joint by supplementing the other

ligaments of the hip joint in extreme range of motion.^[2-6]

Absence of round ligament of femur is a very rare variation with the prevalence of 2.8% in Asian population.^[7] Absence can be unilateral or bilateral. Unilateral absence is more common when compared with the absence on both sides.^[8] Rarely, it will be presented as isolated entity and very often associated with developmental dysplasia of the hip.

Since it is very rare variation, this case reports unilateral absence round ligament of femur with minimal evidence of developmental dysplasia of the hip. To the best of my knowledge, this was the first case report of unilateral absence of round ligament and associated developmental dysplasia of the hip in India. This variation is important for radiologists and surgeons.

Case Report

During routine dissection of the lower limb of an approximately 55-year-old Indian adult male cadaver in the Department of Anatomy, Pondicherry Institute of Medical Sciences. General examination of both limbs showed that the left lower limb was

Divya Umamaheswaran, Nagajyothi Chigurupati, Prince Solomon¹, Rema Devi

Departments of Anatomy and ¹Orthopedics Pondicherry Institute of Medical Sciences, Puducherry, India

Article Info

Received: 22 December 2021

Revised: 25 February 2022

Accepted: 25 March 2022

Available online: 30 June 2022

Address for correspondence:

Dr. Divya Umamaheswaran, Department of Anatomy, Pondicherry Institute of Medical Sciences, Puducherry - 605 014, India.

E-mail: divilatha21@gmail.com

Access this article online

Website: www.jasi.org.in

DOI: 10.4103/jasi.jasi_210_21

Quick Response Code:



How to cite this article: Umamaheswaran D, Chigurupati N, Solomon P, Devi R. Unilateral absence of round ligament of femur - cadaveric case report. *J Anat Soc India* 2022;71:151-3.

This is an open access journal, and articles are distributed under the terms of the Creative Commons Attribution-NonCommercial-ShareAlike 4.0 License, which allows others to remix, tweak, and build upon the work non-commercially, as long as appropriate credit is given and the new creations are licensed under the identical terms.

For reprints contact: WKHLRPMedknow_reprints@wolterskluwer.com

slightly laterally rotated, even though there was no obvious limb length discrepancy or any evidence of previous hip surgeries.

Muscles near both hip joints were dissected out. On opening, the left hip joint by dissecting the iliofemoral ligament, femur head came out immediately without any resistance. Femur head was normal with a complete round contour, smooth surface with normal fovea capitis but the round ligament of femur was absent as shown in Figure 1. Acetabular cavity was also smooth without any evidence of attachment of ligament. Acetabular cup and Acetabular labrum appeared normal. Absence of round ligament of femur was confirmed after discussing with orthopedic surgeon.

Dissection of the right hip joint was proceeded after dissection of iliofemoral ligament, femoral head was observed to be present inside the acetabular cavity and round ligament of femur was present as shown in Figure 2. Because of the presence of the ligament, femoral head did not come out immediately on opening the hip joint. The round ligament of femur was pyramidal in the shape of normal thickness and was well formed. Apex is attached to the fovea capitis and the base was blending with the transverse acetabular ligament. The head of femur was round and normal in contour. Acetabular cavity was normal. Acetabular labrum was normal.

After disarticulating both lower limbs, diameter and the depth of the acetabular cup of both sides were measured and tabulated in Table 1. All the findings in the specimen were photographed and documented.

The left acetabular cavity was found to be shallower than the right acetabular cavity.

Discussion

This report presents the absence of round ligament of femur associated with minimal evidence of developmental dysplasia of the hip. Absence of round ligament of femur is an uncommon variation. Several authors have reported about the biomechanics of round ligament of femur and management modalities for tears but there are very few studies about the incidence of absence of the round ligament of femur and

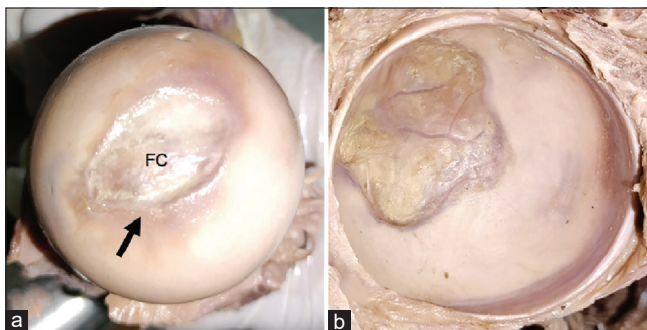


Figure 1: (a) Left femur head, arrow shows fovea capitis (b) left acetabular cavity with no attachment of any ligament. FC – Fovea capitis

so the absence was reported to be 2.8%.^[7] Normally, the ligamentum teres femoris will be formed by the proliferation of mesenchymal cells around the hip joint. Failure of this proliferation is the possible explanation for the absence of round ligament of femur on the left side. As the femoral head was normal and well-formed along with fovea capitis, absence of round ligament was considered to be congenital, especially in the absence of any evidence of surgery. Most of the instances, fovea capitis will be hypoplastic if ligamentum teres is absent but in this case the fovea capitis is well developed.

Initially, it was thought that the main function of round ligament of femur was to transmit acetabular branch of obturator artery which supplies proximal portion of femoral head. However, contribution of this artery to the femoral head is very minimal only to the small subfoveal zone.^[9] Due to the absence of round ligament of femur, acetabular branch of obturator artery is also absent. Major portion of blood supply of femur head is contributed by epiphyseal arteries. In adults, the epiphyseal arteries form an increased number of anastomosis around the femur head. Hence, absence of the acetabular branch of obturator artery would not be a major concern since it supplies only a minimal proximal portion of the femoral head and its absence would be compensated by the increased number of anastomosis around the femoral head by the epiphyseal arteries.

Although acetabular cavity appeared normal, left acetabular cavity is 0.7 cm shallower than the right acetabular cavity which raises a suspicion, as to whether there was an

Table 1: Acetabular cup measurements		
	Left side	Right side
Surface area (cm ²)	21.24	21.24
Depth (mm)	25	32

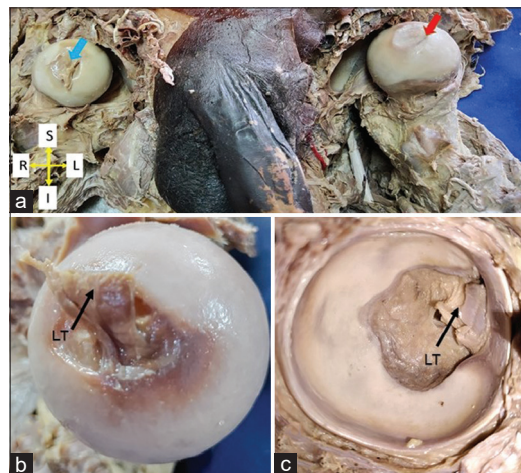


Figure 2: (a) Femur head on both sides, blue arrow showing presence of ligamentum teres, red arrow showing absence of ligamentum teres. (b) Right femur head, arrow shows round ligament of femur. (c) Right acetabular cavity with the attachment of ligamentum teres. LT – ligamentum teres femoris

associated developmental dysplasia of the hip. However, in the absence of indications of surgery and because of the normal contour of the femoral head, associated developmental dysplasia was not considered. Other than shallow acetabular cavity on the left side, there are no other findings of developmental dysplasia of the hip. However, this shallow acetabular cavity is not ignorable because 18.67% of developmental dysplasia of the hip was associated with absent ligamentum teres femoris.^[10]

Hence, in this case, he could have had developmental dysplasia of the hip in childhood which could have been treated conservatively which explains the normal femur head development and almost normally appearing acetabular cavity and explains the extremely laterally rotated left lower limb. Cause for this developmental dysplasia of the hip is attributed to be congenital. To conclude, observations in this case could be due to treated developmental dysplasia of the hip with associated absence of round ligament of femur on the left side.

The clinical significance of this ligamentum teres femoris is it acts as secondary stabilizer of the hip joint. In living beings, isolated absence of ligamentum teres femoris will be asymptomatic. If this absence of ligamentum teres femoris is associated with any osseous abnormalities, then the person will have hip instability and gait changes commonly like limping gait.^[3] In this case, findings of developmental dysplasia of hip associated with absent round ligament of femur on the left side and with extremely laterally rotated left lower limb raises a suspicion that person could have had limping gait.

Conclusion

There is unilateral absence of round ligament of femur associated with minimal evidence of developmental dysplasia of hip which is very rare. Cause of both could be congenital. To the best of our knowledge, this is the first case to report such variation in India. The knowledge of this variation will be important for radiologists and orthopedicians in the management of hip-related problems.

Acknowledgments

The authors sincerely thank those who donated their bodies to science so that anatomical research could be performed.

Results from such research can potentially increase humankind's overall knowledge that can then improve patients care. Therefore, these donors and their families deserve our highest gratitude. Authors also thank all the faculties of the department of Anatomy and nonteaching staffs of the department.

Financial support and sponsorship

Nil.

Conflicts of interest

There are no conflicts of interest.

References

1. Demange K, Kakuda C, Pereira CA, Sakaki M, Albuquerque R. Influence of the Femoral Head Ligament on HIP Mechanical Function; 2007. Available from: <https://www.semanticscholar.org/paper/INFLUENCE-OF-THE-FEMORAL-HEAD-LIGAMENT-ON-HIP-Demange-Kakuda/1dd79ad90f6d36fdf8786287f2d8919a710ebc9b>. [Last accessed on 2021 Dec 22].
2. Kivlan BR, Richard Clemente F, Martin RL, Martin HD. Function of the ligamentum teres during multi-planar movement of the hip joint. *Knee Surg Sports Traumatol Arthrosc* 2013;21:1664-8.
3. Martin HD, Hatem MA, Kivlan BR, Martin RL. Function of the ligamentum teres in limiting hip rotation: A cadaveric study. *Arthroscopy* 2014;30:1085-91.
4. Martin RL, Kivlan BR, Clemente FR. A cadaveric model for ligamentum teres function: A pilot study. *Knee Surg Sports Traumatol Arthrosc* 2013;21:1689-93.
5. Martin RL, Palmer I, Martin HD. Ligamentum teres: A functional description and potential clinical relevance. *Knee Surg Sports Traumatol Arthrosc* 2012;20:1209-14.
6. van Arkel RJ, Amis AA, Cobb JP, Jeffers JR. The capsular ligaments provide more hip rotational restraint than the acetabular labrum and the ligamentum teres: An experimental study. *Bone Joint J* 2015;97-B:484-91.
7. Perumal V, Techataweewan N, Woodley SJ, Nicholson HD. Clinical anatomy of the ligament of the head of femur. *Clin Anat* 2019;32:90-8.
8. Tan CK, Wong WC. Absence of the ligament of head of femur in the human hip joint. *Singapore Med J* 1990;31:360-3.
9. Kirici Y, Kilic C, Oztas E. The ligament of head of femur and its arteries. *J Clin Anal Med* 2010;1:22-5.
10. Li T, Zhang M, Wang H, Wang Y. Absence of ligamentum teres in developmental dysplasia of the hip. *J Pediatr Orthop* 2015;35:708-11.

An Optimal Palpation Method to Locate the Pubic Tubercle

Pubis is an angulated bone. It comprises a body, superior, and inferior ramus. Superior ramus helps in the formation of acetabulum. The thickening on the superior border of the body is the pubic crest and the most lateral prominent swelling of the pubic crest is named pubic tubercle (PT).

PTs are insertion points for inguinal ligament which extends from the anterior superior iliac spine (ASIS). Furthermore, the anterior pelvic plane which is a practical reference plane for pelvic orientation in space is constituted by a tangent passing between two ASIS and PTs.^[1] In an ideal body posture, this plane is expected to be perpendicular to the ground. This is also the anatomical position of the hip bone. In the clinical setting, PT is used as a landmark for planning of inguinal lymphadenectomy, open inguinal hernia repair, obturator nerve block, and elevation of superficial circumflex iliac artery perforator flaps.^[2,3]

Faulty posture and associated multiple musculoskeletal diseases have been related to nonideal pelvis position.^[4] Asymmetry within the pelvic structures is believed to lead to a cascade of postural compensations predisposing the individual to numerous neuromusculoskeletal dysfunctions.^[5] Displacement of the anterior pelvic plane in a horizontal axis is defined as pelvic tilt. In a normal, asymptomatic population, anterior pelvic tilt was found among 85% of male and 75% of female participants, the

tilt degree was in the range of 6°–7° for both sexes.^[6] If a patient has a pelvic tilt, the anterior pelvic plane cannot be aligned parallel to the table on which the patient is lying.

In 2016, it was estimated for the global adult population, 39% of males and 40% of females were to be overweight.^[7] We have been observing a similar increase in body mass index (BMI) among our inpatients.

This tendency of increased BMI hinders the location of the bony prominences. In an operation scenario where the patient is positioned supine, if the patient has an asymptomatic anterior pelvic tilt and has increased BMI, the superficial fascial system and the subcutaneous fat within the periphery of the pelvis will be displaced in an anterior-inferior direction. Moreover, if PT will be used as a landmark in this patient, a finger palpation directed from inferior to superior to locate PT will probably be misleading, as there will be excessive subcutaneous fat between palpating finger and bony prominences due to the positional displacement [Figure 1]. To avoid this pitfall, we suggest, the palpation to be made along the superior border of pubis and directed laterally. The edge point of the superior margin will correlate with PT [Figure 2].

We argue that this is a reliable method to locate PT as the anterior pelvic tilt will most probably go unnoticed during preoperative patient examination.



Figure 1: Typical palpation method oriented obliquely



Figure 2: Proposed palpation method oriented transversely

Ethical statement

All authors certify that they have no affiliations with or involvement in any organization or entity with any financial interest or nonfinancial interest in the subject matter or materials discussed in this manuscript. Informed consent of the participant individual was obtained. The Local Research Ethics Committee has confirmed that no ethical approval is required as this study is based on observation.

Financial support and sponsorship

Nil.

Conflicts of interest

There are no conflicts of interest.

Dağhan Dağdelen, Erol Benlier

Department of Plastic, Reconstructive and Aesthetic Surgery, Trakya University School of Medicine, Edirne, Turkey

*Address for correspondence: Dr. Dağhan Dağdelen, Department of Plastic, Reconstructive and Aesthetic Surgery, Trakya School of Medicine, General Hospital Block, 8th Floor, Balkan Campus, Edirne 22030, Turkey.
E-mail: dagdelend@trakya.edu.tr*

References

1. Digioia AM 3rd, Jaramaz B, Plakseychuk AY, Moody JE Jr., Nikou C, Labarca RS, *et al.* Comparison of a mechanical acetabular alignment guide with computer placement of the socket. *J Arthroplasty* 2002;17:359-64.
2. Al-Refaie WB, Ross MI. Inguinal lymphadenectomy for malignant melanoma. *Oper Tech Gen Surg* 2006;8:90-102.
3. Yoshimatsu H, Yamamoto T, Hayashi A, Iida T. Proximal-to-distally elevated superficial circumflex iliac artery perforator flap enabling hybrid reconstruction. *Plast Reconstr Surg* 2016;138:910-22.
4. Sahrman SA. *Movement System Impairment Syndromes of the Extremities, Cervical and Thoracic Spines*. St. Louis: Mosby; 2010.
5. Juhl JH, Ippolito Cremin TM, Russell G. Prevalence of frontal plane pelvic postural asymmetry – Part 1. *J Am Osteopath Assoc* 2004;104:411-21.
6. Herrington L. Assessment of the degree of pelvic tilt within a normal asymptomatic population. *Man Ther* 2011;16:646-8.
7. World Health Organization. *Overweight and Obesity*; April 01, 2020. Available from: <https://www.who.int/news-room/fact-sheets/detail/obesity-and-overweight>. [Last accessed on 2020 Dec 23].

This is an open access journal, and articles are distributed under the terms of the Creative Commons Attribution-NonCommercial-ShareAlike 4.0 License, which allows others to remix, tweak, and build upon the work non-commercially, as long as appropriate credit is given and the new creations are licensed under the identical terms.

Article Info

Received: 19 August 2021

Accepted: 25 March 2022

Available online: 30 June 2022

Access this article online

Quick Response Code:



Website: www.jasi.org.in

DOI: 10.4103/jasi.jasi_143_21

How to cite this article: Dağdelen D, Benlier E. An optimal palpation method to locate the pubic tubercle. *J Anat Soc India* 2022;71:154-5.

© 2022 Journal of the Anatomical Society of India | Published by Wolters Kluwer - Medknow

Basic Rules for Naming Sutures

Dear Editor,

The development of skull bones is a process that begins in the early embryonic period and continues until adulthood.^[1] The number of bones which consists of 28 parts at birth decreases to 22 in adults. Since the ossification of the newborn skull has not yet been completed, the bones are joined by fibrous or cartilage tissue. In parallel with the progress of the ossification process, structures that we call suture will emerge in the region of these fibrous or cartilage tissues.^[2]

In an adult skull, there are a total of 33 sutures. These are given collectively under the heading “Suturæ cranii” on page 26 in Terminologia Anatomica (TA).^[3] Considering the names of these 33 sutures, some of them are named according to the course of suture (sutura coronalis, etc.), some according to the shape (sutura lambdoid), some according to the structure (sutura squamosa, etc.), some according to the region (sutura palatina mediana, sutura palatina transversa, etc.) but most of them are named according to the names of the bones (sutura sphenothmoidalis and sutura frontonasal, etc.).

The names are created by giving the name of two bones but nomenclature rules about which bone will come first are not known, today.

In the face of questions from students about this topic, the lack of satisfactory answers of educators causes problems. To eliminate this distress to some extent, we aimed to develop an empirical study on the names of sutures.

The existing sutura names in Nomina Anatomica (NA; this book contains lists accepted in 1895, 1933, and 1955 in 3 columns),^[4] NA (1985), and TA (1998) were compared. Current rules for naming sutures are empirically introduced.

On page 26 of (TA), there are a total of 34 terms of suture. (1) The first one is the general title named “Sutura cranii” coded A03.1.02.001.

(2) The names of the four sutures found in Calvaria have been put forward by considering the course, shape and structure of the suture

- A03.1.02.002: Sutura coronalis
- A03.1.02.003: Sutura sagittalis
- A03.1.02.004: Sutura lambdoidea
- A03.1.02.005: Sutura squamosal.

(3) Some sutures belong to a single bone or formed between right and left bones of the same name.

A03.1.02.012: Sutura squamomastoidea (also known as “Fissura tympanomastoidea” because it is not a real suture)

- A03.1.02.023: Sutura internasalis
- A03.1.02.029: Sutura intermaxillaris

- A03.1.02.034: (Sutura frontalis persistens; Sutura metopica).

(4) When sutures belonging to the palate (or sutures including “os palatinum”) are named, the palate is taken as the basis

- A03.1.02.03: Sutura palatoethmoidalis
- A03.1.02.030: Sutura palatomaxillaris
- A03.1.02.032: Sutura palatina mediana
- A03.1.02.033: Sutura palatina transversa.

(5) While the 21 remaining sutures were named, the names of the bones that make up the suture are used together. In this way, the question of which bone’s name will take the first and which bone’s name will take place at the end comes up. We conducted our study to find reasonable answers to this question.

In our empirical examination, we identified four different criteria and obtained the following results.

(A) In anatomical terminology, some of the bones receive “os” while others do not receive “os.” Bones receiving “os:” os frontale, os parietale, os occipitale, os temporale, os ethmoidale, os sphenoidale, os lacrimal, os palatinum, os zygomaticum and os nasale, bones without “os:” concha nasalis inferior, vomer, maxilla, and mandibula

If a suture occurs between a bone that receives “os” and a bone that does not receive “os,” the bone that receives “os” always comes first.

These include:

- A03.1.02.015: Sutura frontomaxillaris
- A03.1.02.018: Sutura zygomaticomaxillaris
- A03.1.02.019: Sutura etmoidomaxillaris
- A03.1.02.021: Sutura sphenovomeris
- A03.1.02.023: Sutura sphenomaxillaris
- A03.1.02.026: Sutura nasomaxillaris
- A03.1.02.027: Sutura lacrimomaxillaris
- A03.1.02.028: Sutura lacrimoconchalis.

(B) If one of the bones that make up the suture belongs to the neurocranium and the other belongs to the viscerocranium, the name of the bone belonging to the neurocranium always comes first

These include:

- A03.1.02.013: Sutura frontonasalis
- A03.1.02.016: Sutura frontolacrimalis
- A03.1.02.017: Sutura frontozygomatica
- A03.1.02.020: Sutura ethmoidolacrimalis
- A03.1.02.022: Sutura sphenozygomatica
- A03.1.02.024: Sutura temporozygomatica
- A03.1.02.015: Sutura frontomaxillaris
- A03.1.02.019: Sutura etmoidomaxillaris

- A03.1.02.021: Sutura sphenovomeris
- A03.1.02.023: Sutura sphenomaxillaris.

There are 10 sutures in this group, but 4 of them (A03.1.02.015: Sutura frontomaxillaris, A03.1.02.019: Sutura etmoidomaxillaris, A03.1.02.021: Sutura sphenovomeris, A03.1.02.023: Sutura sphenomaxillaris) were included in group A before. There are 6 sutures in this group (which were not previously in any group).

(C) When naming a suture formed between the general name of a bone and a part of another bone, the general name comes first.

These include:

- A03.1.02.005: Sutura occipitomastoidea
- A03.1.02.008: Sutura sphenosquamosa
- A03.1.02.011: Sutura parietomastoidea.

(D) There are a total of 4 sutures that do not comply with the above 3 rules. The placement of the bones in the skull is taken into account when naming these sutures. The ones in the center of the skull come first and then the ones around.

These include:

- A03.1.02.006: Sutura sphenofrontalis
- A03.1.02.007: Sutura sphenoehtmoidalis
- A03.1.02.009: Sutura sphenoparietalis
- A03.1.02.014: Sutura frontoehtmoidalis.

Anatomical terms and clinical terms based on them form the basis of communication between people who are engaged in medical science and education in all over the world.^[5-8] Therefore, created terms must comply with certain rules to make this communication in a healthy way.

In TA, which we use today, two of the sutures (sutura ethmoidal lacrimalis and sutura sphenovomeris) named after two bones are present but they are not present in 1895 BNA, 1933 INA, and 1955 PNA. However, it is available in Six Edition NA. The names of some sutures accepted in the BNA (sutura nasofrontalis, sutura zygomaticofrontalis, and sutura temporozygomatica) have been changed to the present state (sutura frontonasalis, sutura frontozygomatica, and sutura temporozygomatica) since they do not comply with the rule B we identified above.

Today, however, students may have difficulty in understanding anatomical terms, and faculty members sometimes have difficulty in answering the question of why from students. In this study, we tried to answer the questions of why. We hope that this study will benefit the new generation of anatomists.

Financial support and sponsorship

Nil.

Conflicts of interest

There are no conflicts of interest.

Erdogan Unur, Ilyas Ucar, Selman Cikmaz¹, Salih Murat Akkin²

Department of Anatomy, Faculty of Medicine, Erciyes University, Kayseri,
¹Department of Anatomy, Faculty of Medicine, Trakya University,
Edirne, ²Department of Anatomy, Faculty of Medicine, Sanko University,
Gaziantep, Turkey

Address for correspondence: Dr. Ilyas Ucar,
Department of Anatomy, Faculty of Medicine, Erciyes University,
Kayseri, Turkey.
E-mail: fzt.iducar@hotmail.com

References

1. Opperman LA. Cranial sutures as intramembranous bone growth sites. *Dev Dyn* 2000;219:472-85.
2. Albay S, Sakallı B, Yonguç G, Kastamoni Y, Edizer M. Incidence and Morphometry of Sutural Bones. *SDU Medical Faculty Journal* 2013;20:1-7.
3. Federative Committee on Anatomical Terminology. *Terminologia Anatomica, International Anatomical Terminology*. New York, USA: Thieme Stuttgart; 1998. p. 292.
4. Kopsch F, von Knese HB. *Nomina anatomica. Comparative overview of Basel, Jena and Paris Nomenclature*. 5 Ed. Stuttgart, Deutschland: Georg Thieme Verlag; 1957. p. 155.
5. Unur E, Ertekin T, Acer N, Cinar S, Ozcelik O, Cay M. Names which originate from plants within terminologia anatomica. *J Turgut Ozal Med Cent* 2016;23:488-91.
6. Kachlik D, Baca V, Bozdechova I, Cech P, Musil V. Anatomical terminology and nomenclature: Past, present and highlights. *Surg Radiol Anat* 2008;30:459-66.
7. Burdan F, Dworżański W, Cendrowska-Pinkosz M, Burdan M, Dworżańska A. Anatomical eponyms – Unloved names in medical terminology. *Folia Morphol (Warsz)* 2016;75:413-38.
8. Sawai T. The emergence of modern muscle names: The contribution to the foundation of systematic terminology of Vesalius, Sylvius, and Bauhin. *Anat Sci Int* 2019;94:23-38.

This is an open access journal, and articles are distributed under the terms of the Creative Commons Attribution-NonCommercial-ShareAlike 4.0 license, which allows others to remix, tweak, and build upon the work non-commercially, as long as appropriate credit is given and the new creations are licensed under the identical terms.

Article Info

Received: 24 August 2020
Accepted: 23 November 2021
Available online: 30 June 2022

Access this article online	
Quick Response Code: 	Website: www.jasi.org.in DOI: 10.4103/jasi.jasi_166_20

How to cite this article: Unur E, Ucar I, Cikmaz S, Akkin SM. Basic rules for naming sutures. *J Anat Soc India* 2022;71:156-7.

© 2022 Journal of the Anatomical Society of India | Published by Wolters Kluwer - Medknow

Why Should Anatomists Underline the Geometry of Some Special Structures?

Dear Editor,

For most of the anatomists, gross anatomy and dissections are cornerstones of traditional medical education. But, we know that exponential growth in medical literature and technological developments have been changing our way of thinking and teaching methods. Gross anatomy education should integrate the traditional and innovative methods today. The development of digital sources such as animations, videos, and three-dimensional reconstructions helps us to deliver more anatomical information during lectures and courses.^[1]

Then comes the question: does the morphology, shape, or geometry of a structure draw any attention to the functional anatomy? This is a good step of learning in medical education; combining the knowledge with the conceptualization by asking the reasons.

Anatomists should underline the geometry of some special structures: Hepatocytes and hepatic lobules are attractive structures concerning the revision of functional anatomy literature. The parenchyme of the liver plays a crucial role in bile production, protein synthesis, chemical processing of molecules of the body itself, and foreign substances. The hepatocytes form the critical cell layer between the sinusoids and the bile canaliculi. They have a unique polarity with the basal membrane facing the sinusoid endothelium, while one or more apical poles can contribute to several bile canaliculi.^[2] Hepatocytes are polygonal in shape and their outer membrane has many facets: two or three facets are in contact with the space of Disse, while the remaining facets make contact with adjacent liver cells. Bile canaliculi run between adjacent hepatocytes. The establishment of hepatocyte polarity and geometry is essential to explain many functions, but this explanation is not enough to understand the relation between physics and functions of the liver. Four to six wedge-shaped hepatocytes arranged in cords are located around the bile canaliculi. Hepatocyte cords and sinusoids run along each other in a branching and interlocking fashion that increases the metabolic interchange between the blood and bile systems. The hepatic lobule is a hexagon with portal triads at each corner. In the hepatic lobular system, periportal areas are supplied by the branches of the hepatic artery and the portal vein to the periphery and the central vein to the center of the lobule which results in centripetal blood flow. The bile flows centrifugally toward the periphery. Another

functional concept is the liver acinus: a diamond-shaped area supplied by the terminal branches of hepatic artery and portal vein. This small unit is important for describing functional and pathological changes of many clinical conditions. Its short axis runs along the borders of hepatic lobules, and its imaginary long axis is located between the two central veins. Hepatocytes are located in three elliptical zones around the short axis.^[3-5]

The systems of lobulation and acinus formation complementing each other prompt the hypothesis that histology dealing with polarity and geometry can be linked to gross anatomy integrating functional modulation. This way of learning anatomy makes hepatocytes and the liver itself highly valuable subjects of medical, biological, and pharmaceutical researches. *In vitro* models of hepatocyte arrangements would be of great importance to understand the physiological functions of the liver and the pathological processes of liver diseases.

The aim of this letter is to encourage the young anatomists to learn microscopical anatomy with gross anatomy and functional anatomy with pathology to drive many researches with the clinicians. Liver is a perfect example to begin...

Financial support and sponsorship

Nil.

Conflicts of interest

There are no conflicts of interest.

Aysegul Firat, Hatice Yasemin Balaban¹

Departments of Anatomy and ¹Gastroenterology, Faculty of Medicine, Hacettepe University, Ankara, Turkey

Address for correspondence: Dr. Aysegul Firat,
Department of Anatomy, Faculty of Medicine, Hacettepe University,
Ankara 06100, Turkey.
E-mail: aysfirat@hacettepe.edu.tr

References

1. Aziz N, Mansor O. The role of anatomists and surgeons in clinical anatomy instruction inside and outside the operating room. *Malays J Med Sci* 2006;13:76-7.
2. Gissen P, Arias IM. Structural and functional hepatocyte polarity and liver disease. *J Hepatol* 2015;63:1023-37.
3. Sun P, Zhang G, Su X, Jin C, Yu B, Yu X, *et al.* Maintenance of primary hepatocyte functions *in vitro* by inhibiting mechanical

- tension-induced YAP activation. *Cell Rep* 2019;29:3212-22.e4.
- Erwin K, Hans-Dieter K. *Hepatology: Textbook and Atlas*. 3rd ed. Heidelberg: Springer Medizin Verlag; 2008. p. 26-8.
 - William KO, Patrick CN. *Netter's Essential Histology*. 2nd ed. Philadelphia: Elsevier Saunders; 2013. p. 314-6.


This is an open access journal, and articles are distributed under the terms of the Creative Commons Attribution-NonCommercial-ShareAlike 4.0 License, which allows others to remix, tweak, and build upon the work non-commercially, as long as appropriate credit is given and the new creations are licensed under the identical terms.

Article Info

Received: 19 December 2020

Accepted: 21 December 2021

Available online: 30 June 2022

Access this article online	
Quick Response Code: 	Website: www.jasi.org.in
	DOI: 10.4103/jasi.jasi_269_20

How to cite this article: Firat A, Balaban HY. Why should anatomists underline the geometry of some special structures? *J Anat Soc India* 2022;71:158-9.

© 2022 Journal of the Anatomical Society of India | Published by Wolters Kluwer - Medknow